ASPECTS OF THE GEOLOGY AND GEOMORPHOLOGY OF LAKE BANGAZI NORTH: A PALAEO-ESTUARY TO THE MKHUZE RIVER

By

Diaksha Ramdhunee

Student number: 216024390

Supervisor: Prof Andrew Green

College of Agriculture, Engineering and Science
School of Agriculture, Earth and Environmental Science
University of KwaZulu-Natal

December 2023

Submitted in fulfilment of the academic requirements for the degree of Master of Science in the School of Agriculture, Earth and Environmental Sciences, University of KwaZulu-Natal, Westville.

COLLEGE OF AGRICULTURE, ENGINEERING AND SCIENCE

DECLARATION 1 - PLAGIARISM

I, ……Diaksha Ramdhunee…….……., declare that

1. The research reported in this thesis, except where otherwise indicated, is my original research.
2. This thesis has not been submitted for any degree or examination at any other university.
3. This thesis does not contain other persons' data, pictures, graphs or other information, unless specifically acknowledged as being sourced from other persons.
4. This thesis does not contain other persons' writing, unless specifically acknowledged as being sourced from other researchers. Where other written sources have been quoted, then:

a. Their words have been re-written but the general information attributed to them has been referenced

b. Where their exact words have been used, then their writing has been placed in italics and inside quotation marks, and referenced.

5. This thesis does not contain text, graphics or tables copied and pasted from the Internet, unless specifically acknowledged, and the source being detailed in the thesis and in the References sections.

Signed

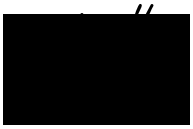

…… ……

As the candidate's supervisor I have approved this thesis/dissertation for submission.

Signed:.…[redacted]…… Name: Prof. Andrew Green… Date: 06/04/2024

Acknowledgements

A special thank you to NRF for providing the funds and giving me the opportunity to further my studies.

A massive thank you to God for allowing me the strength to continue even when things seemed bleak and were overwhelming. For rewarding my faith by allowing me to finish this thesis with strength I did not know I had.

Thank you, Prof. Green for being an amazing supervisor. I have been pushed into new aspects of geology. A big thanks for all your words of wisdom and general life discussions which allowed me to see this thesis and even the world in a new light.

I would like to thank my mom for the endless support and encouragement throughout this year.

Michael, I cannot thank you enough for being the best person I know. For supporting me through everything, forcing me to relax so I could work better. For forcing me to go to sleep when I've been burnt out and being there through the tough times and massive changes in my life over the past few years.

Abstract

This research examines the geological evolution of Lake Bangazi North, on the east coast of northern KwaZulu-Natal, South Africa. Very little research has been conducted on this area and as a result the information provided in this paper will serve as the one of the first research pieces on the area. The geophysical and seismic stratigraphy, changing palaeo-environments relating to the change in contemporary geomorphology using bathymetry and satellite imagery are described for the area of Lake Bangazi. These data were collected and interpreted via geophysical and seismic reflection data, multibeam bathymetry and remote sensing. Geochemical analyses on a core sample taken from the lake provided a quantitative interpretation of the lake sediment, linking the recent development to the broader geological history.

The change in sea level following the Late Pleistocene and Holocene era had a significant effect on coastal systems. Lake Bangazi like other coastal systems along the east coast of KwaZulu-Natal such as St Lucia estuary, Kosi Bay and Lake Sibaya shows similar changes with the interaction of the Pleistocene dune barrier complex influencing the development of these systems. It is theorised that Lake Bangazi was once connected to the St Lucia estuary. Lake Bangazi has been isolated from the St Lucia estuary for a significant period of time where it has only been affected by prolonged periods of drought, thereby ensuring a high preservation potential allowing for an accurate geological evolution to be drawn from the stratigraphic record. An unexpected, yet interesting, aspect of this study shows the relationship that wildlife, specifically hippos, can have with waterbodies and the impact their role as bio-engineers play in the development of these waterbodies.

Table of Contents

List of Figures

List of Tables

Chapter 1

Introduction

Coastal systems are dynamic features which are heavily influenced by various factors such as tectonic activity, sediment supply, climate, storm frequency and intensity, as well as relative sea-level change (Cooper et al., 2018a). Their morphology and stratigraphic evolution are dictated by the above, and are preconditioned by the underlying geological controls of the system, e.g. bedrock and antecedent topography (Cooper et al., 2018b). These systems may also be engineered by biological activity, where biota, especially large herbivores, can create changes to landscape that are inherited through morphodynamic feedbacks to the system (McCarthy et al., 1998, Deocampo, 2002, Chansa et al., 2011).

The various waterbodies that occur along the northern coast of KwaZulu-Natal, South Africa (Figure 1.1.a.), represent a unique opportunity to examine the coastal evolution of the area. These systems have evolved from incised valleys, where rivers extended out past the shelf break during lowstands (Green, 2009a); (Green, 2009b), and have since been backflooded during transgression to form lagoons, lakes and estuaries, the geological evolution of which has been controlled by a limited sediment supply in some cases (e.g. Cooper et al., 2012; Dladla et al., 2022), shallow bedrock control in others (Dladla et al., 2019; Green et al., 2022), and repeated inheritance of old river courses (Wright et al., 2002). The fill of these incised valleys represents a complex response to changing sea level states (Dladla the al., 2021), buffering from open ocean energy by non-migrating and long-lived barriers (Benallack et al., 2016), and changing hydroclimates, especially during the Holocene (Humphries et al., 2016; Humphries et al., 2020).

Over the last ten years, the Universities of the Witwatersrand and KwaZulu-Natal have been engaged in a joint research project aimed at systematically examining the various waterbodies on the coast, especially where they have maintained an open-ocean connection and where they may have potential to act as sea level and climate archives (Humphries et al., 2017). The underlying framework of this research comprises understanding the geological context to coastal waterbody evolution. It is in this context that this research has been carried out at Lake Bangazi North (LBN), a small coastal lake system located approximately 12 km to the south-southwest of Sodwana Bay, KwaZulu-Natal (Figure 1.1.a). LBN occupies an unusual position, fronting the Mkhuze River, yet unlike the other systems of the region, appears to have no visible fluvial connection

(Figure 1.1.). Instead, the river is diverted at 90° to the south where it merges with the Lake St Lucia system to form the Mkhuze River bayhead delta (Figure 1.1.a) (Humphries et al., 2020).

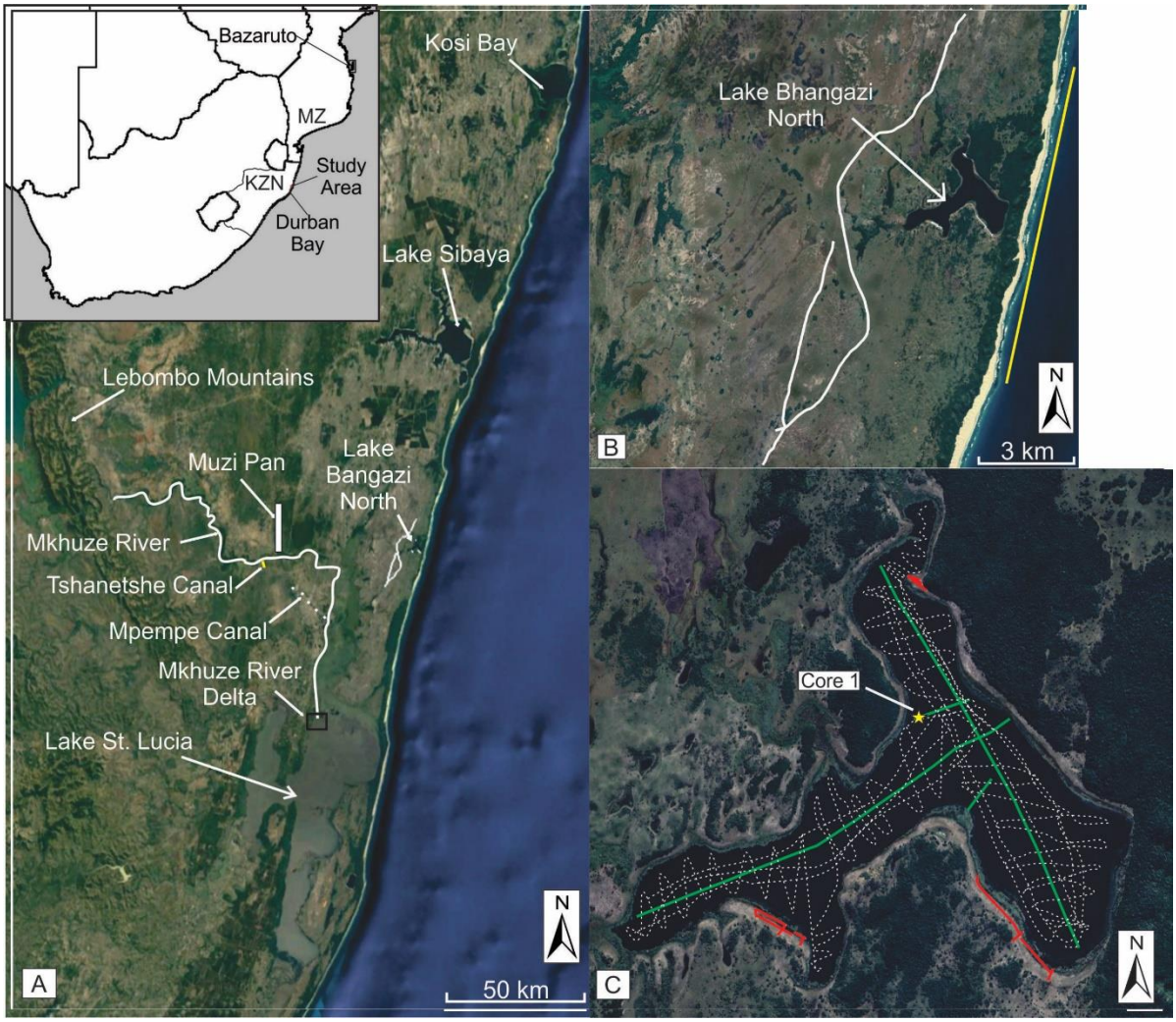

Figure 1.1. Locality map of the study area, highlighting surrounding coastal lake systems and the Mkhuze river. B – Location of regional Ground Penetrating Radar (GPR) data collected along roads inland of LBN. Yellow line represents the offshore seismic data described by Green (2009a). C –the green lines represent the ultra–high resolution sub-bottom profiles. Red lines represent the high resolution GPR data collected around the lake edge. The white dashed lines denote single beam bathymetric data coverage. The yellow star represents the location where the core was collected in the lake.

1.1 Aims and Objectives

This project aims to examine the morphological and stratigraphic evolution of LBN and surrounding coastal plain, paying careful attention to whether this lake comprises a

blocked-valley lake, such as Muzi Pan (Humphries et al., 2019), or if it merely comprises a low-lying dune slack that intercepts the high lying water table of the region (Weitz and Demlie, 2015). The objectives are:

1 – to identify, at a regional (12 x 4 km) scale, the palaeo-drainage courses associated with the Mkhuze River

2 – to link these to local scale channel systems that surround LBN

3 – to examine whether these may merge with a larger palaeo-channel network beneath LBN, and offshore the study area, and to what degree these control the modern lake bathymetry

4 – to core and examine the fill of the LBN system

5 – to identify legacies of bio-engineering in the system that are the result of large herbivore behaviours

Chapter 2

Literature Review

2.1. Coastal Morphological Features

2.1.1. Incised Valleys

Incised valleys are narrow, elongate geologic features which have formed as a result of eustatic sea-level fall, and fluvial or glacial erosion at topographic low points (Zaitlin et al., 1994, Wang et al., 2019). These features form along the coast during the exposure of the shelf and act as a record of palaeo environments following transgression (Nordfjord et al., 2006, Payenberg et al., 2006). The sediment preserved within the fill reveals one of the few pictures of lowstand environments (Posamentier and Allen, 1993, Payenberg et al., 2006) as the valley protects this sedimentary record from the later effects of wave and tidal ravinement processes (Swift and Thorne, 1991, Thorne, 1994, Payenberg et al., 2006). Incised valleys evolve into estuaries through transgression and coastal flooding of the valley form (Nordfjord et al., 2006). Where large barriers form in front of the estuary, these may seal the system to form an impounded coastal lake system, or a blocked valley lake (e.g., Muzi pans, parts of Lake St Lucia and Lake Sibaya) (Wright et al., 2002; Humphries et al., 2019; Green et al., 2022). The evolution of incised valleys records these transgressive phases in the form of tidal ravinement surfaces (Green et al., 2015).

The sedimentary fills that develop within incised valleys can be simple or complex, (Allen and Posamentier, 1994, Zaitlin et al., 1994, Dalrymple and Choi, 2007) and are influenced by a variety of factors. These include their position (coastal plain vs continental shelf-or middle vs outer segments-(Zaitlin, 1994), accommodation space and eustatic sea-level changes (Green, 2009a, Cooper et al., 2012). Fluvial base level is a key factor that controls the formation and infilling of these geologic features. Climate and tectonic processes are the principal factors controlling base level change (Coe et al., 2003, Catuneanu, 2006). Coe et al. (2003) described five orders of cycles recorded in the sedimentary record: first order (c. 50 to c. 200+ Ma), second order (c. 5 to c. 50 Ma), third order (c. 0.2 to c. 5 Ma), fourth order (c. 100 to c. 200 Ka), fifth order (c. 10 to c. 100 Ka).

2.1.2. Blowouts and deflation features

Blowouts are bowl-, saucer- and trough- shaped depressions that form via wind erosion of a pre-existing structure such as a dune or washover hollows and fans (Hesp, 2002,

Hesp, 2011). Two types of blowouts are most common. In the study area, saucer- and trough-shaped are observed. Saucer shaped blowout are shallow depressions that have a saucer shape whereas trough shaped blowouts are more elongate features with deeper depressions and steeper lateral walls/slopes (Figure 2.1.a and b).

2.1.2.1. Formation and Evolution

Blowout features are commonly located on coastal dune environments and/or on receding/eroding beaches (Hesp and Hyde, 1996, Hesp, 2002, Hesp, 2011) and according to González-Villanueva and Hargitai (2021) these are controlled by vegetation. These can also form in high wind/wave environments.

Areas of blowout initiation:

(1) Erosion of dune stoss slope via wave erosion. Thereafter wind further erodes the unvegetated portion of the dune slope.
(2) Change in vegetation - wind erosion of unvegetated portions of a dune during elongated periods of aridity such as drought. A lack of vegetation may also result from vegetation dieback, nutrient depletion, climate change etc.
(3) Wind erosion of overwash fans and hollows.
(4) Hurricanes or high velocity winds act to undermine/erode vegetation, initiating blowouts.
(5) Anthropogenic and local animal activities such as track creation and burrowing respectively.

The knowledge of blowout evolution, from the moment of inception to end, is not fully clear. Various factors affect the growth of these features resulting in the above end-member shapes (Figure 2.1.). Factors such as wind speed, strength and direction, vegetation (dieback and revegetation), occurrence and magnitude of storm events, beach erosion (McKee, 1979, Gares and Nordstrom, 1995, Neal and Roberts, 2001), climate change and human activities (Hesp, 2002).

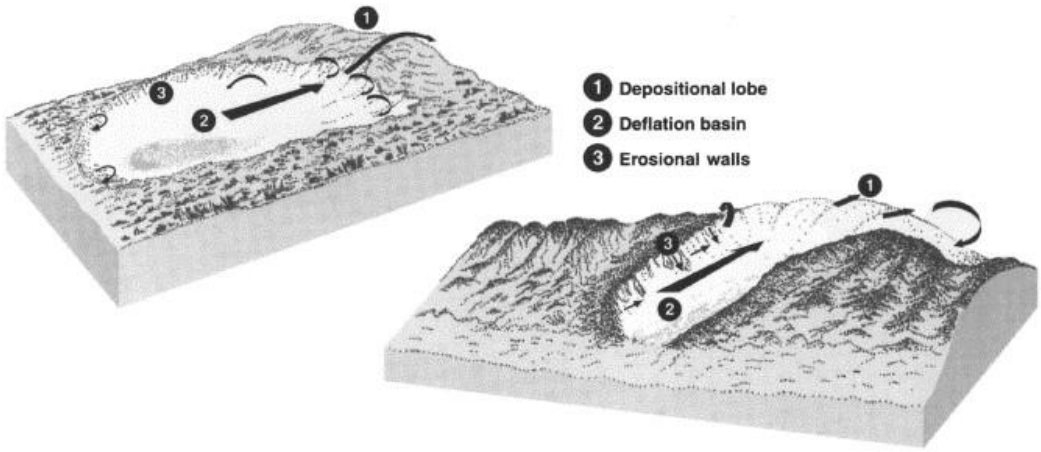

Figure 2.1. Blowout shapes – a) Saucer shaped blowout and b) Trough shaped blowout from Hesp and Hyde (1996). The arrows indicate wind direction.

Correlations between the depositional lobe length and deflation basin length are typically high (González-Villanueva and Hargitai, 2021). A ratio was provided in papers by Hesp (2011), González-Villanueva and Hargitai (2021) showing an evolutionary model of trough and saucer blowouts with a 1:4 and 1:2 to 1:3 ratio between lobe length and basin length (Hesp, 2011, González-Villanueva and Hargitai, 2021). This indicates a trough blowout begins with a narrow-elongated shape with maximum erosion taking place at the base with maximum transport up the central axis (Figure 2.1.). This model describes a greater elongation to widening ratio. A saucer blowout can deepen to a maximum level depending on their morphology (Hugenholtz and Wolfe, 2009) (Figure 2.1.). However, during a period of inactivity, revegetation can occur, stabilizing the feature (Carter et al., 1990). This can also be facilitated by the basin of a saucer blowout reaching a water table promoting the growth of flora in the area. Re-activation can also occur with the erosion of the built-up lobes.

2.1.5. Sediment Geochemistry

Sediment geochemistry plays an important role when reconstructing the palaeoenvironment by aiding in the determination of the sediment provenance (Dellwig et al., 2000, Minyuk et al., 2007), transport mechanism, marine influences and geochemical processes. In dynamic systems such coastal lakes the comparison between relative elemental variation and a conservative element (such as aluminium) proves beneficial as the latter remains unaffected by either post-depositional or biological processes (Schropp et al., 1990).

Iron and aluminium are some of the main elements which are located within a coastal system, typically associated with coastal dunes (Al-Dousari et al., 2020). Aluminium is often associated with alumino-silicates. Silicates have various elements associated with them such as rubidium (Rb), aluminium (Al), titanium (Ti) and iron (Fe). The changes in the ratios of these elements e.g., Rb/Al, Ti/Al, Fe/Al, indicate the variations in mineralogical inputs into the system over a period of time (Haberzettl et al., 2008). Silicon (Si) and aluminium as discussed are often associated with sediments and represented with the ratio (Si/Al). Si is found in coarser sediment such as quartz and Al is found within clay sediments, therefore the aforementioned ratio can be used to indicate the transport mechanism of these sediments i.e., coarser sediment will be deposited within higher energy conditions (Kylander et al., 2011). These elements are the most commonly used proxy indicators for environmental change.

Other important elements include potassium (K), calcium (Ca) and strontium (Misra et al.) (Misra et al., 2017) e.g., K/Al and K/Rb. Coastal lakes are influenced by and act as a depositional site for sediment from marine, aeolian and fluvial aspects, showing ancient climatic conditions of the region. Aspects of these climatic conditions include chemical and carbonate weathering. The ratio of K/Al and K/Rb are good indices for chemical weathering patterns (Zabel et al., 2001, Pattan et al., 2005) due to the difference in size of the cations. The larger cations (Al and Rb) have a tendency to remain within the source rock whereas the smaller cations (K, Sr and sodium (Na)) are selectively leached (Pattan et al., 2005). During chemical alteration, the smaller cations will be leached and the larger, immobile elements will remain behind in the source rock (Hu et al., 2016). Often these elements are used as climatic indicators of a wetter and/or warmer climate in addition to the intensity of chemical weathering (Higgs, 2017).

Calcium and zircon are among the two most commonly used elements to determine the geological history of an environment i.e., zircon indicates a terrestrial environment while calcium indicates a marine environment. Calcium and zircon, share an inverse relationship, were these elements are typically located at specific areas within a dune system as a result of their density (Al-Dousari et al., 2020). Calcium is typically always located upwind and inland, without calcium appearing downwind. These elements can be used as a way to ‘fingerprint’ aeolian sediments (Humphries et al., 2020).

A calcium and strontium ratio can be applied to lake sediments to indicate carbonate weathering, bioclastic material or in-situ precipitation (Shand et al., 2007, Kylander et al., 2011). In-situ precipitation, when carbonate saturation in a lake is reached, occurs because of evaporation or lower lake levels (Cohen, 2003).

2.1.6. Bio-engineering

Hippopotamus amphibius, hereafter hippo, are a locally dominant sub-Saharan animal (Eltringham, 1999) typically known as a megaherbivore due to its size (>1000 kg). They have a semi-aquatic lifestyle (Owen-Smith, 1988) and are known to occupy large freshwater lakes and slow-flowing rivers. Given the combination of the large size of hippos and their movement between terrestrial and aquatic ecosystems, hippos are considered ecosystem engineers (Naiman and Rogers, 1997, Moore, 2006). These creatures spend a large portion of their time in the water, leaving only to graze at night, usually foraging in places that might be a few kilometres away. Hippos tend to follow these established paths to their grazing areas (Lock, 1972) and as they continue to trample along these routes, the routes entrench, often evolving to gullies that alter the landscape (Altamura et al., 2017). These trenches or gullies may harden over time due to compaction, retaining their profile even through seasonal flooding (Altamura et al., 2017).

The geomorphological impact of hippos and the evolutionary pathway of their tracks has been described from the Ngorongoro crater (Tanzania) and the Okavango Delta (Botswana) (Figure 2.2.)(McCarthy et al., 1998, Deocampo, 2002). Ellery et al. (2003) noted transport of clay between the toes of hippos from the aquatic environment to the terrestrial terrain, however, sand was less adhesive and therefore was not transported as frequently to the aquatic environment. Well-established hippo trails are considered especially important as conduits for water flow during a flood, directing water away from perched water tables of certain areas (Ellery et al., 2003).

These pathways can further evolve into sandy ridges as observed by Stanistreet et al. (1993), McCarthy et al. (1998). In Tanzania, McCarthy et al. (1998) observed that hippo pathways act as channels when situated adjacent to lakes or rivers, and these pathways aggrade with the main channel aggradation. These channels evolve and develop into

sinuous sandy ridges, sometimes more than a metre in height (McCarthy et al., 1998). Later, these ridges may create areas where islands form (McCarthy et al., 1998).

Figure 2.2. Images from various hippo trackways of the Ngorongoro area, Kenya (from Deocampo, 2002). Note the relief generated by the trails, and the sandy substrate of the trail floors.

Hippo trails form a radial or a dendritic pattern over time, spreading out from a lake or a river extending for 2 – 3 km, usually with a depth of 1 m and a width of 1 – 5 m (McCarthy et al., 1998, Deocampo, 2002, Ellery et al., 2003), Altamura et al. (2017). At Gombore II-2, in the Ethiopian highlands, fossilized hippo footprints and their resultant load structure features were identified in the stratigraphy of an old hippo trail that had created a channel-like structure filled with sand (Altamura et al., 2017). These had a maximum

width of 2 m and maximum depth of 0.7 m (Altamura et al., 2017), within the known morpho-parameters of hippo paths (Table 2-1).

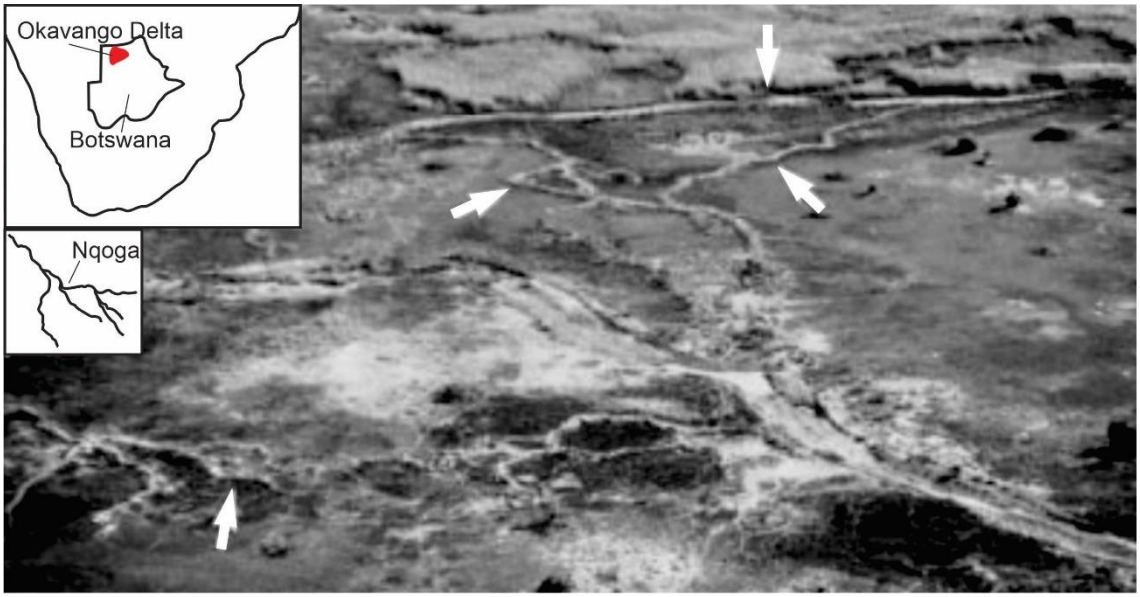

Figure 2.3. Sandy ridges of hippo trails located in Nqoga of the Okavango Delta, in Botswana (McCarthy et al. (1998)).

Table 2-1. Collation of quantified hippo trails found in studies with similar environments.

Hippo Trails (m)	Width	Depth
(Deocampo, 2002)	1 – 5	~ 0.5
(McCarthy et al., 1998)	2	> 1
(Altamura et al., 2017)	2	~ 0.7
(Ellery et al., 2003)	6 – 10	< 2

Fritsch et al. (2022) conducted a recent study in the Ndumo Game Reserve (NGR) located along the northern border of South Africa with Mozambique (MZ). This study noted the movement of hippo pods within an area that is seasonally flooded (typically a floodplain), with seasonal pans. Fritsch (2020), Fritsch et al. (2022) further identified the relationship between hippo movement and hippo pod size (including adults and juveniles), showing that hippo pod size and hippo density decreases with an increasingly inundated area. During the dry season, when the water level is low, hippos are densely crowded into small bodies of water such as the lakes (Shurin et al., 2020). Prinsloo et al. (2020) conducted a

study in the St Lucia estuary, south of Lake Bangazi North, on the distribution habits of hippos within the system. Both Chansa et al. (2011), Prinsloo et al. (2020) noted that hippos congregate in pods with individuals ranging between 1 – 100.

These creatures are known to live for long periods of time with each generational pod following the same selected path of movement. Hippos can physically alter their environment by deepening the pool/riverbed through their movement, in addition to creating incised, vegetation free pathways or channels that increases the activity between the terrestrial and aquatic environments (Naiman and Rogers, 1997). This shows the extent to which hippos can and have influenced an environment over time. To date, no studies have examined the degree to which hippos can modify their environment from geophysical techniques which provide a means to observe further into the geological past.

Chapter 3

Regional Setting

The Northeastern coastal plains of KZN consist of coastal waterbodies developed following the rise in sea level from the Last Glacial Maximum (LGM) of 18 000 – 23 000 yr BP when sea level was ~120 – 130 m below present (Green and Uken, 2005). In many cases, such as Lake St Lucia, their evolution has been strongly controlled by the geological framework in which the incised valleys were formed and then filled (Dladla et al., 2019).

3.1. Regional Geology

3.1.1. Gondwana

The south-eastern African coastline has a dynamic history of different geological and geomorphological activities, taking place over 180 million years since the Gondwanan period (Watkeys et al., 1993, Botha, 2015, Botha, 2018). Continental rifting of Gondwana, together with the extraction of the Falkland Islands, created a sheared passive margin (Green, 2011) that has accumulated significant volumes of material since the Mesozoic (Botha, 2018).

3.1.2. Zululand Group

Post Gondwana breakup, the main unit of deposition comprises the Zululand Group of the Zululand Basin. This is divided into three formations that span the Late Jurassic to Cretaceous i.e., Makatini, Mzinene and St Lucia Formations (Ware, 2001, Botha, 2015, Hicks, 2017). These formations are overlain by Cenozoic to Holocene cover sediments of the Maputaland Group. The Zululand Group comprises 1 500 m of fossiliferous siltstone (Botha, 2015) deposited as a result of marine transgressions over the tilted Lebombo Group (Ware, 2001).

The Makatini Formation forms the base of the sequence and comprises conglomerates, siltstones and minor limestones, capped by marine sandstones (Wolmarans and Du Preez, 1986, Chabangu et al., 2014). These rocks reach a thickness of 80 m (Chabangu et al., 2014, Botha, 2015) and are of Barremian to early Aptian in age. This formation was

considered to be the result of a braided fluvial system that entered into a shallow sea 120 – 114 Ma ago (McCarthy et al., 1993, Tankard et al., 2012).

The Mzinene Formation varies from early Albian to late Cenomanian in age. This sedimentary sucession comprises shallow marine, glauconitic siltstones that are richly fossiliferous, in addition to fine grained sandstones with shelly concentrations (Watkeys et al., 1993).

A major hiatus separates the Mzinene Formation and the overlying St Lucia Formation. Onshore, this hiatus is identified as mid-Cretaceous in age, whereas in the distal portion of the basin McMillan (1993) identified late Cenomanian and early Turonian lithologies along this contact. Chabangu et al. (2014) identified the contact between the two formations as marked by a ~30 m thick, laterally extensive, gritty, quartz sandstone that shows evidence of wave sorting.

The St Lucia Formation is late Cretaceous in age and comprises greenish grey, richly fossiliferous, glauconitic mid– to outer-shelf deposited siltstones and fine-grained sandstones (Chabangu et al., 2014). This sandstone has large calcareous concentrations interbedded within it and mirrors the Mzinene Formation, representing a transgressive state that recommenced in the Zululand Basin (Chabangu et al., 2014, Botha, 2015).

3.1.3. Maputaland Group

The Maputaland Group was formed during the Cenozoic era and consists of the Uloa, Umkwelane, Port Dunford, Kosi Bay, Kwambonambi, and Sibayi (Holocene) Formations (Miller, 1998). The Maputaland Group is exposed along the beaches and dune systems located in northern KZN (Ware, 2001), extending along the eastern coast of South Africa up to the southern Mozambique border (Figure 3.1). The deposits of this group comprise sediments which have accumulated as a result of eustatic sea-level changes during the Pliocene to Pleistocene period (Botha (1997).

The basal layer of the Uloa Formation consists of a thin conglomerate layer overlain by coquina (2 – 3 m thick) (Dingle et al., 1983, Liu, 1995). Overlying the Uloa Formation is the Umkwelane Formation. In some areas there is a marked lithological break between the underlying coquina and the aeolian cross-bedded calcarenite layer of the Umkwelane Formation (Miller, 1994, Miller, 1998, Wright et al., 2000), with the basal layer of the

Umkwelane Formation identified as a succession of beachrock (Miller, 1994, Miller, 1998, Wright et al., 2000).

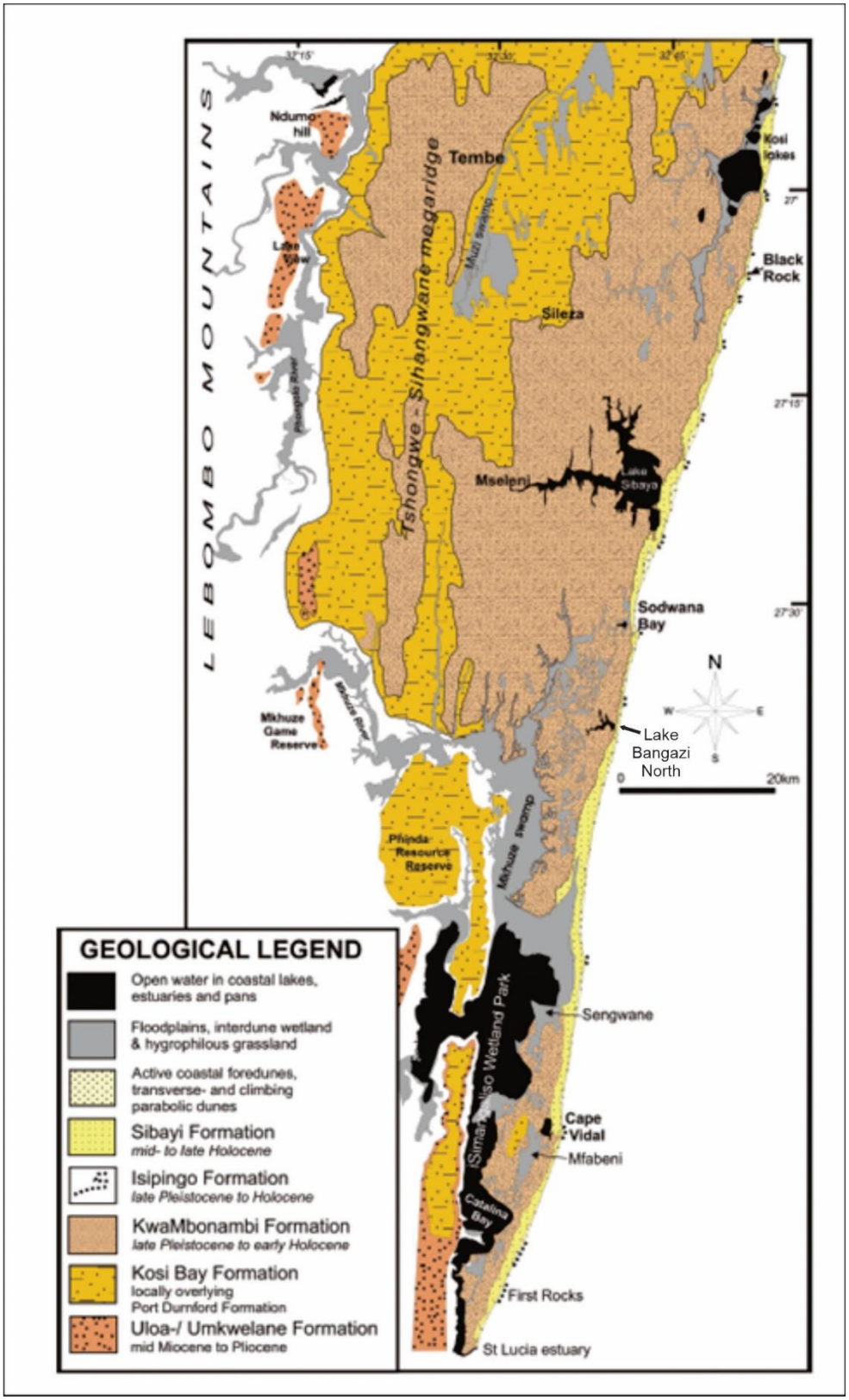

Figure 3.1. Distribution of the Maputaland Group along the northeastern KwaZulu-Natal coast from Botha (2018).

The overlying sediments of the Port Dunford, Kosi Bay, KwaMbonambi and Sibayi Formation have been identified as mid-to-late Pleistocene in age (Miller, 1998, Sudan, 1999, Ware, 2001). The Port Dunford Formation comprises a basal layer of fossiliferous argillite member (Ware, 2001) discontinuous aeolian sediments unconformably overlain by a ±10 m thick fossiliferous shallow marine sands and organic-rich lagoonal clays (Hobday and Orme, 1974, Maud, 1993). Hobday and Orme (1974), Maud (1993) noted a lignite horizon (1 – 1.5 m thick) above the layer of marine sands and lagoonal clay. The Port Durnford Formation is considered to be a transgressive barrier-lagoon complex related to the last interglacial highstand ±120 000 BP (Hobday and Orme, 1974, Maud, 1993).

The Kosi Bay Formation (up to 50 m thick) unconformably overlies the Port Durnford Formation. The formation consists of a basal lignite layer averaging 1.3 m thickness (Ware, 2001). This unit is overlain by ~15 m of weathered, semi-consolidated dune sands above which semi-consolidated clayey sands (Botha, 1997, Botha, 2015). The Kwambonambi Formation formed during marine regression which resulted in the erosion and reworking of dune sands (Kosi Bay Formation) and aeolian deposition (Botha, 1997). This formation comprises 5 – 15 m of redistributed unconsolidated dune sands (Ware, 2001, Botha, 2015).

The Sibayi Formation consists of an extensive coastal dune barrier system in addition to acting as a marker for the Holocene transgression (Miller, 1998, Sudan, 1999). This is noted in the basal marine washover and lagoonal sediments found in areas where the dunes are known to have been breached during the LGM (Miller, 1998). The high coastal dune barrier consists of calcareous, fine-grained and well sorted aeolian sediment which has also been reworked building the dune even further (Botha, 1997, Miller, 1998, Sudan, 1999, Wright, 1999). Buried palaeosols within the dune structure provide evidence for multiple phases of dune building within the Holocene dune system which now separates contemporary lake systems from the ocean (Botha, 1997, Sudan, 1999). These sands have been noted by Ware (2001) to have abundant heavy minerals in economic concentrations.

3.1.4. Regional climate and oceanography

Lake Bangazi North is located on the eastern coast of South Africa within a subtropical coastal climate with a temperate inland climate (Wright et al., 2000). The warm Agulhas

Current sweeps along the eastern coastline resulting in the warmer climate experienced along this coastal region (Government, 2023). Thunderstorms and mid latitude cyclonic activity dominate the weather patterns (Wright et al., 2000). Coast parallel winds are dominant (Wright et al., 2000); during summer, north to north-easterly winds are dominant whereas in winter north-easterly and south-easterly winds prevail (Wright, 1999).

The large amplitude south-easterly swells generated by mid latitude cyclones are distinctive of the wave climate within this region (Rossouw, 1984). Long period swells within this region have a modal height of 2 m, with tidal ranges less than 2 m, thus a wave dominated and microtidal region (Ramsay and Cooper, 2002, Schoonees et al., 2006).

3.1.5. The Mkhuze River

The Mkhuze River is the largest river associated with the study area, with a catchment size of ~5 250 km^2 extending toward Vryheid. The Mkhuze River flows eastwards towards the coast from Vryheid, creating a deep gorge, gradually becoming confined as a result of entrenched meanders through the Lebombo Mountains. The Mkhuze floodplain extends along the eastern coast bound by the Lebombo mountains in the west. This forms part of the Maputaland coastal plain system, which is a mosaic of lakes and wetlands (Watkeys et al., 1993). Ramsay (1996) noted the replenishment of coastal river systems by the Mkhuze River during the LGM when the sea level was ~120 m below present level. Following a rise in sea level during the Holocene, major rivers were blocked causing incised valleys to flood (Higgs, 2017). Erosion and deposition of sediment formed a barrier which cut off Lake St Lucia and the Mkhuze River from the ocean (Higgs, 2017). The Mkhuze Delta grew (laterally) over ~6 000 years at an average of 3 m yr^{-1} (Higgs, 2017).

The Mkhuze River has been affected by many hydrological and climactic changes, most notably tropical cyclones (Higgs, 2017). During tropical cyclones, the river becomes inundated with water, often flooding the surrounding floodplain, leading to recharge of surrounding wetland systems (Humphries et al., 2010). However, in comparison, the Mkhuze wetland has been most affected by human activity as the western portion of the river does not fall under the protection of the iSimangaliso Wetland Park authority (Whitfield and Taylor, 2009). As a result of human interferences, two canals were

constructed to divert the freshwater from the Mkhuze River namely the Mpempe Canal and the Tshanetshe canal (Figure 1.1.). The Mpempe Canal was constructed in the 1960's, directing the freshwater towards the St Lucia estuary during a drought period when the St Lucia estuary experienced a period of high salinity (Alexander et al., 1986, Goodman, 1987). As a result of the construction of this canal, the flow of water bypassed part of the wetland, disrupting the recharge of several pans in the Mkhuze floodplain (Goodman, 1987). The Tshanetshe canal was constructed in the late 1980's directing water from the Mkhuze River to the Tshanetshe Pan by a farmer to irrigate farmland and water livestock (Goodman, 1987). This canal was built by enlarging an existing hippo trail which underwent rapid erosion. Restoration of the original flow of the Mkhuze River has proven unsuccessful (Ellery et al., 2003). The Mkhuze River remains the largest supplier of sediment and freshwater to the Lake St Lucia estuary system via the bayhead delta located in the northern portion of the estuary (Higgs, 2017).

3.2. Coastal Lake Systems of the region

The KZN coast is a patchwork of lake and pan systems (Figure 1.1.). The most prominent and well–known coastal lakes relevant for this study include Lake St Lucia, Lake Sibaya and the Kosi Lake system. All these lakes provide insight into the development of the KZN coast over the LGM (Pleistocene through to Holocene).

3.2.1. St Lucia

Lake St Lucia has long since been an area of interest for geological and economic purposes. These aspects play a dual role in the survival of the geomorphological features of the system. Lake St Lucia estuary is currently characterized as an estuarine–lake system and forms Africa's largest estuary (Wright et al., 2000, Dladla et al., 2019a, Green et al., 2022). The Lake St Lucia estuary provides pivotal insights into the geological workings of a large back barrier lagoon system (Wright et al., 2000, De Falco et al., 2015, Benallack et al., 2016). Many systems similar to this are present around the world but are not as well preserved therefore studies conducted on this area provide valuable information.

The history of Lake St Lucia estuary shows the ever–dynamic environment of the system as the transition from an open marine-dominated embayment to a lagoonal system

numerous transgressions and regressions (Gomes et al., 2017). The northern parts of Lake St Lucia receive their main source of freshwater from the Mkhuze river, however, during the drought period of 2002 – 2007, the river dried up resulting in an increase in salinity in the northern parts of St. Lucia, where the only source of freshwater during this time was groundwater (Whitfield and Taylor, 2009).

Geological exploration for oil and associated seismic profiling revealed a deeply buried, narrow, fault-bounded graben along the western boundary of Lake St Lucia, infilled with sediment 820 m thick, possibly spanning the Jurassic-Cretaceous boundary (Botha, 2015, Botha, 2018). Following an early Cretaceous transgression, the rift was buried under approximately 1000 m of marine sediment (Botha, 2015, Botha, 2018).

Benallack et al. (2016) were the first to publish a high-resolution seismic stratigraphy of the northern parts of the system (False Bay and North Lake) (Figure 3.2). False Bay is dominated by a series of bayhead deltas that create a shallow and isolated basin, whereas North Lake's sediment fill relates to a palaeo-inlet that exited at Leven Point (Figure 3.2). Incised valleys resulting from sea-level lowstands mark both areas, with the oldest phase linked to a period of Pliocene uplift (Benallack et al., 2016). These fills preserve and reflect the geological history of the area beginning with a mixed wave–tide dominated environment. Thereafter sediments of an estuarine central basin were deposited following the sea–level rise to ~30 m. This is coeval with the barrier development on the seaward side of North Lake with estuarine conditions developing in False Bay. This barrier acted to prevent the St Lucia Estuary from further marine influences. This created a transition of a shallow area to deepening area, estuarine to lagoon respectively with a reduction in energy change occurring from the creation of the deep back–barrier lagoon with predominantly tidal influence. This tidal influence is observed in the tidal ravinement surfaces. This controlled the sedimentation in the North Lake, similar to the coeval sedimentation in False Bay, also indicative of a mixed wave–and–tide dominated estuary.

The high dunes located along the eastern coast of South Africa act as source of groundwater which may have an impactful influence on lake systems. Groundwater discharge simulations conducted by Taylor et al. (2006) shows that the groundwater is stored during coastal rainfall periods and the discharge rates are high during moist periods. The discharge contained within the coastal dunes are sufficient to sustain a flow during periods of drought for up to 13 years (Taylor et al., 2006).

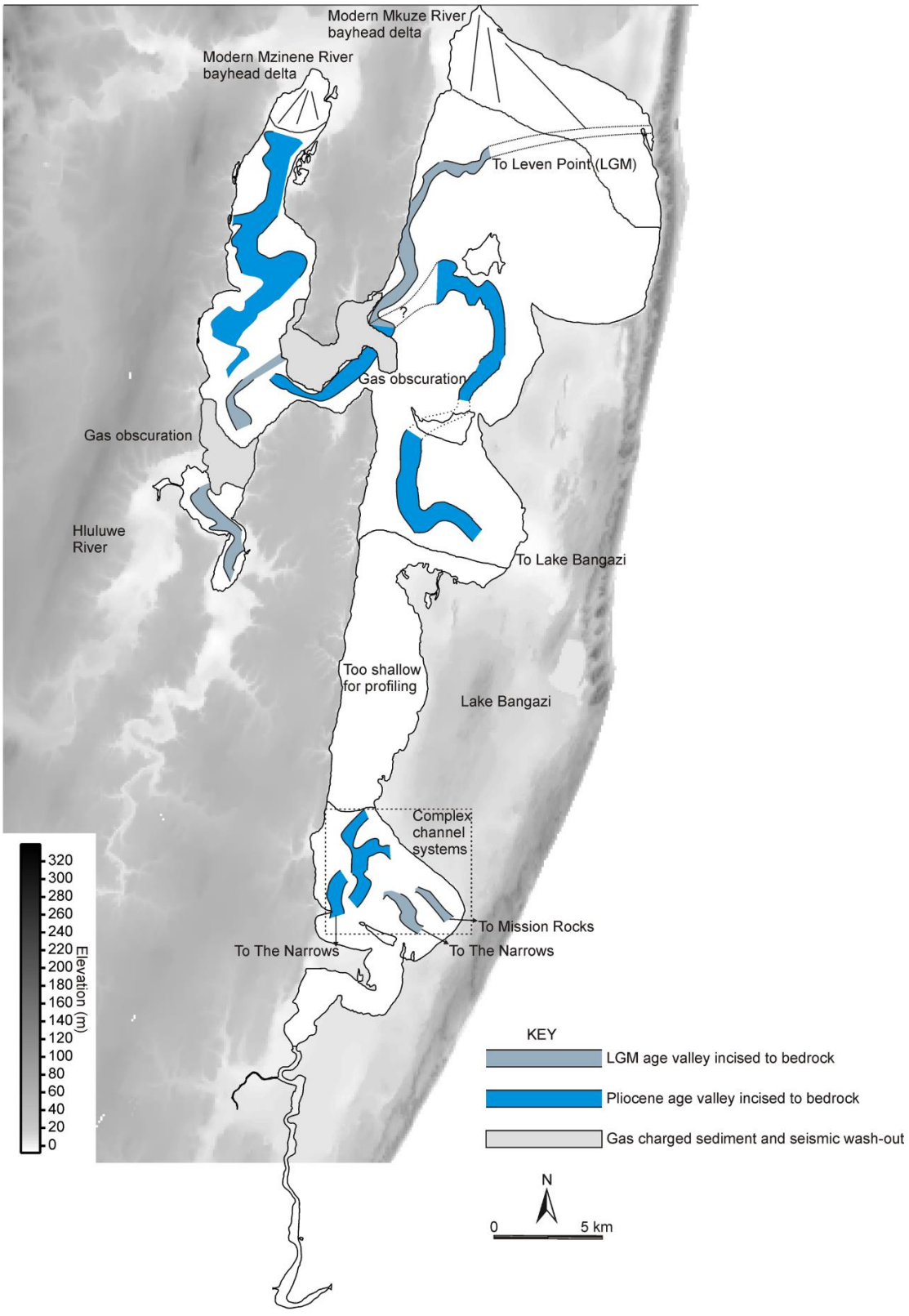

Figure 3.2. Annotated image of Lake St Lucia depicting the location of the bayhead deltas as well as several palaeo–channels (black lines) from Benallack et al. (2016).

3.2.2. Lake Sibaya

Lake Sibaya has a small catchment of 536 km^2, fed by groundwater flow and small streams (Pitman and Hutchison, 1975). The water level of the lake is situated approximately 21 m above mean sea level (Gumsley et al.) (Wright et al., 2000). The lake water level fluctuates depending on the amount of groundwater discharge and loss of water through the coastal dunes including evaporation (Miller, 1994, Miller, 1998).

Seismic evidence collected from Lake Sibaya shows Palaeogene sediments deposited on a gently dipping erosional surface during fluctuations in sea level that occurred during Tertiary period (Siesser and Dingle, 1981, Kruger and Meyer, 1988). Following this deposition phase, small scale faulting occurred during the early Miocene as a result of uplift (Partridge and Maud, 1987). The regressive phase occurring during the late Miocene to Pliocene period, featured the deposition of the Uloa Formation littoral sediments (Liu, 1995) and the aeolian sediments of the Umkwelane Formation (Maud and Orr, 1975). These aeolian sediments built the first phase of the dune cordon during the stillstands related to this regression (Wright, 1999). These sediments were extensively eroded during the Plio/Pleistocene regression (Wright et al., 2000). During the early to mid–Pleistocene, subaerial weathering of the Plio/Pleistocene dune ridges occurred to form the "Berea type" red sand (Botha, 1997). During this same time, a renewed transgression occurred, and the old Pliocene coastal dune barrier was breached and the Port Dunford Formation was deposited under oscillating sea level conditions (Hobday and Orme, 1974, Maud, 1993, Botha, 1997).

The transgressive event terminated at the Last Interglacial high stand with a surface elevated 4 – 5 m amsl (Wright, 1999, Wright et al., 2000, Cooper et al., 2012). The initial transgression resulted in the deposition of littoral sediments in a seaward thickening wedge above the Uloa and Umkwelane Formations (Wright et al., 2000). Land that previously gently dipped in an easterly direction, was levelled out through erosion occurring during a gradual regressive stage (Wright, 1999, Wright et al., 2000). Drop in sea level resulted in the incision of the proximal coastline where the topography was at an elevation of -10 m below sea level (Compton, 2011, Ludt and Rocha, 2015). Once the sea level stabilized, the second phase of the coastal barrier building began, creating lagoon conditions behind it. The lagoons were infilled with washover sediments from the coast and inland aeolian processes (Wright et al., 2000). Minor reworking of the Port Dunford

and Tertiary age sediments deposited into channels within the lagoon. According to Hobday and Orme (1974) there was no evidence of a second marine incursion inland.

The Port Dunford sediments deposited below the mid to late Pleistocene aeolian sediments with a conformable relationship between them. This sequence marked start of the Last Interglacial high stand by a regressive phase (Wright et al., 2000). This regressive period, between 117 000 to 22 000 BP, was marked by the development of palaeo-shorelines consisting of beachrocks and aeolianites (Ramsay, 1996, Ramsay and Cooper, 2002). The re-established coastal dune barrier (ca. 60 000 BP) (Wright et al., 2000, Cooper et al., 2018b) promoted the development of large coastal lake systems.

Following the onset of the LGM, the dune barrier system was breached as a result of the difference in the hydraulic head, between the coastal water and the sea level, draining the coastal wetland system (Smith et al., 2011, Liu et al., 2016). This erosive event, consequently formed the Northwest-Southeast orientated channel (Wright, 1999) which has depths up to -40 m below sea level proximal to the breach (Wright et al., 2000, Green, 2009a). At approximately ca. 7 000 BP, the sea level stabilised at a position similar to current sea level (Ramsay, 1996). Marine overwash deposits filled the inlet. Thereafter lagoon conditions were dominant until ca. 5000 BP (Miller, 1994, Miller, 1996). Thin veneers of gyttja (dark grey to black organic rich mud) are located in the deeper parts of the lake system which rose to 20 m amsl (Wright et al., 2000). Early lake segmentation, where the back barrier waterbody divided into smaller, isolated water bodies occurred (Miller, 1994), characterized in the Lake Sibaya system by prograding sand spits and cuspate forelands. The spits prograde as a result of high wind activity with a large amount of sediment sourced from aeolian dunes during high lake levels (Miller, 1994, Wright et al., 2000).

3.2.3. Kosi Lake system

The Kosi Lake system is a large lake system which comprises a series of interconnected lakes which increase in salinity as the lakes get closer to the inlet (Wright et al., 2000). This lake systems are the northernmost lake system in KZN situated ~5 km from the Mozambique border with a drainage system of 540 km^2 (Wright et al., 1997). This area receives most of its freshwater from the local drainage and the coastal characteristic high groundwater table (Meyer, 1997).

Lake Nhlange is the largest water body of this four–lake series (Figure 3.3.). Bathymetric data collected within the largest of the lakes, Lake Nhlange, shows a palaeo-valley with a deep scour within the stratigraphy extending ~35 m (Wright et al., 2000). Following a rise in sea level the palaeo–channel gradually closed with a decreasing gradient (Wright et al., 2000).

Figure 3.3. Annotated image of the Kosi Lake system. Contemporary inlet to the Kosi Lake system in the north.

This blockage resulted in the formation of a lagoon environment (Wright (1999). Following the sea-level rise of the LGM, the partial infilling of these palaeo-valleys are comprised of homogenous central basin deposits (Dladla et al., 2022). Dladla et al. (2022)

took note of active wind currents driving the development of spits within the system, promoting the early stages of lake segmentation. Kosi Lake and Lake Sibaya are some of the only lakes that preserve these palaeo–topographic features. Margin slumping, as a result of lake segmentation processes caused some infilling of Lake Nhlange during the LGM (Wright, 1999). Four main palaeochannels were located within the lake leading out to a palaeo–inlet at Bhanga Nek (Wright et al., 2000). These channels may have drained the hinterland via the northernmost channel (deepest channel) approximately 16 000 BP to 18 000 BP. An erosional surface demarcating a transgressive-regressive surface, formed approximately 4 500 BP when sea level was 3.5 m above present (Ramsay, 1996). The lake has since had very little sedimentation added during the Late Holocene, with system modification the result of margin progradation and the settling of fine organic detritus within the lake basin (Cooper et al., 2012).

Sand would have been transported into the system via the dynamic barrier system, initially as flood tidal deltas, then washover fans and finally as parabolic dunes burying the previous features in the area such as the underlying spits (Dladla et al., 2022). A combination of a large tidal prism and spit accretion followed by sea level fall after the Holocene maximum at 5 000 BP further segmented the system (Dladla et al., 2022). Rapid barrier accretion during the late Holocene resulted in the Bhanga Nek inlet being permanently closed around 3 160 and 2 900 cal. BP (Cooper et al., 2012, Dladla et al., 2022). This resulted in the mouth moving Northwards near where the present-day Kosi mouth formed 1 500 BP, during the 1.5 m last Holocene high (Cooper et al., 2012). During the relative sea level stability and an increase in arid conditions at ~2 900 BP resulted in further development of marginal spits (Dladla et al., 2022). Wright et al. (2000) used aerial photography to determine a palaeo-inlet closed by dune formation, located North of the present inlet indicating a Holocene dune barrier palaeo–environment. Coral *Favites* located within the rock sequence dated to 1 610 ± 70 BP indicating that the barrier was breached at this time (Wright et al., 2000). This breach was noted by Cooper et al. (2012) during ~1 500 BP, with a small peak in sea level following a long period of back barrier flooding.

The Kosi system acts as a template for the effects of segmentation and the development of segmented lagoon systems over time. Segmentation within the Kosi Lake system occurred as result of wind-blown cuspate spits growing and merging into a large barrier which divided the system into the current known lakes (Wright et al., 2000). Fluctuations

in sea level during the Holocene may have contributed to the development of these cuspate spits by elevating part of the spit which were below lake level (Cooper, 1994, Cooper et al., 2012).

3.3. Relative sea-level changes

The East African coast is located in an area which is tectonically stable (Camoin et al., 1997). Changes in relative sea level (RSL) during the late Pleistocene/Holocene are however poorly constrained (Camoin et al., 2004), despite being an attractive area in which to reconstruct a global sea level curve (Cooper et al., 2018). The local changes in RSL are inferred from global eustatic sea-level changes or from areas near the study area (Ramsay and Cooper, 2002; Cooper et al., 2018).

3.3.1. Pleistocene

Ramsay and Cooper (2002) compiled a comprehensive paper outlining the sea level changes during the Late Pleistocene/Holocene period. Sea level during the early Pleistocene (1 – 1.5 × 106 yr B.P.) was postulated to be at 6 – 8 m amsl as indicated by fossil evidence collected by Hendey and Volman (1986). Hendey and Volman (1986) also placed the peak sea level at 4 m amsl between 98 000 and 110 000 yr B.P. However, data collect from Sodwana Bay indicate a sea level of -44 m below sea level showing the development of a shoreline prior to the dates previously stated (Ramsay and Cooper, 2002). Two sets of shorelines separated by an unconformity are noted by Maud (1968), Hobday (1976) situated at 4 m amsl in KwaZulu-Natal. This shows a cyclical event in which the sea level during the initial highstand was at 4 m amsl depositing the first shoreline sequence, then dropped to -44 m below sea level creating this unconformity followed by a rise in sea level (second highstand) depositing the second shoreline sequence. These highstand sequences mark the last interglacial period (Ramsay and Cooper, 2002).

Ramsay and Cooper (2002) showed a stabilisation in sea level between 55 000 – 40 000 yr B.P., with sea level situated between -40 to -60 m below sea level. This sea level coincides with evidence of a major submerged shoreline offshore the study area observed by Ramsay (1994). At the end of this period (~40 000 yr B.P.) an extreme fluctuation (rapid rise and fall in sea level) in sea level was noted within the wetland peat of Durban

Bay, with a possible connection to the interstadial record of the Huon Peninsula (Chappell and Veeh, 1978). The penultimate Glacial Maximum marked the lowest sea level of time during the mid–Pleistocene period (Green and Uken, 2005). The Huon Peninsula recorded the depth of the penultimate Glacial Maximum, to be between -130 m and -145 m at 135 000 BP (Green and Uken, 2005). The LGM (112 000 ± 23 000) marks the change between the Late Pleistocene – Holocene period with a significant drop in sea level between -125 m and -130 m (Green and Uken, 2005).

3.3.2. Holocene

Most representative of this epoch is the notable 120 m rise in sea level from the LGM, the result of the solar radiative forcing along with the melting of ice sheets (Bard et al., 1996, Törnqvist and Hijma, 2012). The grey blocks in Figure 3.4 shows important sea level states, especially rapid jumps in sea level called melt water pulses (MWP's). MWP's can be described as a period of rapid melting, due to catastrophic ice sheet collapse, added to a continuous and steady sea–level rise (Bard et al., 1996).

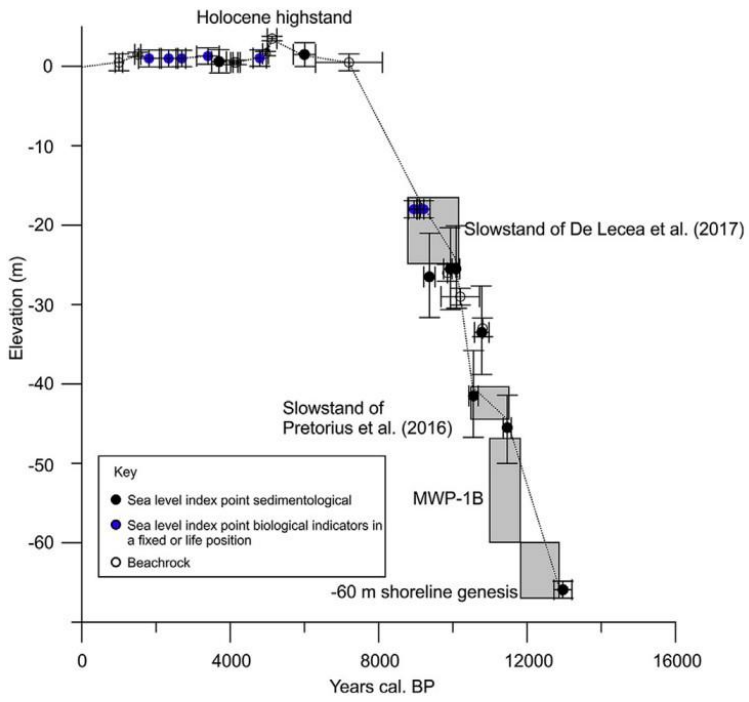

Figure 3.4. Sea level curve for the SE African coast from 13000 BP to present day. Grey blocks denote major sea level events identified along the East coast of southern Africa (Cooper et al., 2018a).

The Holocene epoch ranges from ~11 650 BP till present according to the International Commission on Stratigraphy (ICS). This period represents a time of environmental change when the temperature rose following the last glaciation. The early Holocene epoch ranges between 11 650 BP and 7 000 BP and is marked by a rapid rise in sea level, an effect of deglaciation (Zong, 2004). This caused a relative sea-level rise in low latitudes which resulted in sea level highstands (Sloss et al., 2007). On the east coast of South Africa, sea level rose from approximately -13 m to a maximum of 3.8 m (the Holocene highstand), over a short period (7.6 and 5.8 ka yr BP) (Cooper et al., 2018a). Sea level then dropped to 1 m between 5.3 to 4.2 ka yr BP with sea level at 0 m at 2 ka yr BP (Figure 3.5.) (Cooper et al., 2018a). Sea level data from Bazaruto in Mozambique (MZ) (Figure 1.1.) show sea level to have reached its present level at 7.2 ± 0.9 ka BP, and again at 1.0 ± 0.1 ka BP (Armitage et al., 2006).

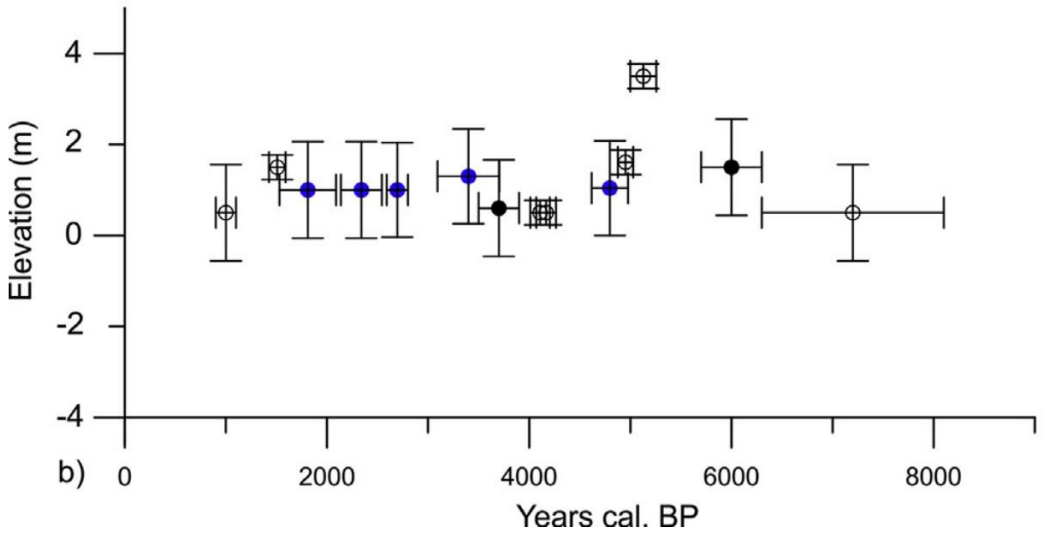

*Figure 3.5. Holocene sea level curve from the South African east coast (*Cooper et al. (2018a)).

Chapter 4

Methods

A variety of remote sensing, geophysical and sedimentological tools were used to gather data on the lake and its surroundings. These encompassed satellite and aerial imagery, ground penetrating radar, ultra-high resolution seismic reflection profiling and piston coring.

4.1. Shuttle Radar Topography Mission, remote aerial imagery and LiDAR dataset

The general coastal plain geomorphology and lake configuration was examined using a combination of LiDAR, Shuttle Radar Topography Mission (SRTM) and high-resolution aerial photographic data. The SRTM data were used to produce a regional elevation grid of the study area; the digital terrain model generated had a resolution of 30 x 30 m and was used to outline the broad geomorphic features of the area. This was supplemented by LiDAR data collected from a 2016 survey of the Greater St Lucia Wetland Park. These included the area immediately surrounding Lake Bangazi North. The terrestrial LiDAR was acquired from a fixed wing aircraft flying at an elevation of ~1 050 m. A vertical accuracy of ~10 cm in the z domain was achieved, with a mean density of 1.5 strikes per meter. The digital terrain model generated has a horizontal resolution of ~ 0.5 x 0.5 m and covers an along coast length of ~ 47 km, with a width of 5 km and an area of ~257 km^2. High resolution aerial orthophotographs were collected simultaneously with the LiDAR. These data have a horizontal resolution of ~ 20 cm.

4.2. Ground penetrating radar

Two ground penetrating radar systems were used to collect data on the sub-surface stratigraphy of the lake margins. A regional set of lines were collected using a 40 MHz GPR along the various roads and paths that surround Lake Bangazi North (Figure 1.1.b). These spanned ~ 17–line km. Along the lake edges, a second set of higher resolution, 200 MHz data were collected in order to assess the palaeo-drainage entryways and the stratigraphy of emergent sediment bodies. The GSSI radar antennae were coupled to an RTK–DGPS system, however the vertical component of the system proved unreliable in post-processing and topographic corrections could not be made on the data post survey. The radar stratigraphy was analysed using the principles described by Neal (2004).

The raw geophysical data was processed using Radan7. A variety of processes including distance normalization, horizontal scaling, noise band removal and time-varied gains were applied to all sets of data. Finite Impulse Response (Smith et al., 2011) Filter and Infinite Impulse Response (IIR) Filter was applied to all datasets with different values corresponding to the data collected with the different equipment. FIR filtered values for the 40 MHz GPR ranged from 10 – 110 MHz and for the 200 MHz GPR ranged from 50 – 400 MHz. IIR filtered values for the data were a constant 4.

4.3. Seismic reflection profiling

Three seismic reflection profiling techniques were applied in the study area. A towed 200 MHz GPR was initially used as a proxy for seismic reflection, however, the data returned were chaotic, likely the result of solutes in the water column.

Approximately 13–line kilometres of seismic reflection data were then collected using an Applied Acoustics AA301 boomer and an 18 element, single–channel hydrophone. A trigger rate of 500 ms and a sweep of 100 ms were used, and the data recorded in Hypack. The data had a central frequency of 800 Hz, with a vertical resolution of ~ 50 cm. Bottom tracking, bandpass filtering and AGC were applied to all data. A regional image of the underlying stratigraphy could not be achieved due to gas blanking in the system.

The final geophysical survey that was conducted used a SILAS, ultra-high resolution acquisition system coupled to a dual frequency (24 to 400 KHz) transducer. These data were collected with a trigger of 200 ms and a sweep rate of 50 ms. The lower frequency spectrum was recorded in SILAS and merged in post-processing with the navigation provided by a DGPS of ~10 cm accuracy. The data were then band pass filtered and bottom tracked using the SILAS processing software, where a basic deconvolution was further applied to limit source ringing in the record. A total of 12–line kilometres of data were collected.

4.4. Bathymetry and Side scan sonar

The lake bathymetry and seabed character were examined using a Garmin echoMAP Chirp 72SV echosounder. Over 25–line kilometres of data were collected. Portions of the lake floor were examined using the system’s Downvuu side scan sonar application. These

were specifically targeted for areas of dense hippo gatherings so that their influence on the lakebed could be examined in detail. Both the bathymetry and side scan sonar data were processed using Sonar TRX. Where the seabed material was particularly fine, the low frequency output of the echosounder provided some penetration and echotraces were captured for further sub-bottom inspection. The bathymetry data were cleaned for spurious readings line by line, and then merged with the navigation inputs and exported as a series of text files. These were gridded to produce a 25 x 25 m bathymetric grid. Side scan sonar data were processed using the autoprocess and bottom track function. A uniform TVG was applied to balance the two channel contrasts and the nadir was removed during mosaic stitching. The final images resolve to ~10 cm in the horizontal.

4.5. Bio-engineering

Aerial photographs with a resolution of 0.5 m x 0.5 m were collected simultaneously with the LiDAR data. A georeferenced orthomosaic was produced of the lake margins and the various hippo paths evident were digitised. The digitised pathways were then compiled to produce a heat analysis of pathway density around the lake margins using ArcGIS.

4.6. Piston Corer

A metal barge was placed on four long tubes and taken out to the deepest portion of the lake using a small engine powered boat. A continuous core of soft lake sediment, 7 m long, was collected from the lake using a hand-driven piston corer. This core was logged and analysed for chemical content.

Chapter 5

Results

5.1. Regional geomorphology

The Mkhuze River extends seaward from the Lebombo mountains and emerges into a broad and flat coastal plain (average 0.07°) where it makes a sharp 90° bend to the south and enters the North Lake Basin of Lake St Lucia (Figure 1.1.). Where the river is deflected to the south, a series of coast-perpendicular elongated mounds, up to 5 m in vertical relief and between 750 m to 1 570 m long are found (Figure 5.1.) These occur at ~18 m above mean sea level. Where they terminate to seaward, the adjacent topography is marked by a flatter and lower-lying depression ~10 m above mean sea level. This is fringed to seaward by an elevated and topographically complex high at +30 m. Lake Bangazi North occurs seaward of this high and occurs directly adjacent to the 90° bend in course of the Mkhuze River.

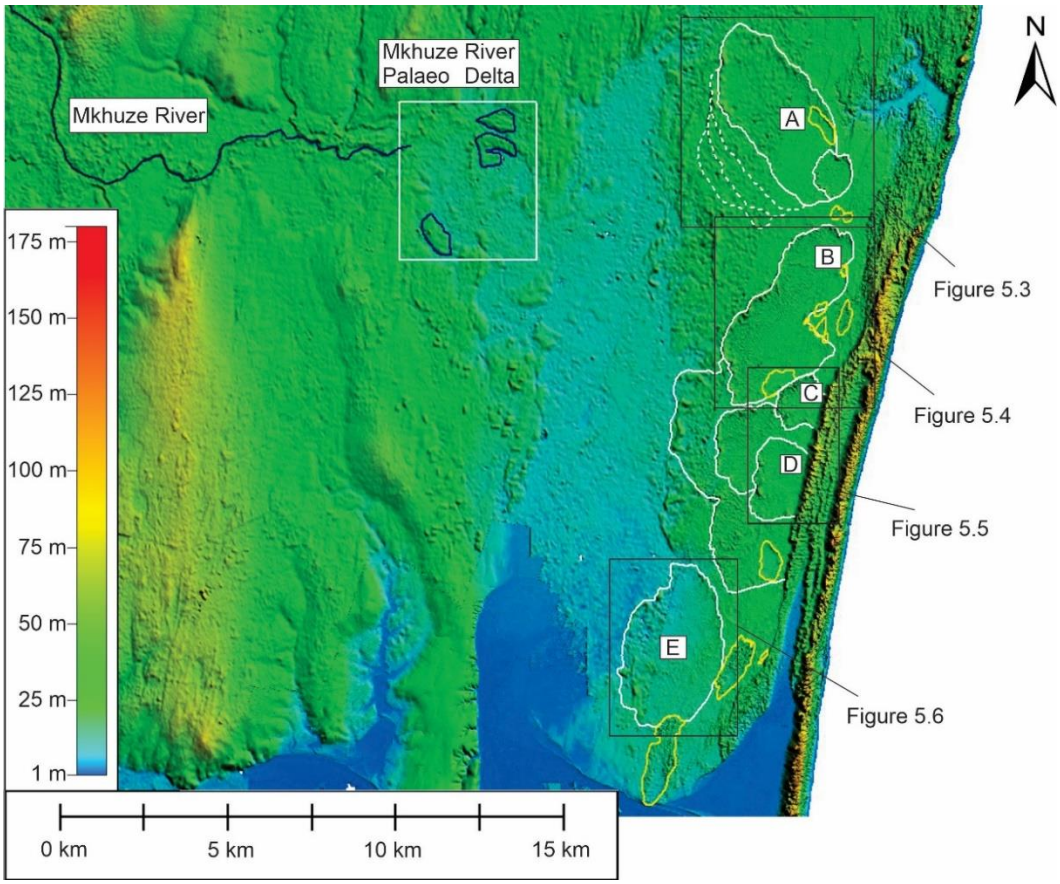

Figure 5.1. Annotated image of geomorphological bodies south of LBN. Black line represents the Mkhuze river which flows from West to East with the coast perpendicular elongated bodies highlighted by the white box. The white line represents the shallow geomorphological depressions whilst the yellow line represents blowout features.

The tall, vegetated barrier frames the coastline (Figure 5.2.) with a maximum elevation of ~115 m and widths that vary from 80 – 150 m. Several low points are evident in the barrier. These are between ~30 m and +40 m amsl (Figure 5.2.).

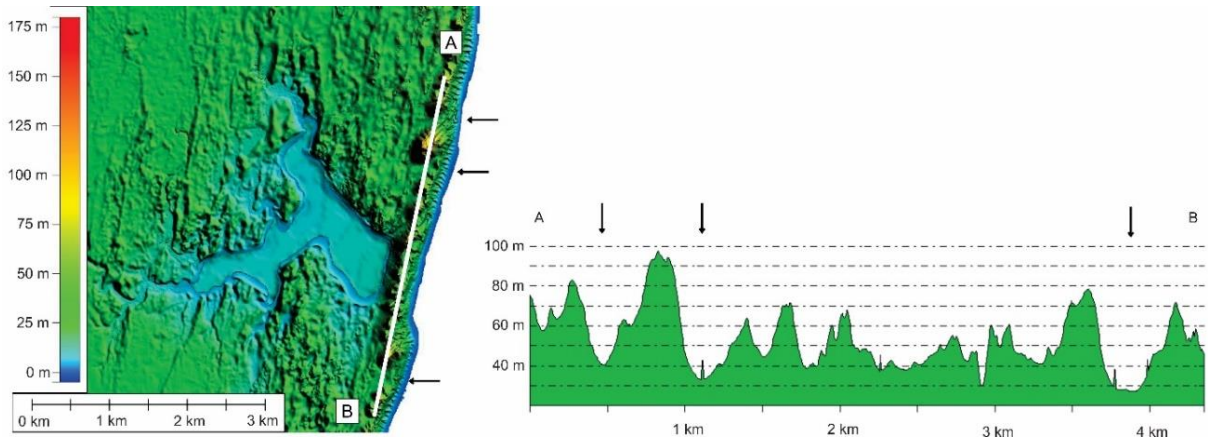

Figure 5.2. Annotated image of the low points in the dune barrier along the East coast of KZN. White line = line of cross section. Black arrows = low points in the barrier.

Several shallow depressions occupy the elevated high point behind the barrier in the stretch of land south and immediately landward of Lake Bangazi North. These form semi-circular to oval shaped landforms (Geomorphological bodies A–E) (Figure 5.1.). Geomorphological body A (Figure 5.3.) comprises an oval-shaped depression with an elevation of +20 m, elongated coast parallel. It is approximately 7 km long and 3 km wide and hosts several raised ridge-like features that vary in relief from ~2 m to ~5 m in the western portion of the geomorphological body with 100 m spacing between these prograding ridge-like features. Further seaward these sedimentary features sharply decrease in height and spacing at ~25 m amsl. These vary in spacing from ~40 m to ~100 m, with reliefs from ~0.5 to ~5 m.

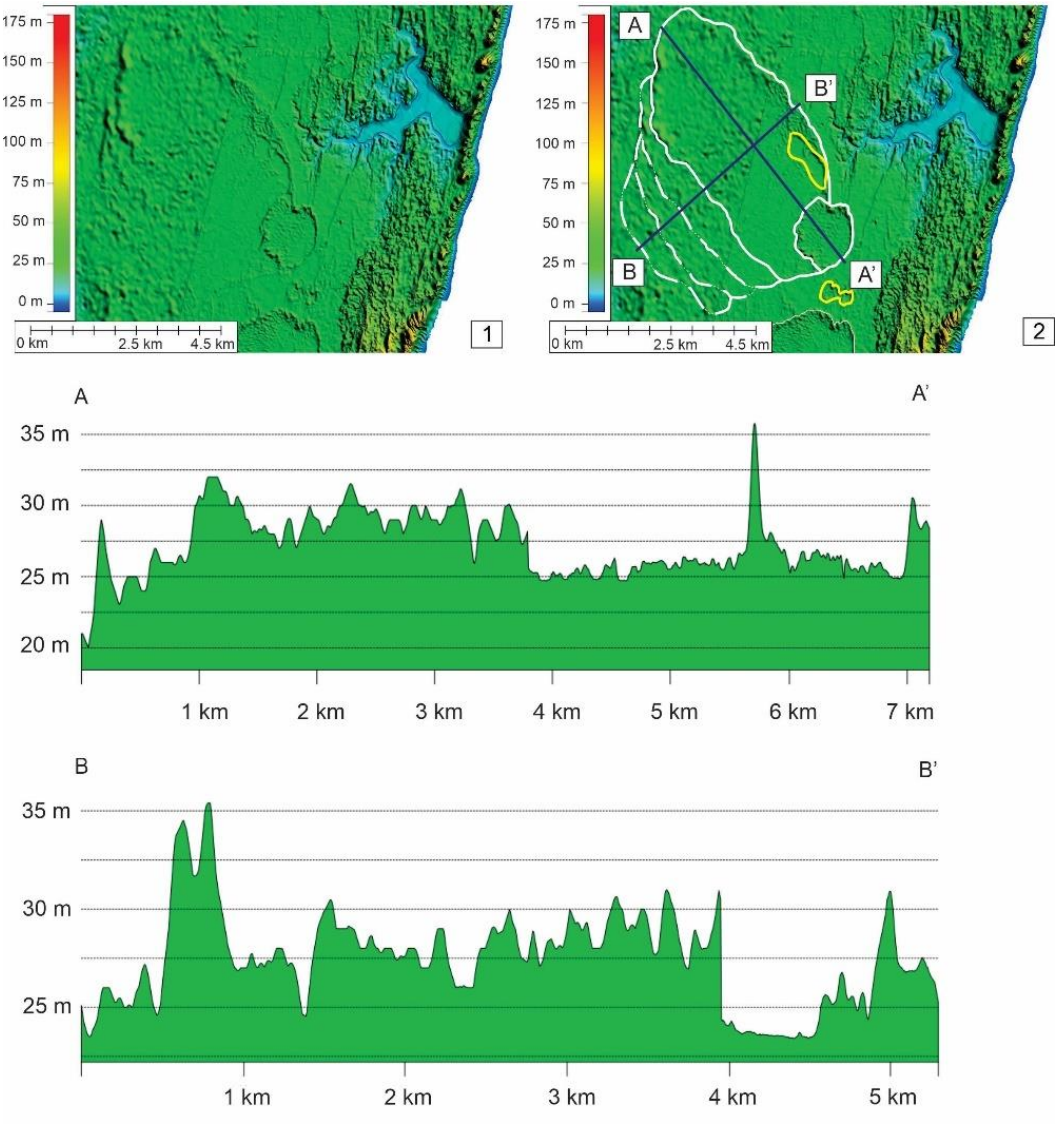

Figure 5.3. 1- LiDAR image of geomorphological body A, 2- Annotated image of geomorphological body A, cross sections of lines A-A' and B-B'.

Figure 5.4 reveals the largest of these features, Geomorphological body B. This comprises a kidney-shaped sedimentary depression with a raised outer rim 10 to 20 m higher than the features contained within the landform (16.38 km^2). The floor of the depression occurs at ~ +20 m elevation and consists of aeolian dunes spaced on average ~70 m, with reliefs between 1 and 2 m. This feature is similarly aligned coast-parallel, with a long axis of 7.25 km and a width of 3.43 km. Occasional cuspate high points protrude from the seaward margin into the depression, partially segmenting the depression into smaller sub-basins. Along the southernmost margin, a small, aeolian-bedform free depression is

evident. This is ~1 km long and 600 m wide, with multiple cuspate edges. The depression is aligned ENE-WNW and fringed by a 2 m–high ridge with several cuspate intrusions.

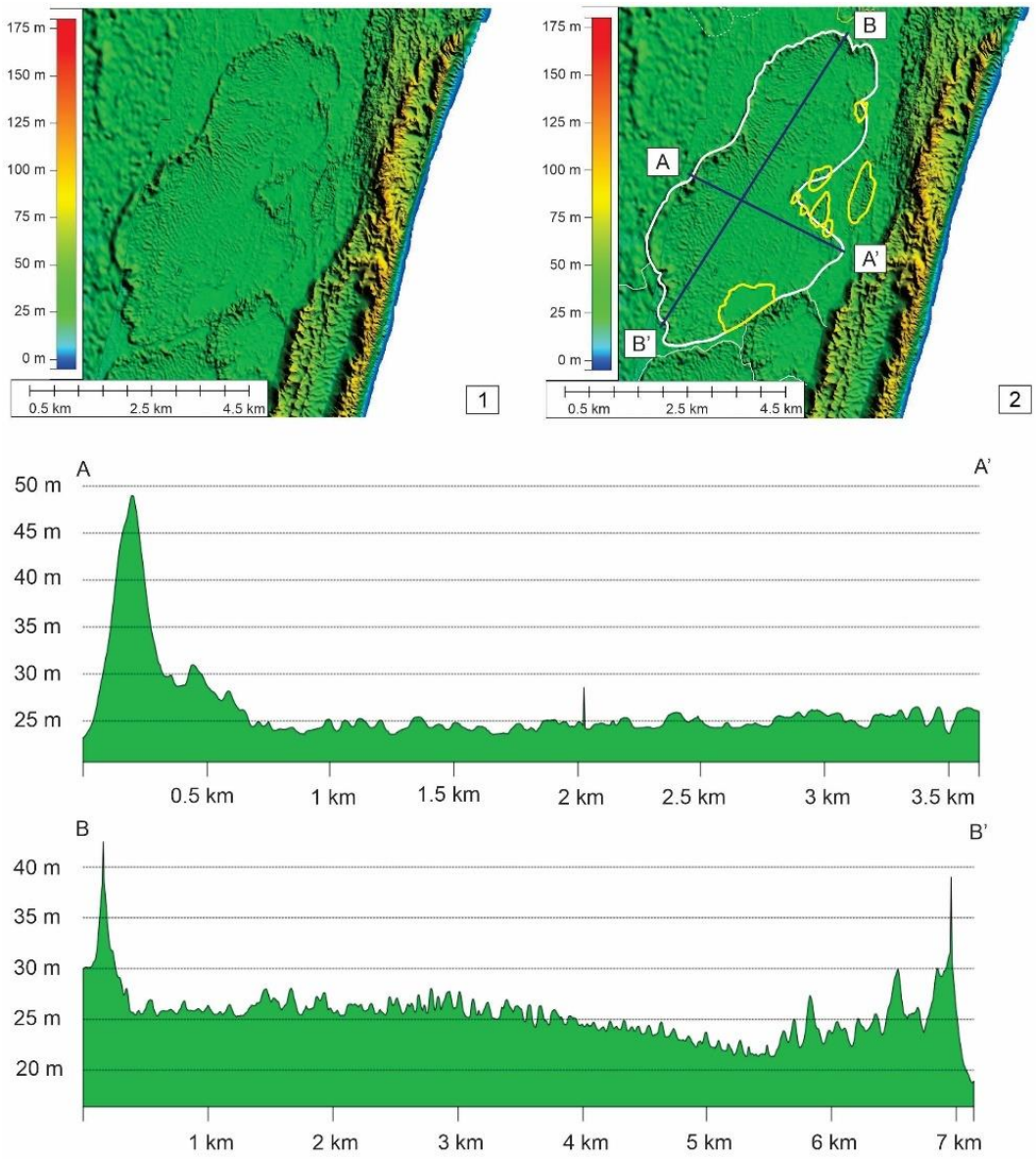

Figure 5.4. 1- LiDAR image of geomorphological body B, 2- Annotated image of geomorphological body B, cross sections of lines A–A' and B–B'.

Geomorphological bodies C and D (Figure 5.5.) comprise fan-like aprons that abut the barrier to seaward. Each has a narrow passage proximal to the shore, and fan to landward, terminating in a 10 – 12 m high semi-circular ridge. These features sit at approximately +22 m and appear to overlie a 130 m wide and 2 m-deep depression that separate the outer

rims of sedimentary body B from an adjoining depression. These fan–like features are in turn buried by the landward edge of the adjoining barrier.

Geomorphological body E (Figure 5.6.) is a shallow depression with an irregular circular shape that spans 5.95 km by 3.59 km. This feature sits at an elevation of ~20 m. The raised rim has a relief of 4 – 20 m on the landward side and the seaward rim with a lower relief of <1 – 3 m. The surface within the depression gently undulates (A–A' cross section) with less well developed aeolian dunes covering it (Figure 5.6. 2).

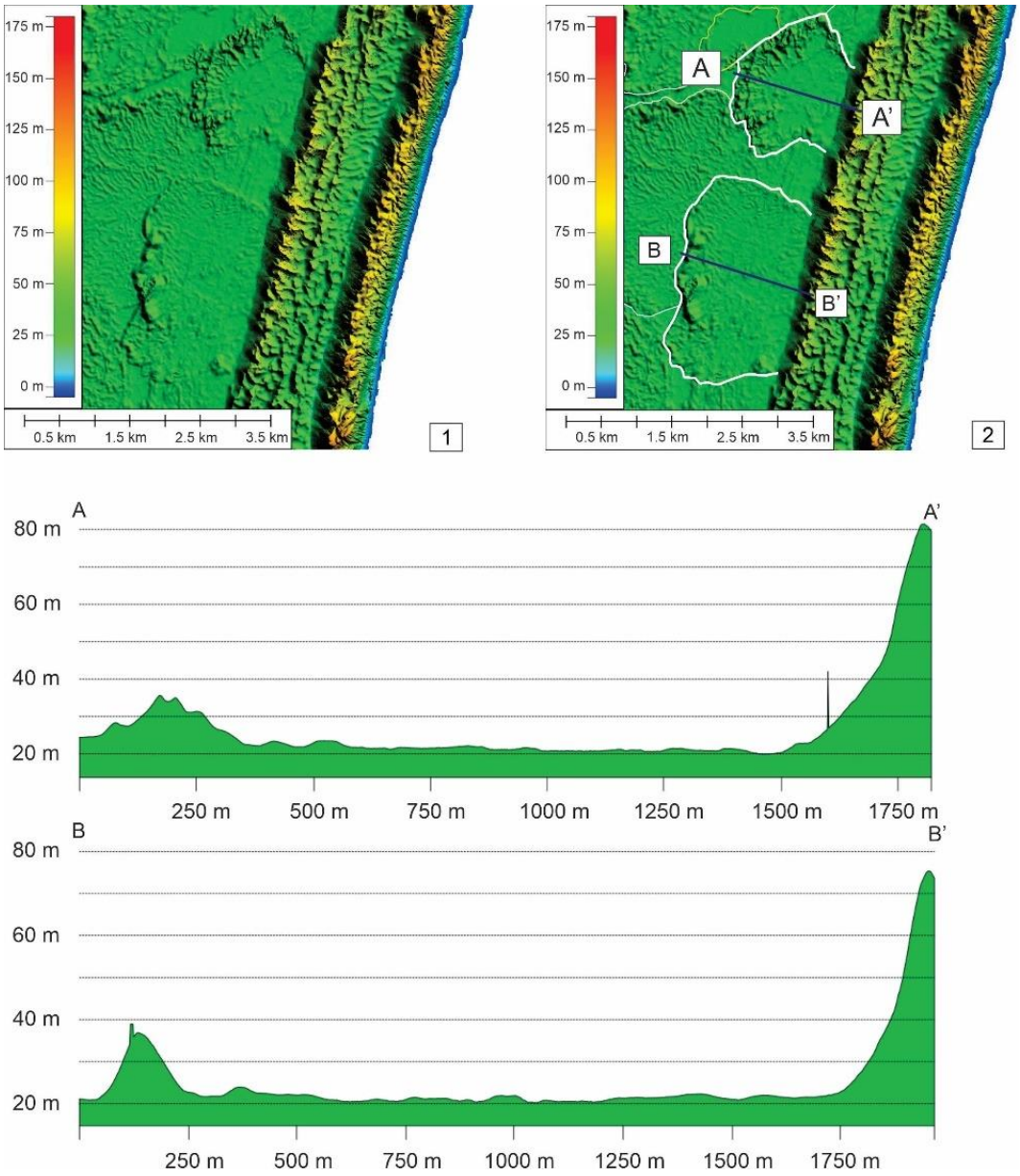

Figure 5.5. 1- LiDAR image of geomorphological body C and D, 2- Annotated image of geomorphological body C and D, cross sections of lines A–A' and B–B'.

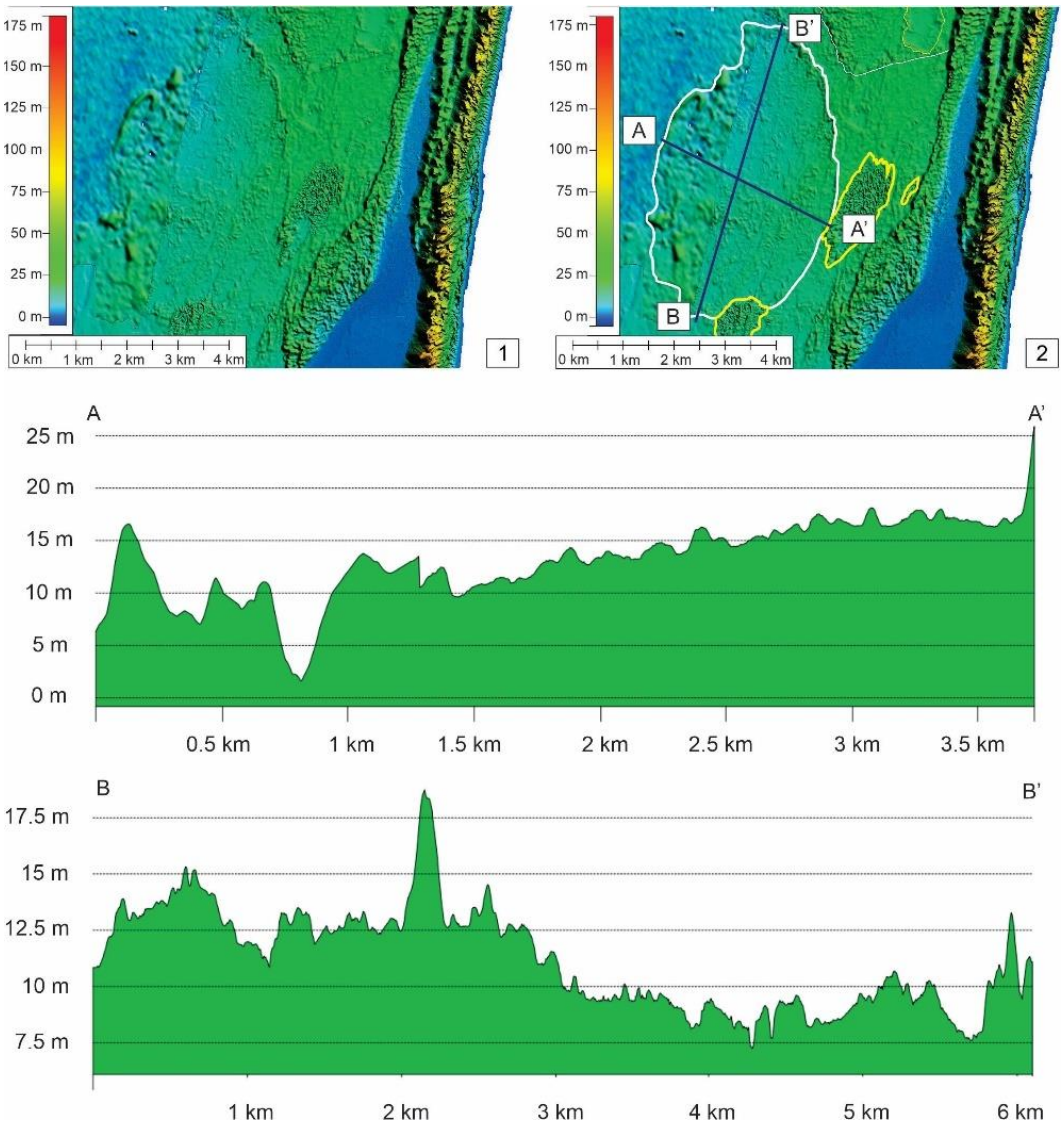

Figure 5.6. 1- LiDAR image of geomorphological body E, 2- Annotated image of geomorphological body E, cross sections of lines A-A' and B-B'.

5.2. Bathymetry of Lake Bangazi North

Figure 5.7 outlines the lake bathymetry highlighting key features within the lake. The lake can be subdivided into a shallow western limb and a slightly deeper eastern limb that rests in the lee of the coastal dune complex. The lake is dominated by a southwest-northeast trending channel that bifurcates into two channels aligned parallel with the coast. The deepest portions of the lake are associated with these channels, where relative depths of up to 9 m (-2.5 MSL) are found in the northern channel bifurcation. A distinct bayhead delta is located in the western limb (Figure 5.7.), forming a lobate, seaward

sloping feature with a relief of ~1 m relative to the surrounding lake floor. In places, the lake floor shallows forming elongated mounds that trend parallel to the lake margins.

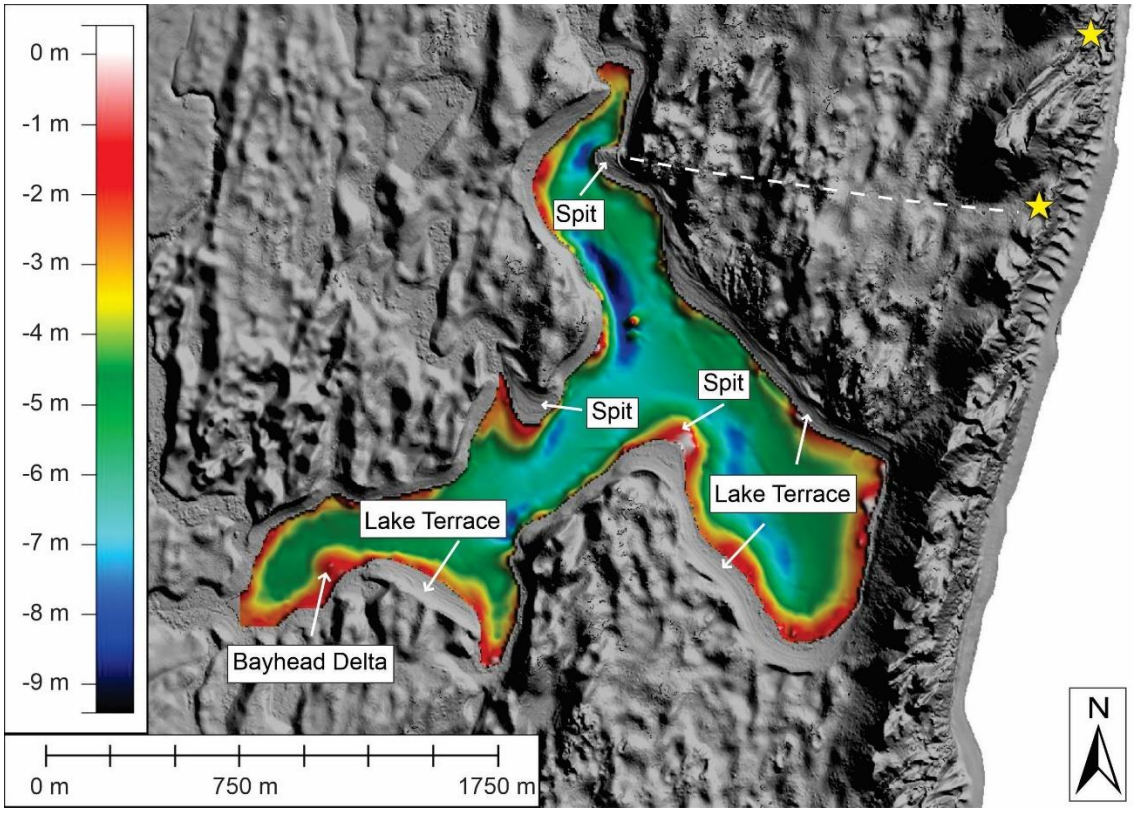

Figure 5.7. Lakebed bathymetry of Lake Bangazi North highlighting spits within the lake and the step-like terrace feature along the lake edge. The yellow stars highlight the low points along the dune barrier. The dash line shows a path linking the yellow star to the spit in the northern limb.

The lake basin shows partial segmentation with several spits orientated both parallel and perpendicular to the lake shorelines (Figure 5.7). The spits extend distances of 35 m to 190 m into the lake. A well-developed spit in the northern limb partially isolates a portion of the limb from the rest of the lake (Figure 5.7.), orientated 100° – 280°. The spit has the only orientation perpendicular to the contemporary coastline, aligned with a low point in the dune cordon, as shown by the yellow star and white, dash line in Figure 5.7. These spits have a gentle dip between 2 – 3˚, with reliefs between 3 – 5 m. The emergent surfaces of the spit have several parallel ridges arranged in a step-like feature leading towards the lake (Figure 5.7) and which are extended around the lake margins (Figure 5.8.).

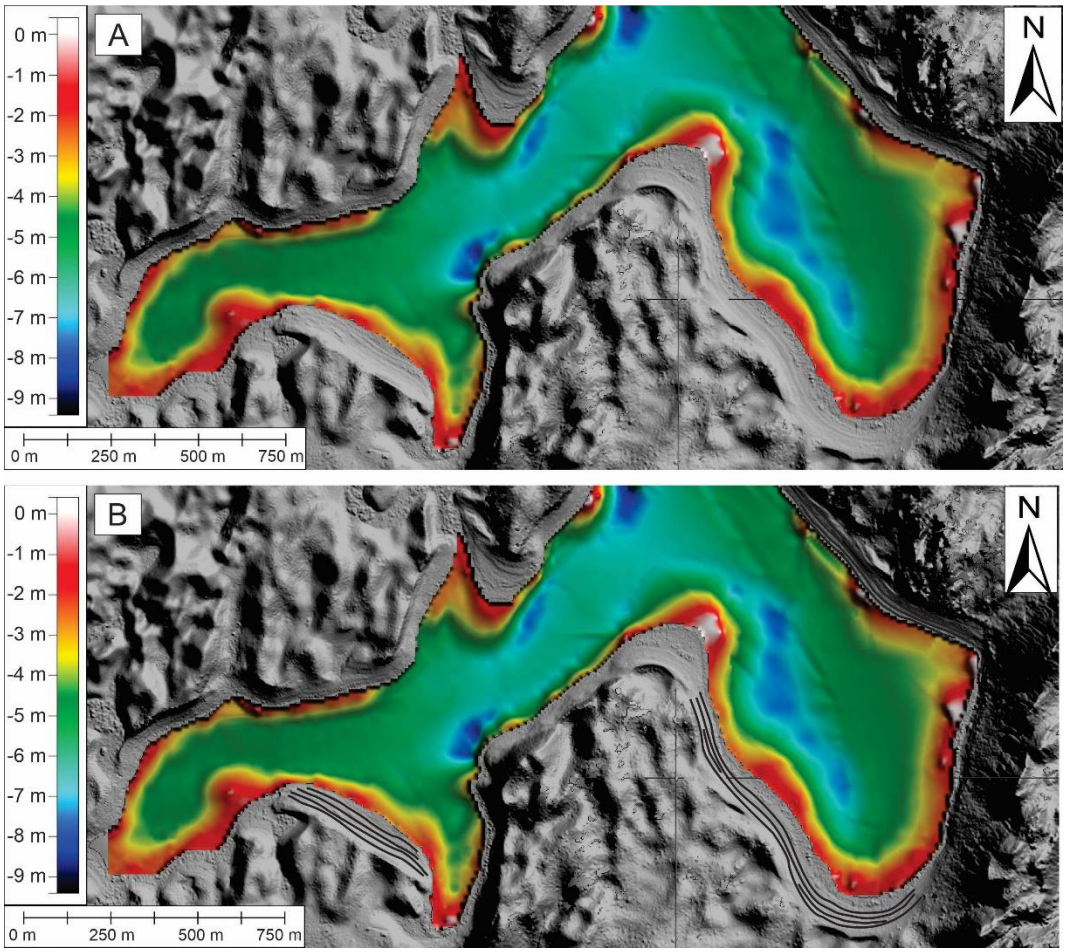

Figure 5.8. A – Mergend LiDAR and bathymetry data detailing the lake terraces concentrated in the bottom half of LBN. B – annotated image of the lake terraces along the lake edge (black lines).

The northern and eastern limb have a similar lakebed topography. The deepest section of the lake is in the northern limb with depths between 5 and 9 m (-2.5 MSL), forming the deepest channel feature (Figure 5.9.). The western limb is characterised by a steep drop at the lake edge, followed by a flat lakebed that is typical of the western basin (Figure 5.10.).

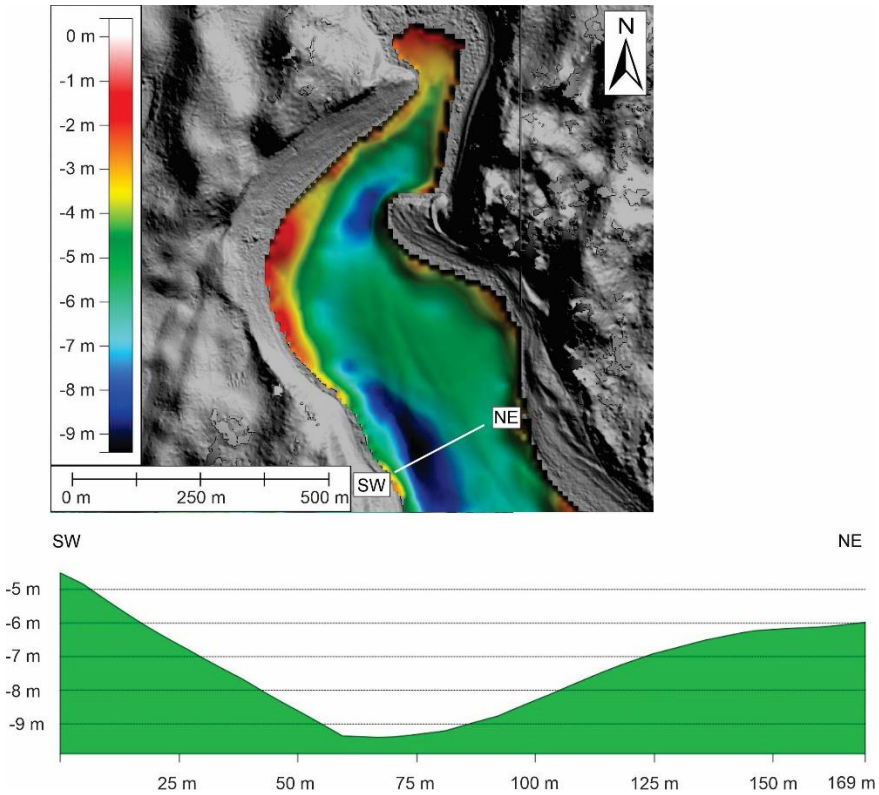

Figure 5.9. Bathymetric cross section of channel located in the northern limb of Lake Bangazi North.

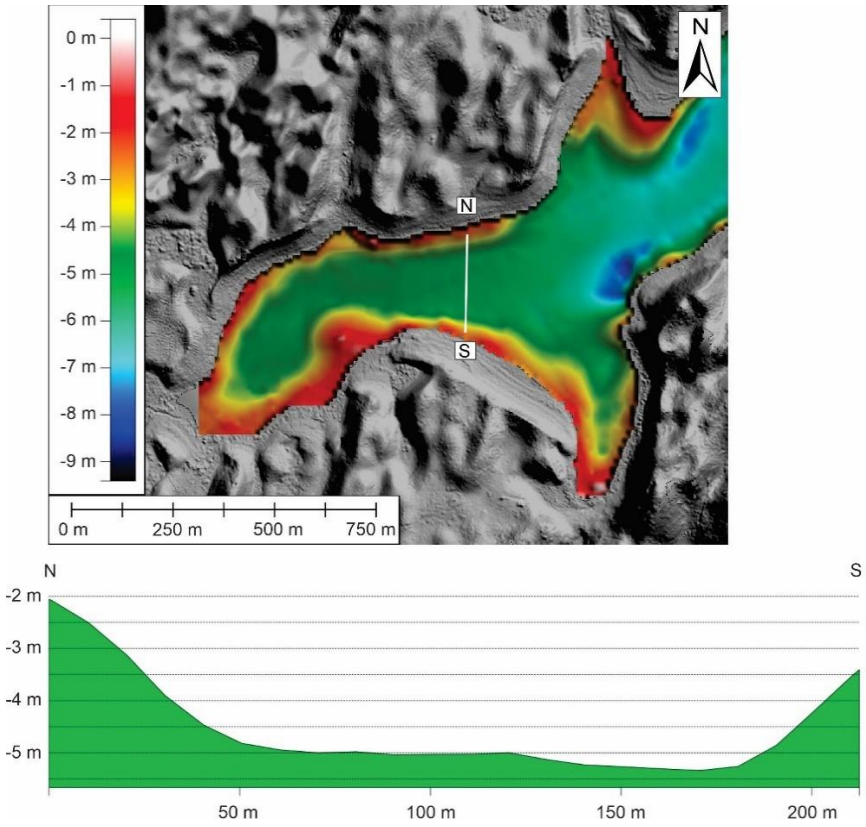

Figure 5.10. Bathymetric cross section of western limb of Lake Bangazi North.

5.3. Regional GPR Stratigraphy

Several incised valleys are identified throughout the data as highlighted in Figure 5.11. These incised valleys are located at a minimum depth of -5 m below ground level and reach a maximum depth of -13 – -20 m below ground level (+5 to +12 MSL). These valleys vary in width ranging from 20 – 250 m wide and incise older substrate, as represented by inclined reflections that dip to the south–west. The fill of the incised valleys are characterised by obliquely inclined reflections with overlapping concave reflectors that onlap valley walls. These are at times incised by secondary, smaller incisions with further tertiary–scale incisions in some areas. These multiple levels of incisions are most prevalent within geomorphological Body A (Figure 5.11.b). The incised valley network is truncated by an undulating reflector (that to some degree inherits the incised valleys beneath). This is overlain in turn by a flat–lying unit characterised by low amplitude reflections. Several sets of prograding reflections are located within this unit forming small-scale prograding bodies that fill the undulations in the basal reflector. These reflectors comprise two sets, characterised by the direction of dip. The first set dips in a south to south–westerly direction whilst the second set dips in a north to north–easterly direction. These packages are highlighted in Figure 5.11 by the red arrows. These often prograde from small, mounds that form high points in the post–valley stratigraphy. The stratigraphy is capped by mostly transparent, indistinct reflections in the radargrams (Figure 5.11.), in which modern blowouts have formed (yellow lines in Figure 5.1.).

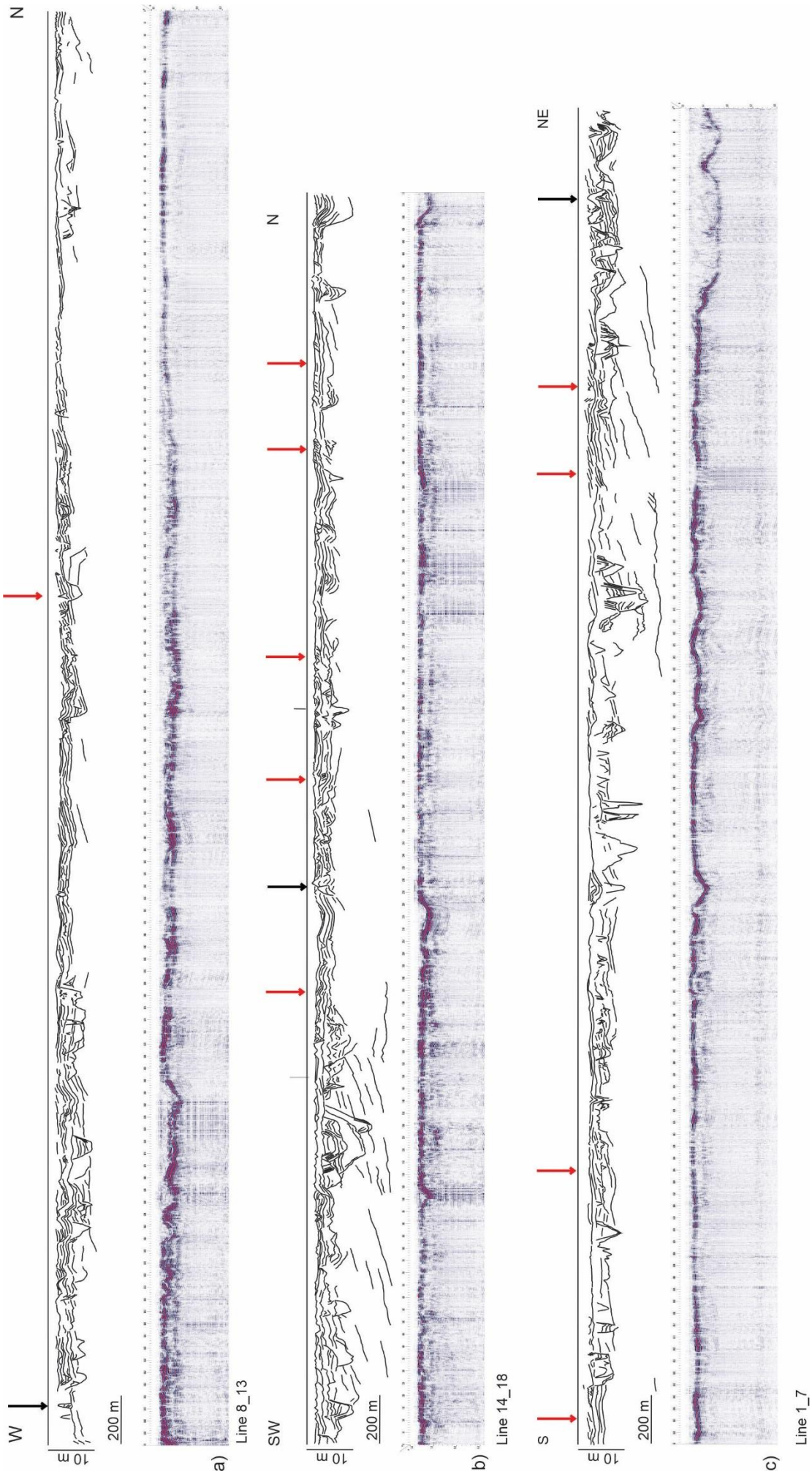
W
N
10 m
200 m
a)
Line 8_13
SW
N
10 m
200 m
b)
Line 14_18
S
NE
10 m
200 m
c)
Line 1_7

Figure 5.11. Interpreted and uninterpreted regional GPR profiles taken west of Lake Bangazi North as seen in Figure 1.1.B. a – GPR data taken from W – N with the raw data below and the interpreted data above. Profile a was taken along the eastern border of geomorphological body A. b – GPR data taken from SW – N with the raw data below and the interpreted data above. Profile b was taken within geomorphological body A. c – GPR data taken from S – NE with the raw data below and the interpreted data above. Red arrows point out small scale bodies of inclined reflectors. Black arrows pointing out small mounds in the subsurface.

5.4. Lake Sub-bottom Data

The stratigraphy comprises a lowermost basal reflector that is characterised by an irregular, moderate amplitude surface with several valleys evident. This surface intersects a non-descript, acoustically opaque basal-most acoustic basement. Overlying this surface are several key landforms. The submerged/emergent spit of the eastern lake limb (evident from the LiDAR and bathymetry) comprises a set of prograding reflections that downlap the basal reflector (Figure 5.12.a). These high amplitude, parallel reflections are interspersed by acoustically opaque materials, the sum of which forms a package 2 m thick, with the reflectors dipping in a northeasterly direction.

Sub-bottom data from the deepest portions of LBN show an underlying depression in the basal reflector that incises to -14 m below sea level (Figure 5.12.b). The filling material comprises non-descript, irregular and chaotic reflections with evidence of gas charging (brightened stratigraphy). The same channel can be seen in Figure 5.12.b., incising to below -13 m MSL, with similar seismic facies for the fill. Reflectors identified within the western limb of the lake show inclined sigmoidal prograding reflectors to the east. These overlie the basal reflector and prograde towards another channel incised to -12 m. These reflections characterise the internal structure of the bayhead delta. The stratigraphy, including channels and prograding bodies, is capped by an acoustically transparent/indistinct package that drapes the underlying stratigraphy and forms the modern lake floor (Figure 5.11. to Figure 5.13.).

The palaeo-channels observed within the regional GPR data (Figure 5.14.) were identified and their seaward continuity inferred. Figure 5.15 includes the main palaeo-channel locations of the coastal plain and within LBN, juxtaposed with seismic reflection profiles (Green, 2009a) from offshore the study area. It appears that the channel network observed in these two images, converges towards LBN, yet these do not appear to discharge towards the main palaeo-channel located seaward (~90 m below the surface) (Figure 5.15), nor associate with a barrier low point (see Figure 5.2.).

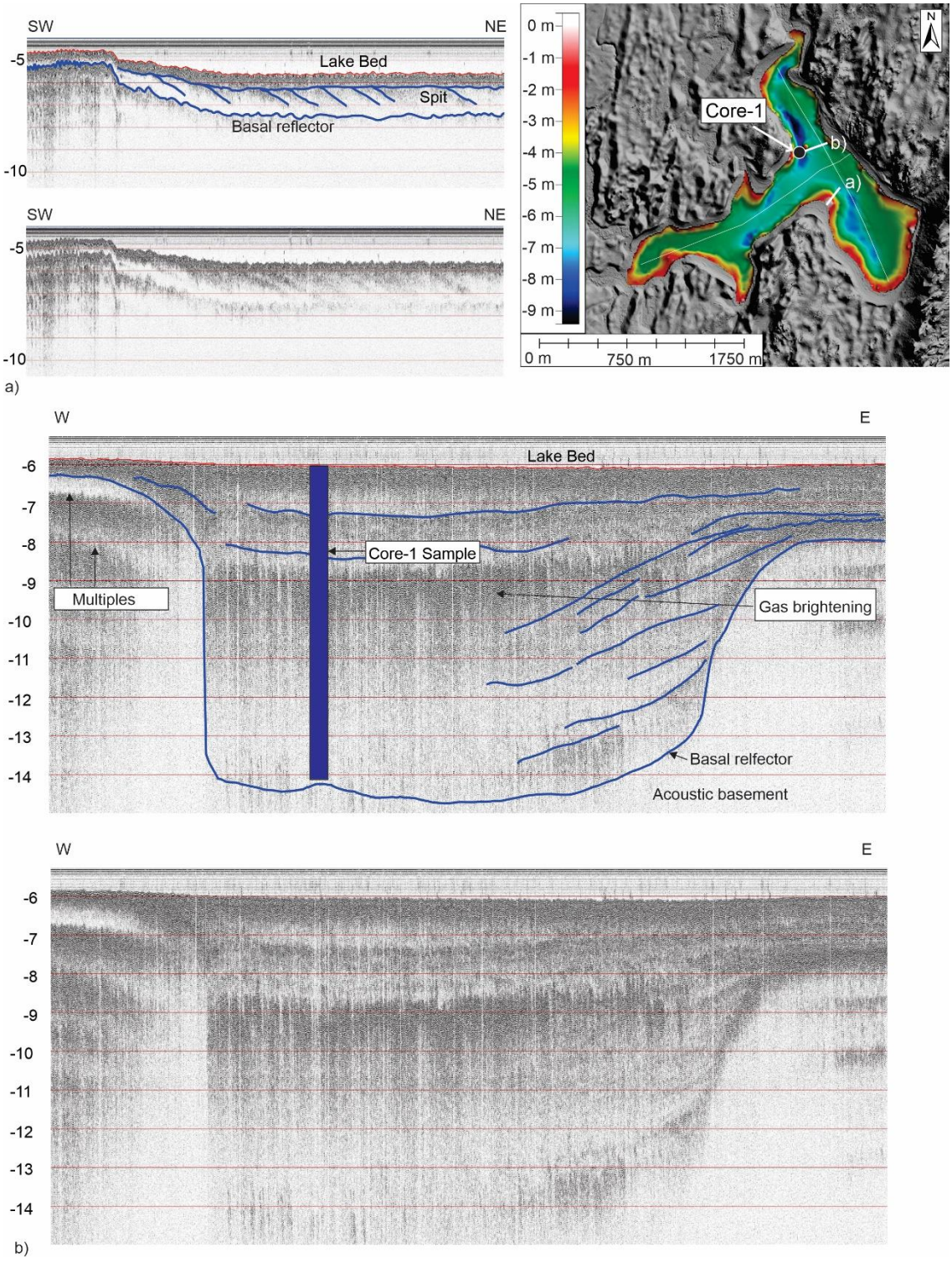

Figure 5.12. Interpreted and uninterpreted subbotom profiles. a – Profile continuing into the lake from a spit body, showing continuing prograding reflections, now covered by an acoustically opaque layer. b – Profile through the core sample point, showing the core sited in a channel dominated by draped reflections and gas brightening. The core terminates at the basal reflector. Inset show's location of specific lines.

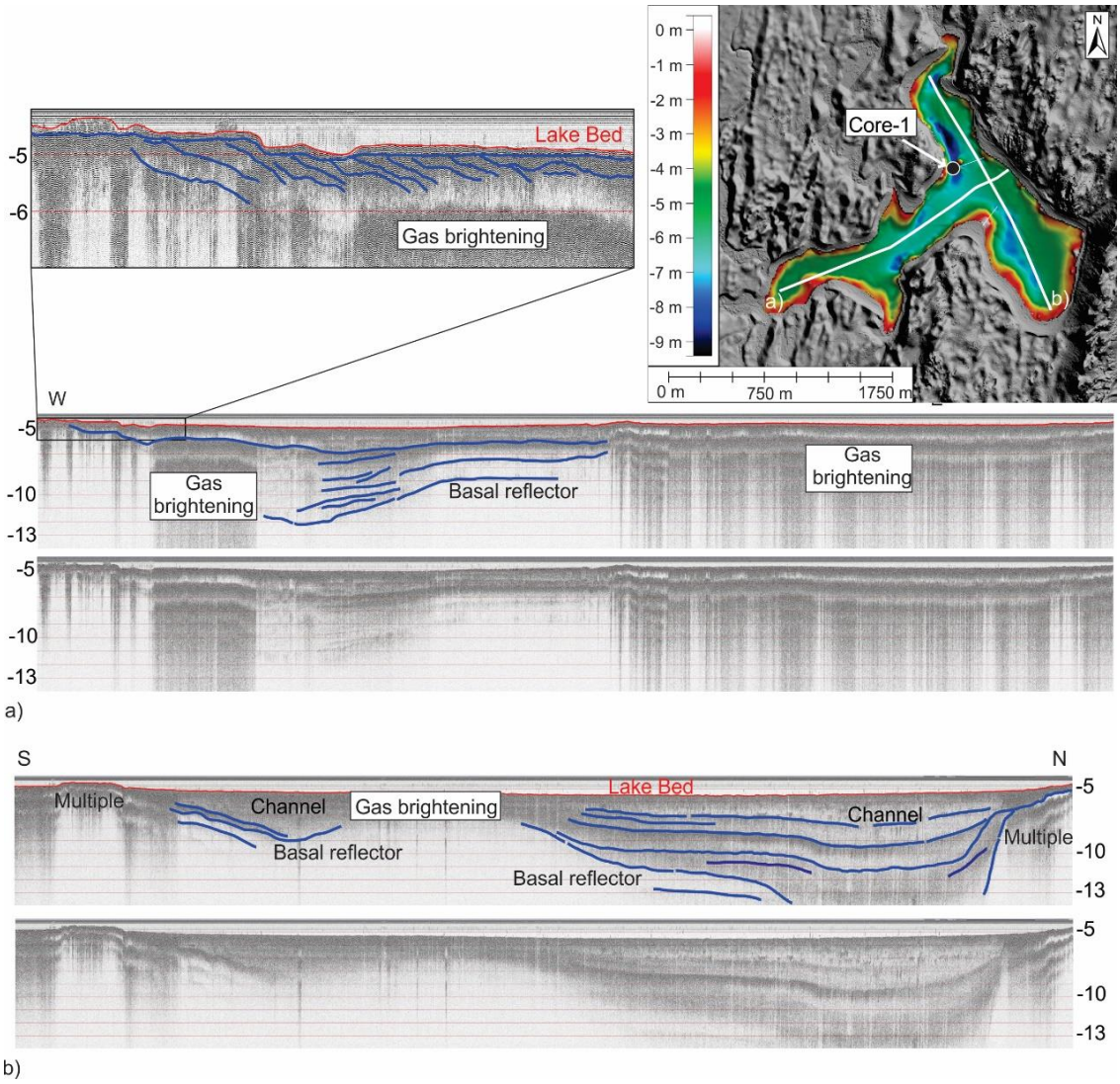

Figure 5.13. Interpreted and uninterpreted sub-bottom profiles. a - West to east profile revealing seaward prograding sigmoidal reflections. b – Coast parallel south-north profile showing a channel form develop din the basal reflector. Inset show's location of specific lines.

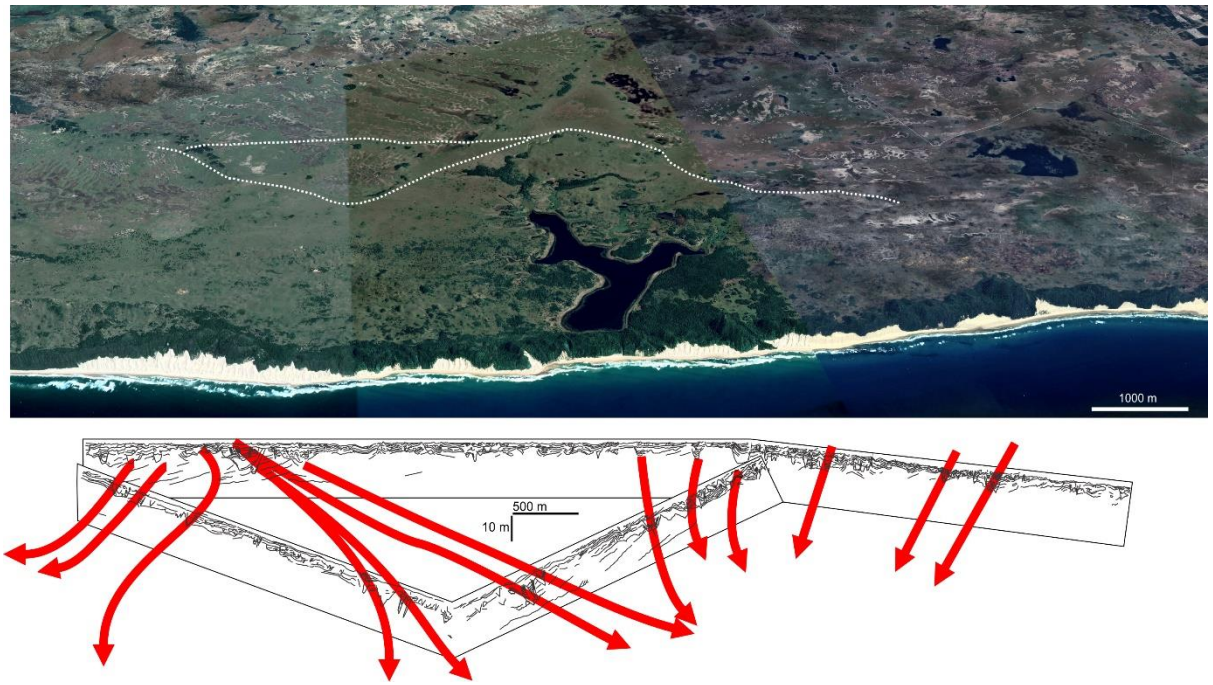

Figure 5.14. Top image shows a re-orientated annotated image of the regional GPR data. The bottom image shows a 3D interpretative fence diagram of the data. The red arrows indicate the channel pathways.

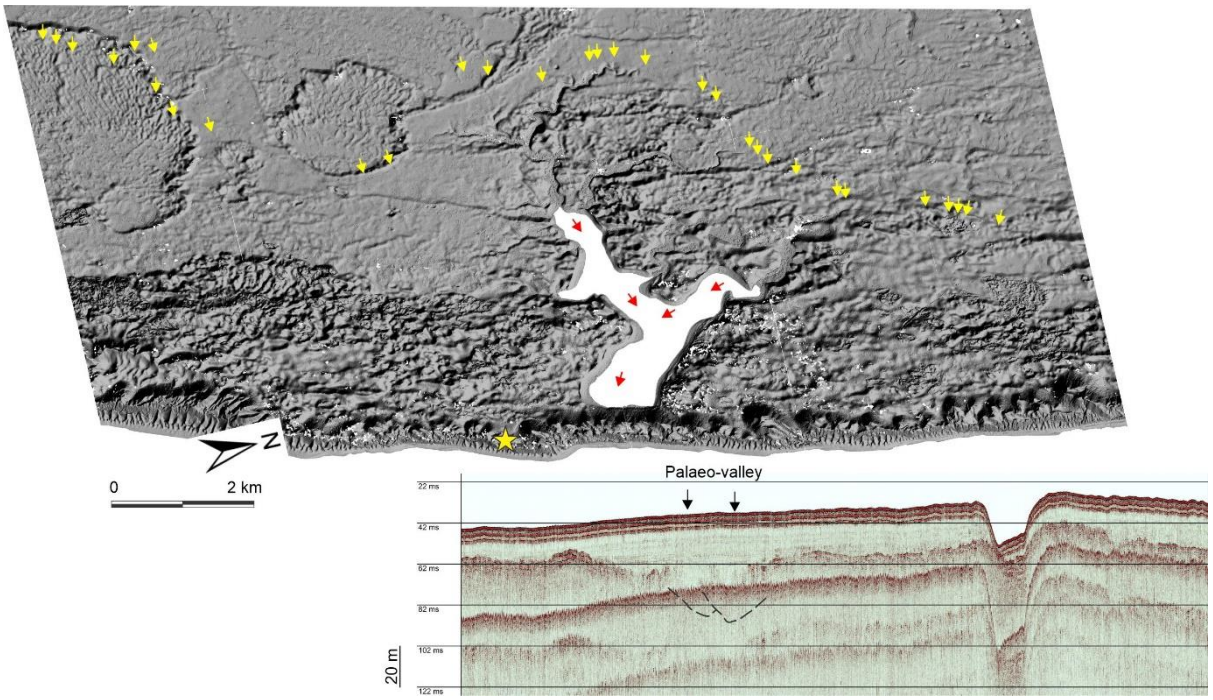

Figure 5.15. Annotated image of the regional channel locations and inferred flow directions (yellow arrows) from regional GPR and sub-bottom profiling in the lake, juxtaposed with seismic reflection data from immediately offshore the study site on the inner shelf. The offshore data show a palaeo–valley (black dashed lines) seaward of LBN, but not aligned to the palaeo–valleys, nor located adjacent to a barrier low (yellow star) (see Figure 5.1., section 5.1. Regional geomorphology).

5.5. Lake Margin GPR Data

The prograding bodies and palaeo-channels seen at a regional scale in the 40 MHz GPR and sub-bottom profile data, are mirrored within the GPR data collected along the lake edges. This now also includes several minor channel incisions (Figure 5.16.) and packages of chaotic reflectors that form within these. The larger channels have a maximum width of ~70 m, with depths up to 7 m below the surface (Figure 5.16.) and are thus similar in scale to the channels identified inland.

Several sets of steeply inclined prograding reflections are interspersed within these data, highlighted by the red arrows in Figure 5.16. These reflectors dip to the northwest and comprise the only dipping component to the channel fills and are usually interleaved with flat–lying and undulating reflections.

Several small (20 – 40 m wide and ~3 m deep) channels occur within the larger palaeo-channel/valley as described in the previous section. A small number of mounds and pinnacles of sediment are also evident. These mounds are concentrated within the western limb of the lake. The internal geometry of the mounds shows semi-transparent, high amplitude, parallel reflectors with the mounds displaying a convex up geometry (black arrows in Figure 5.11.a. and c. and Figure A.4). Low amplitude, parallel reflections cap the uppermost layers of the stratigraphy.

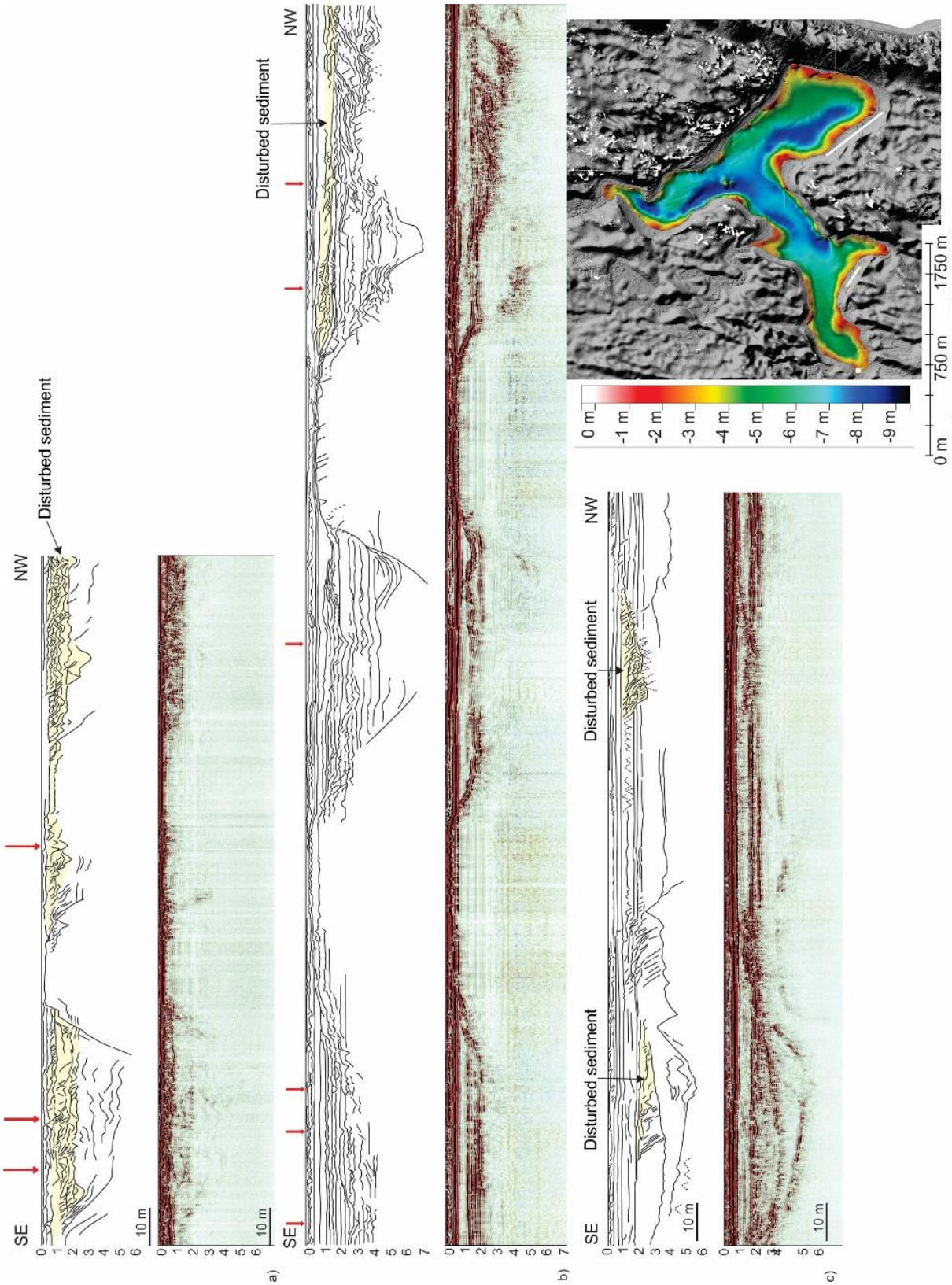

Figure 5.16. Interpreted and uninterpreted GPR data collected parallel to the lake edge in the eastern and western limbs. Red arrows – small channels. Yellow – chaotic, disturbed sediment package filling small corrugations.

5.6. Unusual sub-bottom and surface structures

Many unusual chaotic sediment packages, associated with closely spaced corrugations of the substratum, are noted around and in the lake (Figure 5.17.). These are filled by a chaotic to wavy mix of high amplitude reflections. In many areas where these are encountered, margin-perpendicular linear depressions along the lake shorelines were observed. Upon further investigation, these linear features were identified as hippo pathways.

The hippo pathways have a dendritic pattern and are densely packed around the lake. The highest density of hippo tracks occurs along the western and northern shorelines of the northern limb of the lake. Isolate hotspots do occur along the lake's southern margin, with few to no tracks evident in the southeastern portion of the main lake basin. The tracks had a maximum depth of <1 m with an average width of <3 m. Pathways traced to the lake edge in the field show disturbed vegetation along the path.

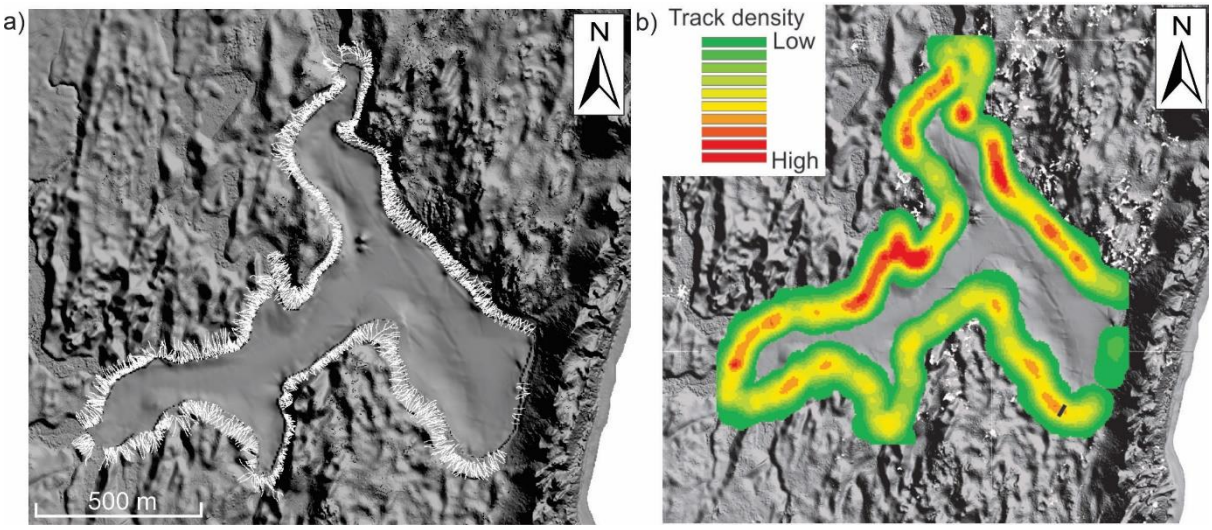

Figure 5.17. A- Hippo pathways around the lake edge. B- Density of tracks/pathways (green representing low density and red representing high density).

The packages of chaotic, disturbed sediment observed within both the GPR and seismic data (Figure 5.16., Figure 5.19. and Figure 5.19.) occur at a maximum depth of 2 m below the surface, the corrugations they associate with have an average width of 1.5 m and a depth of between 0.5 and 1 m (Figure 5.19.). These form amalgamated patches of disturbed stratigraphy up to 150 m wide (Figure 5.18.), and ≤ 4 m thick.

When juxtaposed with side scan sonar and bathymetry data, a variety of similarities can be seen between the onshore disturbed sediments, the submerged equivalents, the lake margin hippo tracks, and the modern lake floor. The dimensions of these pathways coincide with the dimensions of the unusual/disturbed sediment identified within the sedimentary stratigraphy in and around the lake (Table 5-1).

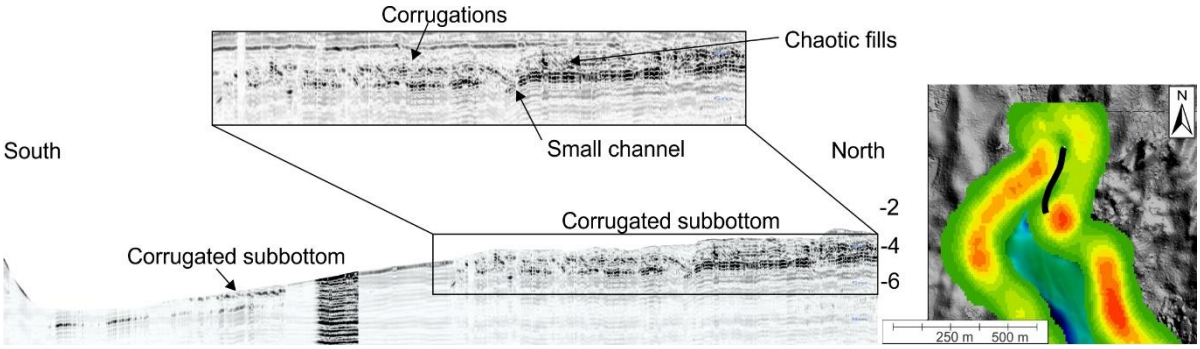

Figure 5.18. Seismic reflection profile (boomer) from the northern limb of the lake showing corrugations and chaotic fills, overlapping to produce a disturbed patch of sediment within the lake stratigraphy. Black line in inset denotes profile position relative to maximum hippo track densities.

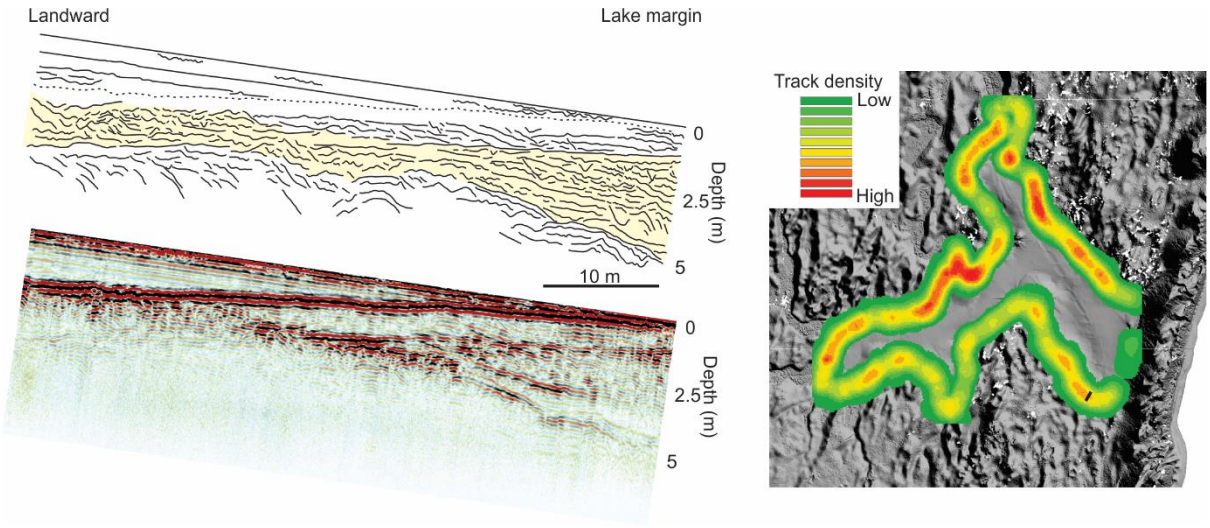

Figure 5.19. Image showing high resolution interpreted and uninterpreted GPR data through an area delineated as a high track density zone.

Echograms from the single beam echosounder that reveal some subsurface structure in the lake have been compiled into Figure 5.20. Figure 5.20.b and d, show the clear outline

of small depressions within the system. These depressions are no more than 1.5 m deep and are less than 2 m wide. The dimensions noted within the boomer and GPR data along the lake edge are similar in both width and depth (Table 5-1). Figure 5.20.c and e, show the concentration of multiple stacked depressions in the underlying sediment. The small depression have a vertical relief of <1.5 m whilst the concentration of packages of amalgamated small depressions reach a maximum thickness of 4 m. Figure 5.20.d shows an irregular surface formed with minor corrugations, overlain by acoustically transparent material.

Table 5-1. Morphometry of corrugated reflection packages compared to hippo tracks observed from aerial imagery.

Average (m)	Width	Depth
Hippo Track	< 3	0.5
GPR	1.5	≤ 0.5
Boomer	1.25	≤ 0.75
Echogram	≤ 1	≤ 0.5

5.7. Lake Floor Texture

Figure 5.20.a shows a selected side scan sonar graph from the northern limb of the lake. Areas of high backscatter correspond to the light parts of the image and low backscatter are shown by the darker parts i.e., mud-like substances will have a lower reflectance and higher absorption of sound (dark) than a sandy substrate (light). Several small circular depressions show an outer rim of high backscatter with a lower backscatter centre (Figure 5.20.a). These features range between 0.2 m to 0.9 m wide, with perimeters ranging between 1 – 2 m long. These depressions are arranged in a linear pattern along the lake edges (Figure 5.20.a) and several are strongly concentrated within a band of high backscatter ~ 2m wide that cross the northern limb of LBN. This high backscatter band appears to be the offshore extension of a path trunk where several hippo paths merge onshore (Figure 5.20.a.). When compared to the sub-bottom data, these depressions and the stripe of high backscatter correlate to small channels and corrugations in the subsurface (Figure 5.18.).

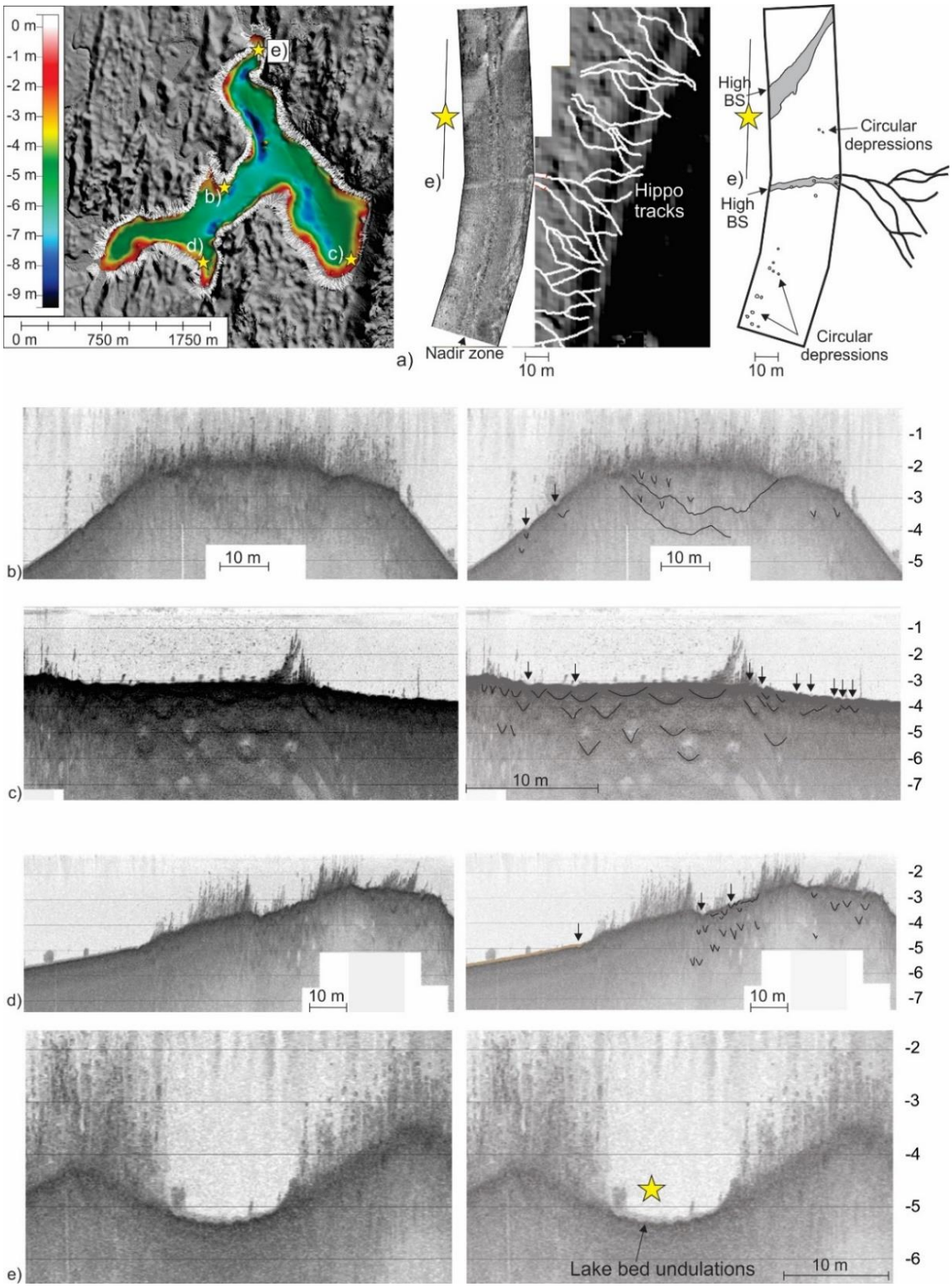

Figure 5.20. a) side scan sonargram and interpretation outlining hippo tracks merging into a stripe of high backscatter. Several circular depressions are also observed, with a centre of low backscatter and rimmed by high backscatter b) sonar graph of a wide channel, with several small narrow and shallow channels within. c) echogram in eastern limb, depicting several stacked wide and shallow channels/depressions. d) echograph in the western limb, with several small and narrow channels/depressions. e) echogram associated with the side scan sonar graph showing an irregular, corrugated surface, overlain by acoustically transparent material. The yellow star in inset a) denotes the location of this relative to the side scan sonargraph.

5.8. Sediment fill of LBN

The almost 8 m-long piston core reveals a relatively monotonous fill sequence within the deepest parts of LBN, terminating at the basal reflector (Figure 5.12.b.). The basal unit, comprising the lowermost reflector was a well packed, 50 cm thick, medium sand (Figure 5.21.). Directly overlying this is a 1.5 m thick package of clayey silt. The remaining length of the core consists of gyjtta, the presence of which correlates to the gas brightening of the sub-bottom record (Figure 5.12.b.). Several thin layers of sand less than 0.5 cm thick punctuate the core throughout.

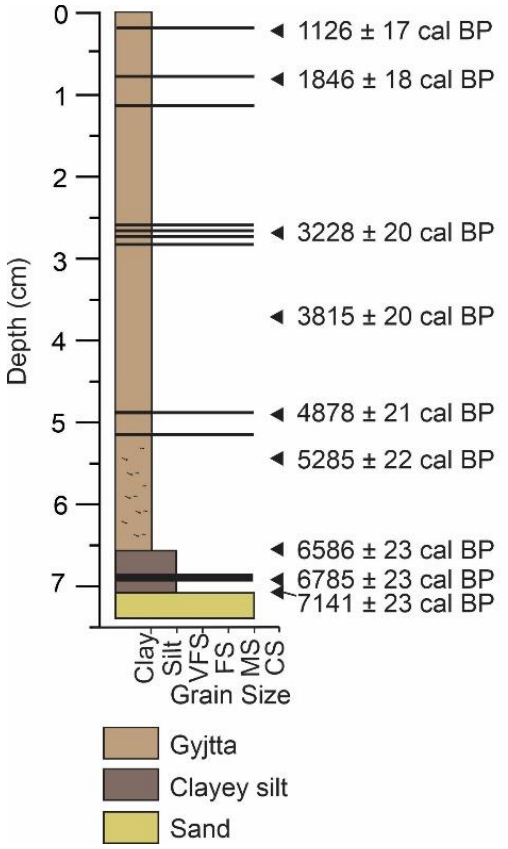

Figure 5.21. Core-1 stratigraphy and geochronology.

5.9. Down core major element geochemistry

The downcore variation in major element oxides is presented in Figure 5.22. Calcium (Ca) and zircon (Zr) follow a similar trend with two distinct spikes at ~670 cm and the very top of Core-1 (Figure 5.22.). When compared to the core lithology, the second spike located further down the core coincides with the change in sediment from gyttja to clayey

silt. Ca has several small spikes with a pronounced spike at the top of the core. Three zircon spikes were noted within the first 120 cm of the core, each correlating to sand horizons (Figure 5.22.). Three distinct titanium spikes are noted within the core, two within the first meter of the core and the third at ~720 cm. These correlate to zircon spikes (sand horizons) and the sandy layer at the base of the core.

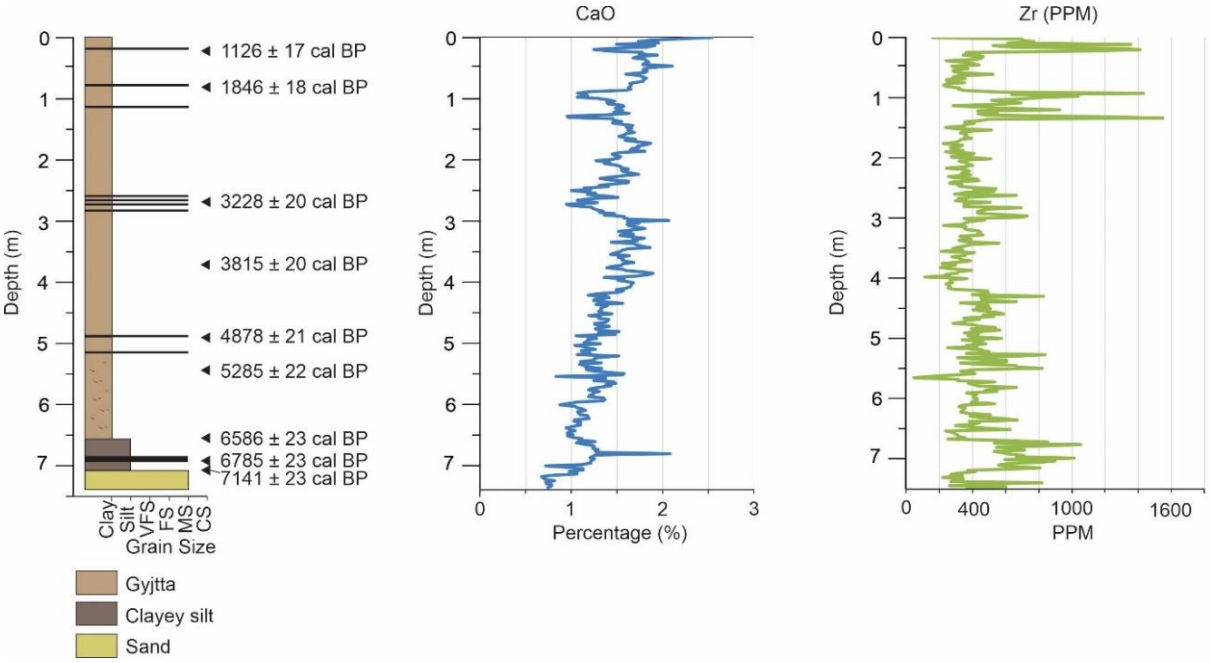

Figure 5.22. Core lithology and associated downcore abundances of calcium (%) and zircon (ppm) in Core-1.

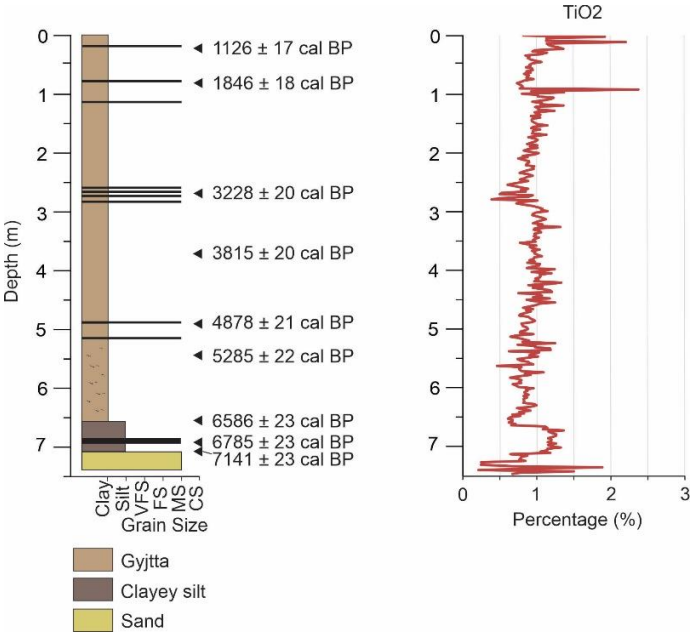

Figure 5.23. Core lithology and associated downcore abundances of calcium (%) and zircon (ppm) in Core-1.

5.10. Geochronology and sedimentation rates

The lowermost organic sediment in the core dated to 7 141 ± 23 cal BP, with all subsequent dates returning a relatively monotonous and constant rate of deposition up to 2.76 m downcore. This first portion has a sedimentation rate of ~1.09 mm per year. Thereafter, the remaining sediment up to the core top accumulated at ~ 1.21 mm per year, a period marked by sharp increases in the terrestrial element Zr.

Chapter 6

Interpretation and discussion

6.1. Regional Geomorphology

The most significant and unusual features that are evident from the LiDAR data are the semicircular depressions that occur directly landward of LBN, and which form an interlinked series of depressions that extend almost to Lake St Lucia (**Error! Reference source not found.Error! Reference source not found.**.). These bodies vary in shape and size and overlap each other in some cases, however their overall geomorphology is very similar (elongated ellipses) to contemporary segmenting coastal lagoons seen along the Mozambiquan coastline i.e., Lagoa Quissico, Lagoa Maiene and Lagoa Uembje. Their along-coast length spans ~ 27 km, comparable to the Kosi Lake system's extent (24 km), with the semi-circular depressions also similar in width to the Kosi Lake basins. These depressions also possess seaward stepping ridges (**Error! Reference source not found.**) akin to the shorelines of almost all segmented coastal waterbodies found in northern KwaZulu-Natal and southern Mozambique.

Geomorphological bodies C and D (Figure 5.5.) possess a fan-like morphology that overlies the broader semi-circular depressions. They appear very similar to washover fans, with narrow necks and an outward fanning series of lobes (Donnelly and Sallenger, 2007, Hudock et al., 2014). Given the context of a long-lived barrier system to seaward (Benallack et al., 2016), and the general heights of the dunes (~80 m-Figure 5.5.), it seems implausible to suggest these are washover fans. Similar types of deposits can be formed from debris flows, where a similar geomorphology is shared (Takahashi, 1981, Zhou et al., 2019, Pánek, 2021). Debris flows are a mass wasting event where, weakening of the slope causes a large amount of sediment to move down the slope and fan out once at the base. Given the regional climate of the area has been characterised by dry periods, especially during the Holocene, when significant amounts of dune vegetation died and mass deflation occurred (Humphries et al., 2020), these may represent slope failures when binding vegetation was scarce.

The high-resolution LiDAR data show the Mkhuze River extending seaward, with several raised topographic lobe-like features found where the 90° bend occurs and the river changes course towards Lake St. Lucia (Figure 1.1.). These lobes are orientated perpendicular to the coast. These features are of similar shape and scale to the bayhead

deltas that are found in many of the microtidal estuaries of KwaZulu-Natal (Cooper, 2001, Dladla et al., 2021), most notably those that now enter the St Lucia lake system (Green et al., 2022). They are also broadly comparable with the examples of bayhead deltas outlined by Simms et al. (2018). If these are relict bayhead deltas (as suggested by their size and shape), they imply coastal waterbody shoreline approximately coast-parallel at ~ +18 m, into which the Mkhuze River discharged.

The tall, vegetated dune barriers along the coastline prevents any interaction between the lake and the ocean. However, three low points are observed along the length of the dune near LBN (Figure 5.2.). The low point located to the south of LBN, with an elevation of less than 30 m, could have possibly been an inlet linking LBN and the ocean at one point (Figure 5.15). The offshore seismic reflection data shows a palaeo-valley system developed adjacent to the location of LBN (Figure 5.15.), and in line with the low point immediately north of LBN, however there was no associated seaward palaeo-channel with the southernmost low point in the dune (Green, 2009a) (Figure 5.2.).

A similar connection has been noted for the lakes of northern KwaZulu-Natal e.g., Lakes St Lucia, Sibaya and Nhlange where low points in the barrier correspond with palaeo-channels and later inlets that breached these dunes (Green, 2009, Green et al., 2022, Dladla et al., 2022). It thus seems probable that a land-ocean connection existed where LBN is located, marked by the barrier low and offshore palaeo-valley.

6.2. GPR Stratigraphy and sub-bottom data

The regional GPR data reflect numerous channels that incise the stratigraphy to landward of LBN (Figures 5.11., 5.14. and 5.15.). These channels underlie the semicircular depressions and appear to converge toward LBN, where palaeo-channels can also be seen entering the lake from the shoreline GPR data (Figure 5.16.). Where the modern Mkhuze river traverses the coastal plain, channel dimensions are quite similar and range from 6 m wide and 3 m deep (cf. Ellery et al. (2003)), to at least 150 m-wide (as seen from the DEM data in Figure 5.15.). These valleys may be compound (Figure 5.11.b), eroding into previous valleys, thus indicating the reactivation and re-inheritance of the drainage systems over time. Each channel may not represent a distinct river, but rather the same river, meandering over the coastal plain and re-incising older, low-lying topography.

The channel fills mostly consist of drapes that fill the channel body. These are similar in form to the valley fill of LBN, characterised by low to moderate amplitude reflections that drape the topography and onlap the valley walls (Figure 5.12. and 5.13.). These appear to correspond to the central basin fill of a wave-dominated estuary (cf. Zaitlin et al., 1994).

Prominent sets of inclined reflections occur throughout the study area and comprise the first radar package that occurs above the draped, central basin-style channel fills (Figure 5.11.). These prograde from mounded highpoints that are located between channels on the interfluves. Similar seismic architectures have been recognised from segmented coastal waterbodies that are submerged and preserved offshore (Green et al., 2013, Pretorius et al., 2016, Green et al., 2020), in addition to those on the modern coastal plain of KwaZulu-Natal (Benallack et al., 2016, Dladla et al., 2019a, Dladla et al., 2022, Green et al., 2022). In these cases, the transgressive filling of the incised valley overspills the valley interfluves and lagoonal or estuarine/lake materials were deposited over the palaeo-coastal plain to form a shallow muddy low-energy system.

The mounded features may be interpreted as the waterbody shorelines, that over time shift toward the valley as the system slowly segments due to sea level stasis or fall and shoreline reworking e.g. Zenkovitch (1959). The prograding reflections represent the development of cuspate spits and prograding shoals that mark system shallowing and separate basin development (Green et al., 2022). The progradational architecture is identical to the internal geometry of the contemporary spits that now segment LBN, as evidenced in the sub bottom profiles (Figure 5.12.a.). Likewise, these bear a close similarity to the internal structure of the encroaching bayhead delta of LBN (Figure 5.13.a.).

The capping, acoustically indistinct or transparent layer is correlated to the modern aeolian cover sediment. This fills the underlying depressions to some extent and is characterised by the development of blowouts.

The GPR data collected around the lake margins likewise reveals channels entering the lake system. These are all a similar scale to those channels observed to landward of LBN. The channels converge and match with the channels evident in the sub-bottom record of LBN (Figure 5.12. and 5.13.). Though the sub-bottom data are sparse, the presence of multiple channel incisions along individual profiles (Figure 5.13.b.) suggest several

channel courses, or a meandering system constrained by pre-existing palaeo-topography e.g. Dladla et al. (2019a).

When the various channel locations are noted (Figure 5.15.), they indicate a general convergence of channels towards LBN, with the majority joining the channel in the eastern limb of the lake where the modern bayhead delta exists. A second channel enters from the northern limb and combines to exit the system. The exact exit point is not clear and the channel location in the sub-bottom records likewise does not closely match the low-points in the barrier, or the exact position of the incised valley observed in the offshore records. It may be that the valley meanders between the onshore data sites and those offshore. This is confirmed to some extent by the large (< 7 m-deep; < 50 m-wide) channel observed in the GPR data on the southwestern-most part of the lake (Figure 5.16.b.), and to which the channel preserved in the bathymetry extends toward (see below). The lake was without doubt connected at some point via an inlet to the south.

6.3. Bathymetry of Lake Bangazi North

The most significant bathymetric features of LBN are the channels preserved on the lake bottom. These are significant in their relief and are similar to those found in Lake Sibaya (Miller, 1998, Wright et al., 2000) and the Kosi Lake System (Dladla et al., 2022). Their presence, especially in the Kosi Lake System, implies a limited sediment supply to the incised valley to the extent that the main channels are not fully inundated with sediment (Cooper et al., 2012). Thus, in contrast to Lake St Lucia, where there are no channels preserved and all the available accommodation space in the incised valleys are filled (Green et al., 2022), the situation has arisen of an incised valley that has not managed to fill completely in line with rising sea levels. This further implies that 1) marine sediment supply was limited to LBN, and 2) once the system was sealed from the ocean, sufficient fluvial sediment supply was unavailable to counterbalance the remaining accommodation space.

The main morphological features of the system are represented by the spits and the small bayhead delta that enters the western limb. Like other coastal waterbodies that are actively segmenting, these are the main sediment inputs to the system that significantly control the system geomorphology e.g. Dladla et al. (2022). The spits represent autochthonous sediment supply from shoreline reworking by wind waves (c.f. Cooper (1994)). The upper

surface of the bayhead delta is covered by a thin veneer of acoustically homogenous/transparent material (Figure 5.13.a.). The acoustic response is similar to the uppermost fill layers of other coastal waterbodies, where that was determined to comprise fluid mud or gyttja (Dladla et al., 2022). In the case of LBN, the veneer covering the bayhead delta implies that there is very little fluvial sediment currently entering the system and the delta itself may be relict.

6.4. Sediment infill and chronology

The fill of LBN reflects a sharp transition from sandy sediment at the base (deposition of which predates 7 141 ± 23 cal BP) to silt, then gyttja (Figure 5.21.). The basal sand correlates to the acoustic basement (Figure 5.15.), with the material overlying the base reflecting the fill succession of the system. The transition from basal siliclastic material to organic deposition is reflected in the reduction in Zr abundance at 6.6 m downcore at 6 586 ± 23 cal BP. The reduction in Zr likely reflects the sudden switch in the system from allochthonous materials (wind-blown, fluvial and marine) to autochthonous sedimentation. Such switches in depositional style have been ascribed to inlet sealing of other related coastal waterbodies such as Lake St Lucia and the Kosi Lake System (Benallack et al., 2016, Dladla et al., 2019a, Dladla et al., 2022). In the case of the former, the basal sand body reflected tidal flats and the latter, flood tide deltas respectively. Both of these environments imply an open marine connection prior to 6 586 cal BP.

In contrast to the above examples, the remaining valley fill of LBN appears to be terrestrial in nature. The seismic stratigraphy is marked by alternating high and low amplitude reflections that drape the valley walls (Figure 5.12.), an arrangement typically interpreted as the central basin environment of wave or mixed wave and tide-dominated estuaries where a mixed fluvial and marine signal is encountered (Zaitlin et al., 1994, Benallack et al., 2016, Dladla et al., 2019a). The core data conversely indicate this to comprise an almost undisturbed sequence of gyttja, a solely terrestrial-forming organic deposit (Stoops et al., 2018). Further, the basal sand of the LBN fill lacked any macrofossils and had a relatively low abundance of Ca when compared to the overlying autochthonous gyttja. The low Ca content is interpreted to represent a lack of marine influence, supported by the higher levels of Zr, likely sourced from fluvial or dune

materials (Humphries et al., 2020) or occasional shoreline reworking. This may explain the relatively high background Zr in the upper sections of the core.

Given LBN's close proximity to the ocean, the terrestrial fill of the valley implies either 1) little to no marine sediment entered the system and a significantly seaward located inlet sealed rapidly causing terrestrial backflooding as opposed to marine inundation, or 2) the core and geophysics do not penetrate sufficiently to image the estuarine succession below and only the progradational bayhead delta is encountered, occurring as an "apparent valley floor" horizon the top of which mirrors the underlying valley morphology. No matter the interpretation, three main points arise:

1) The shift to autochthonous deposition marks a closing of the inlet or cessation of the fluvial inputs.
2) The incised valley architecture differs dramatically from those described from the region. Either a very strongly prograded bayhead delta has filled much of the valley e.g., the incised valleys described by Cooper (1993) and Green et al. (2015), or the main marine depocenter was further seaward and the inner segment of the valley is intersected directly at the coast (Zaitlin et al., 1994).
3) Siliclastic sediment supply to the system ceased abruptly at ~ 6 586 cal BP.

In the case of point two above, the nearby marine seismic profile reflects an acoustically transparent valley fill that Green (2009) interpreted as a central basin deposit. The bayhead delta explanation is thus preferred.

The limited fluvial sediment supply can be related to the Mkhuze River's discharge into the St Lucia system since ~ 7 200 cal BP (Humphries et al., 2020). This likely diverted the main fluvial sediment supply southward, with some smaller systems (as seen in the lakeside GPR records) entering LBN. These too provided very limited fluvial materials. The result is the preservation of the original incised valley form in the modern bathymetry, as seen in the channel system of the lakebed.

The various spikes in both grain size and Ti abundances recorded in the core stratigraphy may be related to dry periods, where vegetation die backs result in increased deflation from the adjoining coastal dune (Humphries et al., 2020). The transported materials settle in the lake as allochthonous sediment horizons that punctuate the background gyttja deposition. It is beyond the scope of this thesis to examine the climate variability of the region, however, the main cluster of sandy lenses at 2.5 – 2.75 m downcore are coeval

with similar layers found in the Mkhuze delta (Humphries et al., 2020). The LBN layers date to 3228 ± 20 cal BP, which overlaps with a period of aridity recognised between 3700–2600 cal yr BP from the Mkhuze delta records (Humphries et al., 2020). These were ascribed to changes in the El Niño-Southern Oscillation (Labaune et al., 2005). A closer examination of the various sand lenses and their relationships to climate is thus strongly recommended.

6.5. Bio-engineering

The margins of LBN are strongly affected by hippo tracks and pathways, with a strong clustering evident in the northern limb, and other isolated hotspots occurring along the southern portions of the system (Figure 5.17.). When observations are extended to the lakebed, certain correlations can be made between lakebed texture and hippo movements.

The bands of high backscatter (white bands) that cross the lakebed in the northern limb of LBN extend directly into the areas of highest track density on the seaward margin of the northern limb. One track can be followed directly into this high backscatter stripe and is evident from the echograms to be underlain by corrugated depressions in the lakebed of a similar scale to those mapped on land (Table 5-1). The high backscatter is likely the result of compaction of the lakebed increasing its density and allowing for higher scattering, in addition to sand being tracked into the lake by the hippos during crossing. Similar features were observed by McCarthy et al. (1998) on dry lakebeds in the Daonara area of the Okavango Delta. Where hippos traversed the lake beds, they formed sandy paths, seen from the air as yellow bands of sandy material encapsulated by the muddy materials of the typical lake sediments (McCarthy et al., 1998).

The corrugated reflections that can be observed in the echograms of the lake's upper stratigraphy are interpreted as being related to hippo movement. Their scale is similarly comparable to those hippo tracks mapped on land in this study and elsewhere (Deocampo, 2002), and their underlying association with tracks followed from onshore to underwater attest to this (Figure 5.20.e.). These can form a single corrugated surface such as in Figure 5.18. and Figure 5.20.e., where tracks amalgamate to produce a corrugated and channelled substrate (as seen in the boomer record too). These surfaces may also stack, indicating that these tracks persist for long periods, that there is morphological feedback between hippos and previous tracks, and that the product of this results in long term preservation

of hippo ecosystem engineering. This is further substantiated by the GPR records along the lake margins. Several corrugated surfaces amalgamate to produce distinct packages of disturbed sediment up to 2.5 m-thick, notably found in areas of high track density (Figure 5.19.).

Several scattered and isolated circular depressions of the lakebed can be seen surrounding the areas of high backscatter (Figure 5.20.a). These have an inner circle of low backscatter and an outer rim of higher backscatter. These are considered as single or random pathways of hippos that have not yet formed a discrete track. The discrepancy in backscatter relates to the individual foot movements, where the foot punches out a plug of muddy upper substrate to leave a lower backscatter crater, with sand mantling the rim introduced from the hippo foot as it enters from the sandy margins (McCarthy et al., 1998). Laporte and Behrensmeyer (1980) document a situation where the foot rather removes mud and then presses into underlying sandy substrate to make such a contrast in sediment, however this is unlikely to be the case here as the upper sediment in LBN is mostly homogenous gyttja. These circular depressions are likely the precursors to the corrugated layers, as with continued trampling, the surface sediment is homogenised and erosional depressions then form as opposed to discrete footprints (Laporte and Behrensmeyer, 1980). A multitude of overlapping small depressions or channels can be seen in the echograms of the lake (Figure 5.20.b-d.). These could be representative of the intermediate stage in a continuum from individual footprints to agglomerated tracks.

6.6. Coastal evolution and LBN

Figure 6.1. outlines the general evolutionary model of LBN and the surrounding coastal plain based on the discussion points raised.

Stage 1). The Mkhuze River and other lesser drainage systems incised the coastal plain (Figure 6.1.a.). The Mkhuze River was diverted through the long-lived coastal barrier and incised the shelf south of the current position of LBN. The river valley formed the proto depression for LBN.

Stage 2). The rising postglacial transgression submerged the river channels as sea level approached the last interglacial highstand of ~ 8 m. Early marine transgressive filling of the more landward river valleys mapped by GPR likely only occurred when the relative sea level elevation of the highstand was equivalent to the basal elevations of the channel

bottoms (Figure 6.1.b.). The remaining fill is likely through fluvial aggradation where these are higher than +8 m.

Stage 3). The highstand was reached and the valleys are flooded (Figure 6.1.c.) A period of prolonged sea level stasis occurred and allowed for the back flooding of the river valleys and submergence of the interfluves, forming a lagoon/perched coastal waterbody It is likely that the coastal barrier sealed, allowing water levels of the lake system to perch at ~ +12 m (Cooper and Green, 2021). A lagoonal system is unlikely to have water levels to that elevation given a sea level of 6 – 8 m for the last interglacial (Cooper and Green, 2021).

Stage 4). Waterbody segmentation began (Figure 6.1.d.). The coastal waterbody developed spits that began to enclose the smaller sub-basins. These prograded from the waterbody shorelines and the system gradually shallowed.

Stage 5). Aeolian conditions began to dominate as sea level started to fall after the interglacial (Figure 6.1.e.) Aeolian deposition covered the waterbody, however depressions inherited from the waterbody sub-basins created conditions optimal for flow steering and deflation to occur. Blowouts formed within these depressions. Sea level fell past the shelf break to ~ 120-130 m depth and an opening was formed again in the barrier.

Stage 6). Rising sea level in the Holocene began to raise fluvial base levels and formed estuaries at the position of the contemporary coastline (Figure 6.1.f.). A large, strongly prograded bayhead delta emerged into the LBN estuary and covered the central basin deposits below. This was ca. 7 140 BP, a time when sea levels stabilised after the rapid rises of the early Holocene (Ramsay and Cooper, 2002). At this stage, the Mkhuze River began to discharge into Lake St Lucia (Humphries et al., 2020), leaving behind a relict bayhead delta.

Stage 7). The barrier inlet sealed at about 6 586 cal BP (Figure 6.1.g.). A switch to autochthonous sedimentation in the form of gyttja occurred, draping the bayhead delta and partly filling the accommodation above it.

Stage 8). Modern day LBN formed, with a gyttja fill, underfilled channels still evident in the bathymetry and contemporary segmentation occurring with spits and a modern bayhead delta (Figure 6.1.h). The relict waterbody to landward shows evidence of

prograded spits and segmentation, with low points now occupied by wetlands and pans and modified by blowout associated deflation.

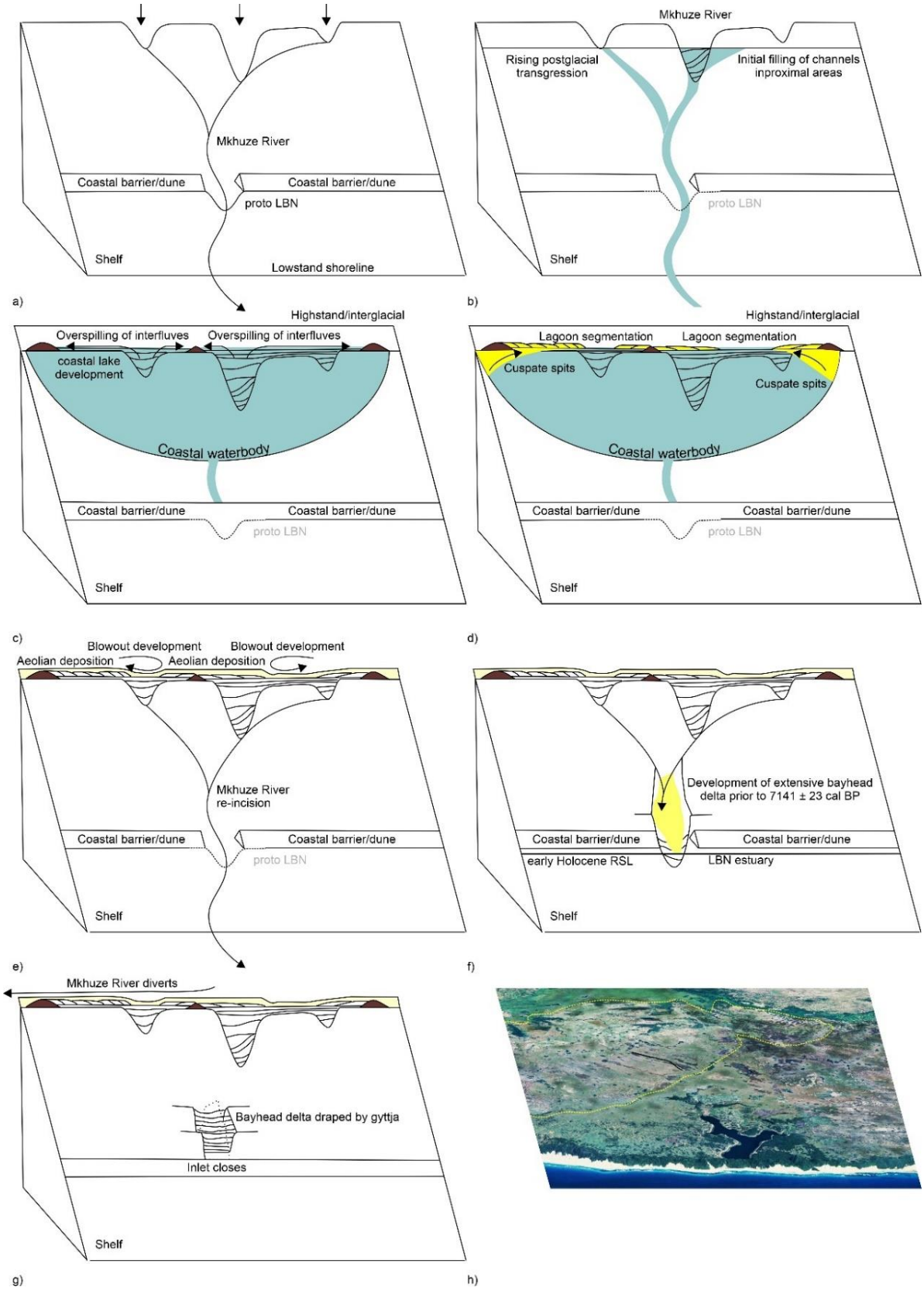

Figure 6.1. A model of the coastal evolution of LBN as a result of changing sea-level and subsequent barrier evolution.

Chapter 7

Conclusion

7.1. Evolutionary Model

The results presented above allows for the construction of an evolutionary model of Lake Bangazi North. The evolution of this area begins with a distinct episode of valley incision that forms during a lowstand in sea level. This marks the lowermost and oldest incision of this nature.

This initial valley infill shows a period of transgression in which the landscape was flooded, drowning these valleys and depositing sediment within them. The flooding of this landscape increases accommodation space thereby depositing sediment further seaward. These deposits formed during a period of stillstand. During this time, spit barriers possibly formed creating, an inlet into the hybrid lagoon-estuary system. This inlet allowed for the influence of tidal currents, forming tidal bedforms and creating tidal channels. The avulsion of these tidal channels are seen as a result of rise in sea level following a period of stillstand (De Lecea et al., 2016, De Lecea et al., 2017). De Lecea et al. (2017), Dladla et al. (2019b) both conclude that these tidal incisions which were overlain by tidal bedforms mark the onset of a lagoon environment.

This partial sealing of the system created a mixed wave-tidal environment with the only freshwater source being the river (Mkhuze). This river is thought to have deposited sediment into the lagoon-estuary system building a large delta plain with many lobes. These delta plains often have distributaries flowing on the lobes. Following a rapid rise in sea level, the delta plain and these small incisions were preserved into which a transgressive fill draped these surfaces. With this increase in accommodation space a new delta formed and built on top of the old one.

Another rise in sea level created the estuary built behind the now well-established Pleistocene dune barrier complex created an inlet system similar to what is seen today with the St Lucia estuary and coastal lake systems such as Kosi Bay and Lake Sibaya. Like these lake systems which have an inlet, this inlet opens and closes due to wave movement depositing sediment across the inlet as well as removing sediment from the inlet. The opening and closing of this inlet alters the back barrier environment from an estuary to a shallow lagoon system. When the inlet was open, the movement of the water

disturbed the sediment possibly eroding the sediment layer beneath before the final closure of the inlet following sea level stillstand.

Following the cut off from the ocean, the system deepened from a shallow lagoon system to a deep lagoon system which caps the regional study area. As seen from other lakes such as the eastern coastal lakes of South Africa and the southern lakes of the Mozambique coast, lake segmentation occurs after there is no longer an influx of water into the system to renew or sustain it including groundwater recharge. The segmentation of the lagoon occurred over a long period of time with the natural build-up of elevated dunes due to aeolian processes, dividing the system. These formed the well-preserved geomorphological bodies identified in the LiDAR data. This area could have a possible source of freshwater in the form of the Mkhuze river prior to its mysterious change in direction.

Palaeo-channels identified throughout the study area indicate the flow of water towards LBN, however the channel flow does not link well to the palaeo-valley identified offshore LBN. Further research will be required for this.

7.2. Conclusion

This project aimed to provide an examination of the morphological and stratigraphic evolution of LBN and the surrounding coastal plain. In this light the following objectives were proposed

1 – to identify, at a regional (12 x 4 km) scale, the palaeo-drainage courses associated with the Mkhuze River.

A well-developed palaeo-drainage network is evident to landward of LBN, representative of the palaeo-Mkhuze River course prior to its debouchement to Lake St Lucia. These channels underlie a series of shallow semicircular depressions that are considered to be relict paleo-coastal waterbodies. The valleys seem to predate the last interglacial highstand and the elevated coastal waterbodies formed during the highstand. These segmented in a fashion similar to the coastal waterbodies of the modern coastal plain of northern KwaZulu-Natal.

2 – to link these to local scale channel systems that surround LBN.

The channels, at a regional scale, seem to link with those of the surrounding lake. Drainage appears to be directed toward the lake, with channels of similar size and scale in both lakeside and regional GPR data.

3 – to examine whether these may merge with a larger palaeo-channel network beneath LBN, and offshore the study area, and to what degree these control the modern lake bathymetry.

When integrated with the channels mapped from sub-bottom profiling, it is clear that the palaeo-Mkhuze River extended through LBN and discharged into the ocean just south of the lake, manifest in a low point in the dune barrier. This river meandered and joined a palaeo-valley evident in seismic reflection profiles on the mid shelf seaward of LBN.

The relative lack of sediment from either marine or fluvial sources resulted in the preservation of underfilled parts of the incised valley. The entire valley may not be imaged by the sub-bottom profiler used. It seems likely that the upper part of a well-defined and strongly prograded bayhead delta of the palaeo-Mkhuze River forms the acoustic basement. The river appears to have disconnected from LBN and diverted to Lake St Lucia ~ 7 100 cal BP.

4 – to core and examine the fill of the LBN system.

The fill above the relict bayhead delta in LBN is almost entirely autochthonously-formed gyttja, the deposition of which commenced ~6 586 cal BP with the sealing of LBN's inlet to the ocean. Occasional sandy lenses mark drought conditions with increased deflation from the coastal dune and surrounding coastal plain. It is strongly recommended that further study be undertaken on the significance of the cycles evident in the core, especially in light of ENSO-driven drought in the area.

5 – to identify legacies of bio-engineering in the system that are the result of large herbivore behaviours.

Modern system change is driven by the segmentation of the system by spits and a bayhead delta entering the western limb of LBN. Superimposed on this are long-term effects of hippo movements that have sculpted parts of the system stratigraphy, in addition to the modern geomorphology. This study presents a continuum of bio-engineering that begins with individual footprints, which over time and persistent trampling, evolve into single corrugated/channelled surfaces. These further amalgamate into shallow depressions filled

with < 4 m-thick corrugated/deformed sediment. It is recommended that a detailed grid of sub-bottom profiles and GPR be acquired to examine these relict hippo pathways in three dimension with the aim of creating an ichnofacies model for ancient rock studies.

Chapter 8

References

AL-DOUSARI, A., PYE, K., AL-HAZZA, A., AL-SHATTI, F., AHMED, M., AL-DOUSARI, N. & RAJAB, M. 2020. Nanosize inclusions as a fingerprint for aeolian sediments. *Journal of Nanoparticle Research,* 22**,** 1-15.

ALEXANDER, W., STORMANNS, C. & BREEN, C. Some aspects of the hydrology of the Mkuze Swamp system. Proceedings of the Greater Mkuze Swamp System Symposium and Workshop, Institute of Natural Resources, Pietermaritzburg, 1986. 4-7.

ALLEN, G. P. & POSAMENTIER, H. W. 1994. Transgressive facies and sequence architecture in mixed tide-and wave-dominated incised valleys: example from the Gironde Estuary, France.

ALTAMURA, F., MELIS, R. T. & MUSSI, M. 2017. A middle Pleistocene hippo tracksite at gombore II-2 (melka kunture, upper Awash, Ethiopia). *Palaeogeography, Palaeoclimatology, Palaeoecology,* 470**,** 122-131.

ARMITAGE, S. J., BOTHA, G. A., DULLER, G., WINTLE, A., REBÊLO, L. & MOMADE, F. 2006. The formation and evolution of the barrier islands of Inhaca and Bazaruto, Mozambique. *Geomorphology,* 82**,** 295-308.

BARD, E., HAMELIN, B., ARNOLD, M., MONTAGGIONI, L., CABIOCH, G., FAURE, G. & ROUGERIE, F. 1996. Deglacial sea-level record from Tahiti corals and the timing of global meltwater discharge. *Nature,* 382**,** 241-244.

BENALLACK, K., GREEN, A. N., HUMPHRIES, M. S., COOPER, J. A. G., DLADLA, N. N. & FINCH, J. M. 2016. The stratigraphic evolution of a large back-barrier lagoon system with a non-migrating barrier. *Marine Geology,* 379**,** 64-77.

BOTHA, G. The Maputaland Group: a provisional lithostratigraphy for coastal KwaZulu-Natal. Maputaland focus on the quaternary evolution of the south-east African coastal plain. International Union for Quaternary Research Workshop abstracts. Council for Geoscience, Pretoria, 1997. 21-26.

BOTHA, G. 2015. The Maputaland Corridor: A Coastal Geomorphological Treasure. *Landscapes and Landforms of South Africa.* Springer.

BOTHA, G. 2018. Lithostratigraphy of the late Cenozoic Maputaland Group. *South African Journal of Geology 2018,* 121**,** 95-108.

CAMOIN, G., COLONNA, M., MONTAGGIONI, L., CASANOVA, J., FAURE, G. & THOMASSIN, B. 1997. Holocene sea level changes and reef development in the southwestern Indian Ocean. *Coral Reefs,* 16**,** 247-259.

CAMOIN, G., MONTAGGIONI, L. & BRAITHWAITE, C. 2004. Late glacial to post glacial sea levels in the Western Indian Ocean. *Marine Geology,* 206**,** 119-146.

CARTER, R., HESP, P. & NORDSTROM, K. Erosional landforms in coastal dunes. Coastal dunes. Form and process, 1990. 217-250.

CATUNEANU, O. 2006. *Principles of sequence stratigraphy*, Elsevier.

CHABANGU, N., BECK, B., HICKS, N., BOTHA, G., VILJOEN, J., DAVIDS, S. & CLOETE, M. 2014. The investigation of CO2 storage potential in the Zululand Basin in South Africa. *Energy Procedia,* 63**,** 2789-2799.

CHANSA, W., MILANZI, J. & SICHONE, P. 2011. Influence of river geomorphologic features on hippopotamus density distribution along the Luangwa River, Zambia. *African Journal of Ecology,* 49**,** 221-226.

CHAPPELL, J. & VEEH, H. 1978. 230Th/234U age support of an interstadial sea level of− 40 m at 30,000 yr BP. *Nature,* 276**,** 602-604.

COE, A. L., BOSENCE, D. W., CHURCH, K. D., DAN, W., FLINT, S. S., KEVIN, D., HOWELL, J. A., JOHN, A. & WILSON, R. C. L. 2003. *The sedimentary record of sea-level change*, Cambridge University Press.

COHEN, A. S. 2003. *Paleolimnology: the history and evolution of lake systems*, Oxford university press.

COMPTON, J. S. 2011. Pleistocene sea-level fluctuations and human evolution on the southern coastal plain of South Africa. *Quaternary Science Reviews,* 30**,** 506-527.

COOPER, J. 1994. Lagoons and microtidal coasts. *Coastal evolution: late Quaternary shoreline morphodynamics***,** 219-265.

COOPER, J. 2001. Geomorphological variability among microtidal estuaries from the wave-dominated South African coast. *Geomorphology,* 40**,** 99-122.

COOPER, J. A. G. 1993. Sedimentation in a river dominated estuary. *Sedimentology,* 40**,** 979-1017.

COOPER, J. A. G. & GREEN, A. N. 2021. A standardized database of Marine Isotope Stage 5e sea-level proxies in southern Africa (Angola, Namibia and South Africa). *Earth System Science Data,* 13**,** 953-968.

COOPER, J. A. G., GREEN, A. N. & COMPTON, J. S. 2018a. Sea-level change in southern Africa since the Last Glacial Maximum. *Quaternary Science Reviews,* 201**,** 303-318.

COOPER, J. A. G., GREEN, A. N. & LOUREIRO, C. 2018b. Geological constraints on mesoscale coastal barrier behaviour. *Global and Planetary Change,* 168**,** 15-34.

COOPER, J. A. G., GREEN, A. N. & WRIGHT, C. I. 2012. Evolution of an incised valley coastal plain estuary under low sediment supply: a 'give-up'estuary. *Sedimentology,* 59**,** 899-916.

DALRYMPLE, R. W. & CHOI, K. 2007. Morphologic and facies trends through the fluvial–marine transition in tide-dominated depositional systems: a schematic framework for environmental and sequence-stratigraphic interpretation. *Earth-Science Reviews,* 81**,** 135-174.

DE FALCO, G., ANTONIOLI, F., FONTOLAN, G., PRESTI, V. L., SIMEONE, S. & TONIELLI, R. 2015. Early cementation and accommodation space dictate the evolution of an overstepping barrier system during the Holocene. *Marine Geology,* 369**,** 52-66.

DE LECEA, A., GREEN, A. N. & COOPER, A. 2016. Environmental change during the Pleistocene and Holocene: Estuaries and lagoons of southern Africa. *Quaternary environmental change in Southern Africa: Physical and human dimensions.* Cambridge University Press.

DE LECEA, A. M., GREEN, A. N., STRACHAN, K. L., COOPER, J. A. G. & WILES, E. A. 2017. Stepped Holocene sea-level rise and its influence on sedimentation in a large marine embayment: Maputo Bay, Mozambique. *Estuarine, Coastal and Shelf Science,* 193**,** 25-36.

DELLWIG, O., HINRICHS, J., HILD, A. & BRUMSACK, H.-J. 2000. Changing sedimentation in tidal flat sediments of the southern North Sea from the Holocene to the present: a geochemical approach. *Journal of Sea Research,* 44**,** 195-208.

DEOCAMPO, D. M. 2002. Sedimentary structures generated by Hippopotamus amphibius in a lake-margin wetland, Ngorongoro Crater, Tanzania. *Palaios,* 17**,** 212-217.

DINGLE, R. V., SIESSER, W. G. & NEWTON, A. R. 1983. Mesozoic and Tertiary geology of southern Africa. *(No Title)*.

DLADLA, N., GREEN, A., COOPER, J. & HUMPHRIES, M. 2019a. Geological inheritance and its role in the geomorphological and sedimentological evolution of bedrock-hosted incised valleys, lake St Lucia, South Africa. *Estuarine, Coastal and Shelf Science,* 222**,** 154-167.

DLADLA, N., GREEN, A. N., HUMPHRIES, M., COOPER, J., GODFREY, M. & WRIGHT, C. 2022. Back-barrier evolution and along-strike variations in infilling of the Kosi Bay lake system, South Africa. *Estuarine, Coastal and Shelf Science,* 272**,** 107877.

DLADLA, N. N., GREEN, A. N., COOPER, J. A. G. & HUMPHRIES, M. S. 2019b. Geological inheritance and its role in the geomorphological and sedimentological evolution of bedrock-hosted incised valleys, lake St Lucia, South Africa. *Estuarine, Coastal and Shelf Science,* 222**,** 154-167.

DLADLA, N. N., GREEN, A. N., COOPER, J. A. G., MEHLHORN, P. & HABERZETTL, T. 2021. Bayhead delta evolution in the context of late Quaternary and Holocene sea-level change, Richards Bay, South Africa. *Marine Geology***,** 106608.

DONNELLY, C. & SALLENGER, A. H. 2007. Characterisation and modeling of washover fans. *Coastal Sediments' 07.*

ELLERY, W., DAHLBERG, A., STRYDOM, R., NEAL, M. & JACKSON, J. 2003. Diversion of water flow from a floodplain wetland stream: an analysis of geomorphological setting and hydrological and ecological consequences. *Journal of environmental management,* 68**,** 51-71.

ELTRINGHAM, S. K. 1999. *The hippos: natural history and conservation*, Princeton University Press.

FRITSCH, C. J.-A. 2020. *Aspects of common hippopotamus (Hippopotamus amphibius) behavioural ecology and their consequences in managed systems in South Africa.*

FRITSCH, C. J., PLEBANI, M. & DOWNS, C. T. 2022. Inundation area drives hippo group aggregation and dispersal in a seasonal floodplain system. *Mammalian Biology,* 102**,** 1811-1821.

GARES, P. A. & NORDSTROM, K. F. 1995. A cyclic model of foredune blowout evolution for a leeward coast: Island Beach, New Jersey. *Annals of the Association of American Geographers,* 85**,** 1-20.

GOMES, M., HUMPHRIES, M., KIRSTEN, K., GREEN, A., FINCH, J. & DE LECEA, A. 2017. Diatom-inferred hydrological changes and Holocene geomorphic transitioning of Africa's largest estuarine system, Lake St Lucia. *Estuarine, Coastal and Shelf Science,* 192**,** 170-180.

GONZÁLEZ-VILLANUEVA, R. & HARGITAI, H. 2021. Blowout Dune and Hollow. *Encyclopedia of Planetary Landforms.* New York, NY: Springer New York.

GOODMAN, P. 1987. Mkuze floodplain and swamps–Wetland management case study. *African Wildlife,* 41.

GOVERNMENT, S. A. 2023. *Geography and climate* [Online]. [Accessed 03 11/2023].

GREEN, A. 2009a. Palaeo-drainage, incised valley fills and transgressive systems tract sedimentation of the northern KwaZulu-Natal continental shelf, South Africa, SW Indian Ocean. *Marine Geology,* 263**,** 46-63.

GREEN, A. 2011. Submarine canyons associated with alternating sediment starvation and shelf-edge wedge development: Northern KwaZulu-Natal continental margin, South Africa. *Marine Geology,* 284**,** 114-126.

GREEN, A., HUMPHRIES, M., COOPER, J., STRACHAN, K., GOMES, M. & DLADLA, N. 2022. The Holocene evolution of Lake St Lucia, Africa's largest estuary: Geological implications for contemporary management. *Estuarine, coastal and shelf science,* 266**,** 107745.

GREEN, A. N. 2009b. Palaeo-drainage, incised valley fills and transgressive systems tract sedimentation of the northern KwaZulu-Natal continental shelf, South Africa, SW Indian Ocean. *Marine Geology,* 263**,** 46-63.

GREEN, A. N., COOPER, J. A. G., DLAMINI, N. P., DLADLA, N. N., PARKER, D. & KERWATH, S. E. 2020. Relict and contemporary influences on the postglacial geomorphology and evolution of a current swept shelf: The Eastern Cape Coast, South Africa. *Marine Geology,* 427**,** 106230.

GREEN, A. N., COOPER, J. A. G., LEUCI, R., THACKERAY, Z. & MALLINSON, D. 2013. Formation and preservation of an overstepped segmented lagoon complex on a high-energy continental shelf. *Sedimentology,* 60**,** 1755-1768.

GREEN, A. N., COOPER, J. A. G., WILES, E. A. & DE LECEA, A. M. 2015. Seismic architecture, stratigraphy and evolution of a subtropical marine embayment: Maputo Bay, Mozambique. *Marine Geology,* 369**,** 300-309.

GREEN, A. N. & UKEN, R. 2005. First observations of sea-level indicators related to glacial maxima at Sodwana Bay, northern KwaZulu-Natal: Research in action. *South African Journal of Science,* 101**,** 236-238.

GUMSLEY, A., STAMSNIJDER, J., LARSSON, E., SÖDERLUND, U., NAERAA, T., DE KOCK, M., SAŁACIŃSKA, A., GAWĘDA, A., HUMBERT, F. & ERNST, R. 2020. Neoarchean large igneous provinces on the Kaapvaal Craton in southern Africa re-define the formation of the Ventersdorp Supergroup and its temporal equivalents. *Geological Society of America Bulletin*.

HABERZETTL, T., KÜCK, B., WULF, S., ANSELMETTI, F., ARIZTEGUI, D., CORBELLA, H., FEY, M., JANSSEN, S., LÜCKE, A. & MAYR, C. 2008. Hydrological variability in southeastern Patagonia and explosive volcanic activity in the southern Andean Cordillera during Oxygen Isotope Stage 3 and the Holocene inferred from lake sediments of Laguna Potrok Aike, Argentina. *Palaeogeography, Palaeoclimatology, Palaeoecology,* 259**,** 213-229.

HENDEY, Q. & VOLMAN, T. 1986. Last interglacial sea levels and coastal caves in the Cape Province, South Africa. *Quaternary Research,* 25**,** 189-198.

HESP, P. 2002. Foredunes and blowouts: initiation, geomorphology and dynamics. *Geomorphology,* 48**,** 245-268.

HESP, P. 2011. Dune Coasts. *Treatise on Estuarine and Coastal Science,* 3**,** 193-221.

HESP, P. A. & HYDE, R. 1996. Flow dynamics and geomorphology of a trough blowout. *Sedimentology,* 43**,** 505-525.

HICKS, N. 2017. *The seismic stratigraphy, geological evolution and CO2 storage potential of the offshore Durban Basin, South Africa.* University of KwaZulu-Natal, Westville.

HIGGS, C. G. 2017. *Geochemical insights into the influence of Holocene sea level change on the evolution of the Mkhuze River Delta, Lake St Lucia, northen KwaZulu-Natal.*

HOBDAY, D. 1976. Quaternary Sedimentation and Development of the lagoonal complex, Lake St Lucia, Zululand.

HOBDAY, D. & ORME, A. 1974. The Port Durnford Formation: a major Pleistocene barrier-lagoon complex along the Zululand coast. *South African Journal of Geology,* 77**,** 141-149.

HU, D., CLIFT, P. D., WAN, S., BÖNING, P., HANNIGAN, R., HILLIER, S. & BLUSZTAJN, J. 2016. Testing chemical weathering proxies in Miocene–Recent fluvial-derived sediments in the South China Sea. *Geological Society, London, Special Publications,* 429**,** 45-72.

HUDOCK, J. W., FLAIG, P. P. & WOOD, L. J. 2014. Washover fans: A modern geomorphologic analysis and proposed classification scheme to improve reservoir models. *Journal of Sedimentary Research,* 84**,** 854-865.

HUGENHOLTZ, C. H. & WOLFE, S. A. 2009. Form–flow interactions of an aeolian saucer blowout. *Earth Surface Processes and Landforms,* 34**,** 919-928.

HUMPHRIES, M., GREEN, A., BENALLACK, K., FINCH, J., DE LECEA, A., GOMES, M., STRACHAN, K. & KIRSTEN, K. 2017. A multi-proxy investigation into past and present environmental change at Lake St Lucia.

HUMPHRIES, M., GREEN, A., HIGGS, C., STRACHAN, K., HAHN, A., PILLAY, L. & ZABEL, M. 2020. High-resolution geochemical records of extreme drought in southeastern Africa during the past 7000 years. *Quaternary Science Reviews,* 236**,** 106294.

HUMPHRIES, M. S., KINDNESS, A., ELLERY, W. N., HUGHES, J. C. & BENITEZ-NELSON, C. R. 2010. 137Cs and 210Pb derived sediment accumulation rates and their role in the long-term development of the Mkuze River floodplain, South Africa. *Geomorphology,* 119**,** 88-96.

KRUGER, G. & MEYER, R. A sedimentological model for the northern Zululand coastal plain. Ext. abstr. 22nd Earth Sci. Congress, Geol. Soc. S. Africa, 1988. 423-426.

KYLANDER, M. E., AMPEL, L., WOHLFARTH, B. & VERES, D. 2011. High-resolution X-ray fluorescence core scanning analysis of Les Echets (France) sedimentary sequence: new insights from chemical proxies. *Journal of Quaternary Science,* 26**,** 109-117.

LABAUNE, C., TESSON, M. & GENSOUS, B. 2005. Integration of high and very high-resolution seismic reflection profiles to study Upper Quaternary deposits of a coastal area in the western Gulf of Lions, SW France. *Marine Geophysical Researches,* 26**,** 109-122.

LAPORTE, L. F. & BEHRENSMEYER, A. K. 1980. Tracks and substrate reworking by terrestrial vertebrates in Quaternary sediments of Kenya. *Journal of Sedimentary Research,* 50**,** 1337-1346.

LIU, K. 1995. Diagenesis of the Neogene Uloa Formation of Zululand, South Africa. *South African Journal of Geology,* 98**,** 25-34.

LIU, X., RENDLE-BÜHRING, R., MEYER, I. & HENRICH, R. 2016. Holocene shelf sedimentation patterns off equatorial East Africa constrained by climatic and sea-level changes. *Sedimentary Geology,* 331**,** 1-11.

LOCK, J. 1972. The effects of hippopotamus grazing on grasslands. *The Journal of Ecology***,** 445-467.

LUDT, W. B. & ROCHA, L. A. 2015. Shifting seas: the impacts of Pleistocene sea-level fluctuations on the evolution of tropical marine taxa. *Journal of Biogeography,* 42**,** 25-38.

MAUD, R. 1968. *Quartenary geomorphology and soil formation in Coastal Natal*.

MAUD, R. 1993. Port Durnford Formation. *Quaternary Geology of the Natal and Zululand coast South Africa. IUGS/CLIP/GSO Fieldguide. 32pp*.

MAUD, R. & ORR, W. 1975. Aspects of post-Karroo geology in the Richards Bay area. *South African Journal of Geology,* 78**,** 101-109.

MCCARTHY, T., ELLERY, W. & BLOEM, A. 1998. Some observations on the geomorphological impact of hippopotamus (Hippopotamus amphibius L.) in the Okavango Delta, Botswana. *African Journal of Ecology,* 36**,** 44-56.

MCCARTHY, T., ELLERY, W. & STANISTREET, L. 1993. Lakes of the north eastern region of the Okavango Swamps, Botswana. *Zeitschrift für Geomorphologie***,** 273-294.

MCKEE, E. D. 1979. Sedimentary structures in dunes. *US Geological Survey Professional Paper***,** 83.

MCMILLAN, I. 1993. Foraminiferal biostratigraphy, sequence stratigraphy and interpreted chronostratigraphy of marine Quaternary sedimentation on the South African continental shelf. *South African Journal of Science,* 89**,** 83-89.

MEYER, R. Geological information from geohydrological investigations on the Zululand Coastal Plain. Maputaland focus on the Quaternary evolution of the south-east African coastal plain. International Union for Quaternary Research Workshop Abstracts, Council for Geoscience, Private Bag X, 1997. 90-99.

MILLER, W. 1994. Morphology and bathymetry of Lake Sibaya. Council for Geoscience, Private Bag X112, Pretoria, 0001. Restricted Report.

MILLER, W. 1996. Sequence Stratigraphy of the Latest Mesozoic and Cenozoic Sediments Below Lake Sibaya, Northern KwaZulu-Natal. *Council for Geoscience, 1996-0318***,** 38.

MILLER, W. R. 1998. *The bathymetry, sedimentology and seismic stratigraphy of Lake Sibaya-Northern KwaZulu-Natal.*

MINYUK, P., BRIGHAM-GRETTE, J., MELLES, M., BORKHODOEV, V. Y. & GLUSHKOVA, O. Y. 2007. Inorganic geochemistry of El'gygytgyn Lake sediments (northeastern Russia) as an indicator of paleoclimatic change for the last 250 kyr. *Journal of Paleolimnology,* 37**,** 123-133.

MISRA, S., SMITH, A. & RAY, D. 2017. KAROO CFB, SOUTHERN AFRICA-EVOLVED FROM MORB BY MIXING WITH A-TYPE RHYOLITE IN BIMODAL ASSOCIATION.

MOORE, J. W. 2006. Animal ecosystem engineers in streams. *BioScience,* 56**,** 237-246.

NAIMAN, R. J. & ROGERS, K. H. 1997. Large animals and system-level characteristics in river corridors. *BioScience,* 47**,** 521-529.

NEAL, A. 2004. Ground-penetrating radar and its use in sedimentology: principles, problems and progress. *Earth-science reviews,* 66**,** 261-330.

NEAL, A. & ROBERTS, C. L. 2001. Internal structure of a trough blowout, determined from migrated ground-penetrating radar profiles. *Sedimentology,* 48**,** 791-810.

NORDFJORD, S., GOFF, J., AUSTIN, J. & GULICK, S. 2006. Seismic facies of incised-valley fills, New Jersey continental shelf: implications for erosion and preservation processes acting during latest Pleistocene–Holocene transgression. *Journal of Sedimentary Research,* 76**,** 1284-1303.

OWEN-SMITH, R. N. 1988. *Megaherbivores: the influence of very large body size on ecology*, Cambridge university press.

PÁNEK, T. 2021. Landslides and Related Sediments. *In:* ALDERTON, D. & ELIAS, S. A. (eds.) *Encyclopedia of Geology (Second Edition).* Oxford: Academic Press.

PARTRIDGE, T. & MAUD, R. 1987. Geomorphic evolution of southern Africa since the Mesozoic. *South African Journal of Geology,* 90**,** 179-208.

PATTAN, J., MASUZAWA, T. & YAMAMOTO, M. 2005. Variations in terrigenous sediment discharge in a sediment core from southeastern Arabian Sea during the last 140 ka. *Current Science***,** 1421-1425.

PAYENBERG, T. H., BOYD, R., BEAUDOIN, J., RUMING, K., DAVIES, S., ROBERTS, J. & LANG, S. C. 2006. The filling of an incised valley by shelf dunes—an example from Hervey Bay, east coast of Australia.

PITMAN, W. & HUTCHISON, I. 1975. A preliminary hydrological study of Lake Sibaya. *Hydrological Research Unit Report*.

POSAMENTIER, H. W. & ALLEN, G. P. 1993. Variability of the sequence stratigraphic model: effects of local basin factors. *Sedimentary geology,* 86**,** 91-109.

PRETORIUS, L., GREEN, A. & COOPER, A. 2016. Submerged shoreline preservation and ravinement during rapid postglacial sea-level rise and subsequent “slowstand”. *Bulletin,* 128**,** 1059-1069.

PRINSLOO, A. S., PILLAY, D. & O'RIAIN, M. J. 2020. Multiscale drivers of hippopotamus distribution in the St Lucia Estuary, South Africa. *African zoology,* 55**,** 127-140.

RAMSAY, P. 1994. Marine geology of the Sodwana Bay shelf, southeast Africa. *Marine Geology,* 120**,** 225-247.

RAMSAY, P. 1996. 9000 years of sea-level change along the southern African coastline. *Quaternary International,* 31**,** 71-75.

RAMSAY, P. J. & COOPER, J. A. G. 2002. Late Quaternary sea-level change in South Africa. *Quaternary Research,* 57**,** 82-90.

ROSSOUW, J. 1984. *Review of existing wave data, wave climate and design waves for South African and South West African (Namibian) coastal waters*, Coastal Engineering and Hydraulics, National Research Institute for ….

SCHOONEES, J., THERON, A. & BEVIS, D. 2006. Shoreline accretion and sand transport at groynes inside the Port of Richards Bay. *Coastal Engineering,* 53**,** 1045-1058.

SCHROPP, S. J., GRAHAM LEWIS, F., WINDOM, H. L., RYAN, J. D., CALDER, F. D. & BURNEY, L. C. 1990. Interpretation of metal concentrations in estuarine sediments of Florida using aluminum as a reference element. *Estuaries,* 13**,** 227-235.

SHAND, P., DARBYSHIRE, D. F., GOODDY, D. & HARIA, A. H. 2007. 87Sr/86Sr as an indicator of flowpaths and weathering rates in the Plynlimon experimental catchments, Wales, UK. *Chemical Geology,* 236**,** 247-265.

SHURIN, J. B., ARANGUREN-RIAÑO, N., DUQUE NEGRO, D., ECHEVERRI LOPEZ, D., JONES, N. T., LAVERDE-R, O., NEU, A. & PEDROZA RAMOS, A. 2020. Ecosystem effects of the world’s largest invasive animal. *Ecology,* 101**,** e02991.

SIESSER, W. G. & DINGLE, R. V. 1981. Tertiary sea-level movements around southern Africa. *The Journal of Geology,* 89**,** 523-536.

SLOSS, C. R., MURRAY-WALLACE, C. V. & JONES, B. G. 2007. Holocene sea-level change on the southeast coast of Australia: a review. *The Holocene,* 17**,** 999-1014.

SMITH, D., HARRISON, S., FIRTH, C. R. & JORDAN, J. T. 2011. The early Holocene sea level rise. *Quaternary Science Reviews,* 30**,** 1846-1860.

STANISTREET, I., CAIRNCROSS, B. & MCCARTHY, T. 1993. Low sinuosity and meandering bedload rivers of the Okavango Fan: channel confinement by vegetated levees without fine sediment. *Sedimentary Geology,* 85**,** 135-156.

STOOPS, G., MARCELINO, V. & MEES, F. 2018. *Interpretation of micromorphological features of soils and regoliths*, Elsevier.

SUDAN, P. 1999. *Sedimentology, stratigraphy and geological history of part of the northern KwaZulu-Natal coastal dune cordon, South Africa.*

SWIFT, D. & THORNE, J. 1991. Sedimentation on continental margins, I: a general model for shelf sedimentation. *Shelf sand and sandstone bodies: Geometry, facies and sequence stratigraphy,* 14**,** 3-31.

TAKAHASHI, T. 1981. Debris flow. *Annual review of fluid mechanics,* 13**,** 57-77.

TANKARD, A. J., MARTIN, M., ERIKSSON, K., HOBDAY, D., HUNTER, D. & MINTER, W. 2012. *Crustal evolution of southern Africa: 3.8 billion years of earth history*, Springer Science & Business Media.

TAYLOR, R., KELBE, B., HALDORSEN, S., BOTHA, G. A., WEJDEN, B., VÆRET, L. & SIMONSEN, M. B. 2006. Groundwater-dependent ecology of the shoreline of the subtropical Lake St Lucia estuary. *Environmental Geology,* 49**,** 586-600.

THORNE, J. 1994. Constraints on riverine valley incision and the response to sea-level change based on fluid mechanics.

TÖRNQVIST, T. E. & HIJMA, M. P. 2012. Links between early Holocene ice-sheet decay, sea-level rise and abrupt climate change. *Nature Geoscience,* 5**,** 601-606.

WANG, R., COLOMBERA, L. & MOUNTNEY, N. P. 2019. Geological controls on the geometry of incised-valley fills: Insights from a global dataset of late-Quaternary examples. *Sedimentology,* 66**,** 2134-2168.

WARE, C. I. 2001. *Evolution of the northern KwaZulu-Natal coastal dune cordon: evidence from the fine-grained sediment fraction.*

WATKEYS, M., MASON, T. & GOODMAN, P. 1993. The role of geology in the development of Maputaland, South Africa. *Journal of African Earth Sciences (and the Middle East),* 16**,** 205-221.

WHITFIELD, A. & TAYLOR, R. 2009. A review of the importance of freshwater inflow to the future conservation of Lake St Lucia. *Aquatic Conservation: Marine and Freshwater Ecosystems,* 19**,** 838-848.

WOLMARANS, L. & DU PREEZ, J. 1986. The geology of the St Lucia area. *(No Title)*.

WRIGHT, C., LINDSAY, P. & COOPER, J. 1997. The effect of sedimentary processes on the ecology of the mangrove-fringed Kosi estuary/lake system, South Africa. *Mangroves and Salt Marshes,* 1**,** 79-94.

WRIGHT, C. I. 1999. *The Cenozoic evolution of the northern KwaZulu-Natal coastal plain, South Africa.* University of Natal, Durban.

WRIGHT, C. I., MILLER, W. R. & COOPER, J. A. G. 2000. The late Cenozoic evolution of coastal water bodies in Northern Kwazulu-Natal, South Africa. *Marine Geology,* 167**,** 207-229.

ZABEL, M., SCHNEIDER, R. R., WAGNER, T., ADEGBIE, A. T., DE VRIES, U. & KOLONIC, S. 2001. Late Quaternary climate changes in Central Africa as inferred from terrigenous input to the Niger Fan. *Quaternary Research,* 56**,** 207-217.

ZAITLIN, B. A., DALRYMPLE, R. W. & BOYD, R. 1994. The stratigraphic organization of incised-valley systems associated with relative sea-level change.

ZENKOVITCH, V. 1959. On the genesis of cuspate spits along lagoon shores. *The Journal of Geology,* 67**,** 269-277.

ZHOU, G. G. D., LI, S., SONG, D., CHOI, C. E. & CHEN, X. 2019. Depositional mechanisms and morphology of debris flow: physical modelling. *Landslides,* 16**,** 315-332.

ZONG, Y. 2004. Mid-Holocene sea-level highstand along the Southeast Coast of China. *Quaternary International,* 117**,** 55-67.

Appendix A

Figure A.1. 200 HS Antenna used to collect GPR data.

Figure A.2. The SIR 4000 GSSI data collection equipment recording data collected.

Figure A.3. Image of Cobra plug-in ground probing radar antenna (SUBECHO 40) mounted onto the back of a vehicle and transported along dirt road to collect data.

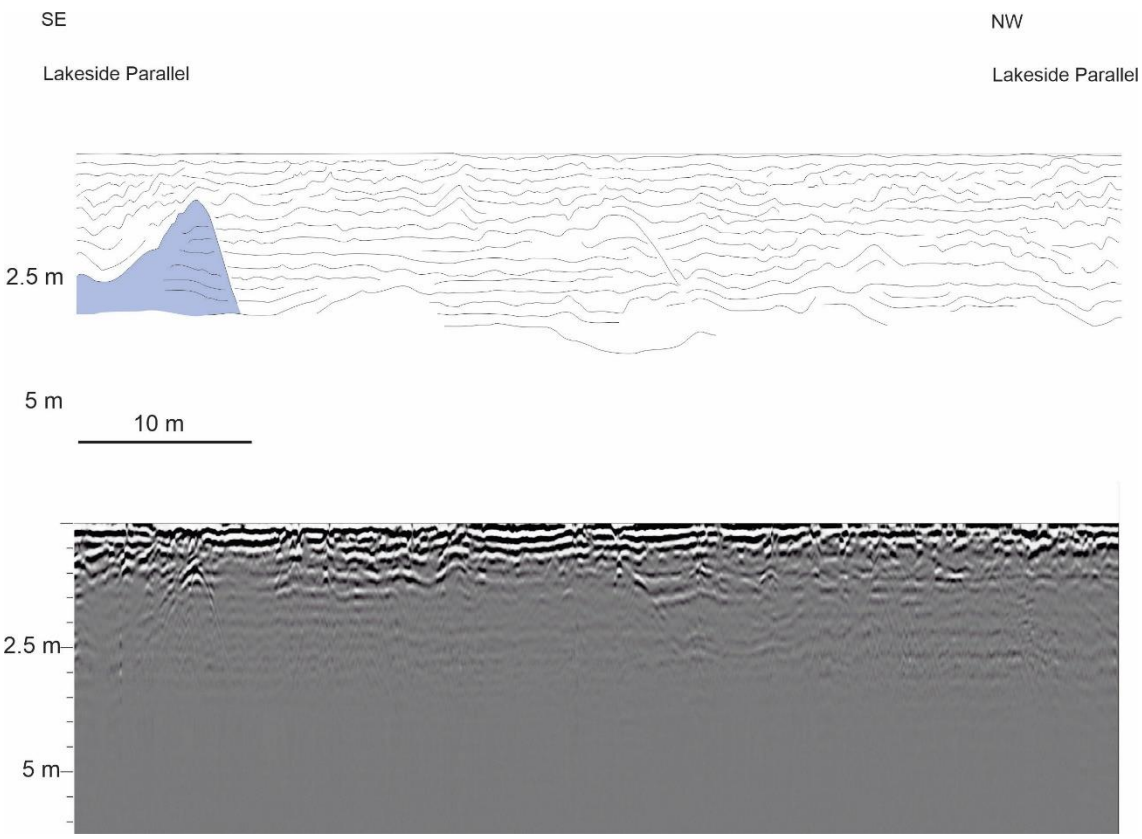

Figure A.4. Interpreted image of GPR data taken along lake margin. Blue colour highlights mound within GPR data.